UNIVERSITÀ
DEGLI STUDI
DI PADOVA

Sede Amministrativa: Università degli Studi di Padova

SCUOLA DI DOTTORATO DI RICERCA IN BIOSCIENZE E BIOTECNOLOGIE
INDIRIZZO BIOLOGIA CELLULARE
CICLO XXIX

MOLECULAR BASIS OF THE INTERACTIONS BETWEEN CARBOHYDRATE ANTIGENS AND MONOCLONAL ANTIBODIES

Tesi redatta con il contributo finanziario di GSK Vaccines

Direttore della Scuola: Ch.mo Prof. Paolo Bernardi
Coordinatore d'indirizzo: Ch.mo Prof. Paolo Bernardi
Supervisore: Ch.mo Prof. Cesare Montecucco
Supervisore GSK Vaccines: Dr. Roberto Adamo

Dottorando: Filippo Carboni

ABSTRACT

Carbohydrate-based vaccines induce an immune response against surface glycans found on pathogenic bacteria and are used to protect children from meningitis and other bacterial diseases. The definition of the epitope targeted by protective antibodies is a crucial information for the design, description and even registration of glycoconjugate vaccines.

The aim of this project is the characterization at atomic level of the interaction between Group B *Streptococcus* (GBS) oligosaccharides with functional antibodies mediating bacterial phagocytic killing. The specificity of anti-GBS type III polysaccharide (GBS PSIII) antibodies has been ascribed to a conformational epitope with an extended helical structure which would be formed by multiple repeating units.

Here fragments of GBS PSIII were obtained by chemical synthesis and by sizing of the native polysaccharide from bacterial source. The oligosaccharides (OSs) were purified by ion exchange chromatography and were characterized by mass spectrometry, HPLC and NMR analysis.

First, the obtained OSs were used to characterize the interaction to protective anti PSIII rabbit monoclonal antibody (mAb) by competitive ELISA and surface plasmon resonance analysis. The dependence of binding affinity on oligosaccharide length was confirmed and the minimal structures showing comparable binding to full-length PS III were identified.

Next, a combination of saturation transfer difference NMR (STD-NMR) and X-ray crystallography was used to map at atomic level the interactions in the rabbit mAb-OS complex. The challenging crystallization of the carbohydrate-protein complex was achieved and the molecular bases of the antigen-antibody interaction were unveiled.

The obtained results were used to optimize a vaccine based on short GBS PSIII fragments.

RIASSUNTO

I vaccini basati su carboidrati inducono una risposta immunitaria contro i glicani della superficie di patogeni e sono usati per proteggere i bambini da meningite e altre malattie batteriche. La definizione dell'epitopo riconosciuto da anticorpi protettivi è un'informazione cruciale per il design e la registrazione di questi vaccini gliconiugati.

L'obiettivo di questo progetto è la caratterizzazione a livello atomico dell'interazione tra oligosaccaridi derivanti dalla capsula di Group B *Streptococcus* (GBS) e anticorpi funzionali che quindi inducono la fagocitosi del batterio. La specificità degli anticorpi verso il polisaccaride del GBS di serotipo III (GBS PSIII) è stata attribuita ad un epitopo conformazionale formato da un'estesa elica che si forma quando si hanno un certo numero di unità saccaridiche che si ripetono nella struttura.

In questo progetto, i frammenti di GBS PSIII sono stati ottenuti sia per sintesi chimica sia tramite depolimerizzazione del polisaccaride nativo estratto dalla capsula del batterio. Gli oligosaccaridi (OSs) sono stati purificati tramite cromatografica a scambio ionico e sono stati caratterizzati tramite spettrometria di massa, HPLC e analisi NMR.

Inizialmente gli OSs ottenuti sono stati utilizzati per caratterizzare l'interazione di un anticorpo monoclonale (mAb), prodotto in coniglio, protettivo e specifico per PSIII, attraverso studi di competitive ELISA e SPR.

In seguito, una combinazione di tecniche diverse, tra cui saturation transfer difference NMR (STD-NMR) e cristallografia a raggi X, è stata utilizzata per mappare a livello atomico l'interazione tra il mAb di coniglio e un OS selezionato sulla base delle analisi precedenti. La riuscita cristallizzazione del complesso carboidrato-proteina ha permesso di rivelare le basi molecolari dell'interazione antigene-anticorpo.

I risultati ottenuti sono stati quindi utilizzati per ottimizzare un vaccino basato su frammenti corti del GBS PSIII.

TABLE OF CONTENTS

6.4. References

7. CONCLUSIONS

CHAPTER 1: INTRODUCTION

1.1. General principles of vaccination

The immune responses of mammals can be divided into innate and adaptive immunity. Innate immunity fights intruding pathogens in a fast, yet non-specific way and can be considered a first line of defense. Onset of adaptive immunity instead is delayed, but all responses are directed specifically against the respective intruder. A multitude of pathogen-specific cells are created by clonal expansion of few, "fitting" pre-cursor cells. And, once infection is resolved, some of these cells survive in the body to form immunologic memory ready to fight the same pathogen faster and more efficiently, when a second encounter occurs. Vaccination takes advantage of this potential of adaptive immunity. The principle of vaccination is that exposure to a small sample of a disease-causing microorganism - or to a part or portion of it - teaches the immune system to rapidly recognize the menace and to create memory that enables the body to fight the real pathogen efficiently during a later encounter. Vaccination basically mimics a natural infection without causing disease. Several are the components of host immune responses that are set in motion following vaccination. Important vaccine-induced immune effectors are antibodies produced by B lymphocytes. These antibodies are capable to recognize and specifically bind to a toxin or a pathogen (or to a portion representative of it).[1] Antibody binding interferes with pathogen entry into host cells or other important functions. Moreover bound antibodies facilitate uptake and elimination of the pathogen by other immune cells. Other important immune effectors are cytotoxic CD8+ T lymphocytes (CTL) that may limit the spread of infectious agents by recognizing and killing infected cells or by secreting specific antiviral cytokines. The generation and maintenance of both B and CD8+ T cell responses is supported by growth factors and signals provided by CD4+ T helper (Th) lymphocytes, which are historically subdivided into T helper 1 (Th1), T helper 2 (Th2) and T helper 17 (Th17) subtypes. These effector cells are controlled by regulatory T cells (Treg) that are involved in maintaining immune tolerance.[2] Most of the antigens and vaccines trigger both B and T cell responses, and the two responses benefit of their interconnection: CD4+ T cells are required for most antibody responses, while antibodies exert significant influences on T cell responses to intracellular pathogens.[3]

Early protective efficacy of a vaccine is often conferred by microorganism-specific antibodies. But just triggering a specific antibody response is not sufficient. The quality of such antibody responses, e.g., antibody avidity, has been identified as a determining factor of efficacy. Although B lymphocytes represent the specialized lineage in antibody production once differentiated in plasma cells, T cells can largely contribute to effective and long-lasting immune responses. In fact, these cells are essential to immune memory, and novel vaccine targets have been identified against which T cells are likely to be the prime effectors.

The stimulation of antigen-specific T cell responses requires their activation by specific antigen presenting cells (APCs), essentially dendritic cells (DCs), which reside in tissues or patrol through the body and are

recruited by inflammatory signals to the site of infection. When exposed to pathogens, immature DCs will phagocyte and process them proteolytically, so that some pathogen components can be loaded on Major Histocompatibility Complex (MHC) class II molecules. DCs then undergo maturation, modulate specific surface receptors and migrate towards secondary lymph nodes, where the trigger of T and B cell responses occurs.

The central role for mature DCs in the activation of vaccine responses reflects their unique ability to provide both antigen-specific and co-stimulation signals to T cells. In fact, T cells require at least two signals to become fully activated:

1. a first antigen-specific signal provided through the T cell receptor which interacts with the antigen peptide-loaded MHC class II molecules on the surface of the APCs;
2. a second antigen-unspecific signal, a co-stimulatory incentive, provided by the interaction between co-stimulatory molecules expressed on the membrane of the APC upon maturation with its counterparts on the T cell.

APCs can also secrete cytokines that are sensed by the interacting T cell and determine its further phenotype (Th1, Th2, Th17).

The very first requirement to elicit vaccine responses is thus to provide sufficient stimuli through vaccine antigens and eventually adjuvants, to trigger an inflammatory reaction that is mediated by cells of the innate immune system[4].

In general, the antibody response to bacterial polysaccharides is poorly affected by adjuvants, IgM represents the major class of antibodies induced and since their immune response does not induce memory, it is not boosted by subsequent immunizations.

These characteristics are due to the fact that, unlike proteins that are T-cell dependent (TD) antigens, polysaccharides are T-cell independent (TI) antigens as they do not require T-cell activation for the induction of specific B-cell (antibody) responses. Polysaccharide antigens directly activate polysaccharide-specific B cells which differentiate then into plasma cells to produce antibodies, but memory B cells are not formed; moreover a pre-existing memory B-cell pool can be depleted by immunization with unconjugated polysaccharide, with risk of hypo-responsiveness on subsequent immunizations[5].

Differently from polysaccharides, proteins are TD antigens; following interaction with antigen-presenting cells (APC) like dendritic cells, macrophages and B-cells, protein antigens are internalized and processed into small peptides which are then re-exposed and presented to T lymphocytes in association with the MHC class II molecules. Interaction with T cells induces B cells to differentiate into plasma cells and memory B cells, thus initiating downstream adaptive immune responses. Unlike TI antigens, TD antigens are immunogenic early in infancy, the immune response induced can be boosted, enhanced by adjuvants and is characterized by antibody class switch and production of antigen-specific IgG.

1.2. Polysaccharide vaccines

Polysaccharides are important virulence factor especially for encapsulated bacteria that present on their surface complex carbohydrate structures. Surface polysaccharides have several functions:

- in some cases they protect microorganisms from desiccation when they are exposed to the external environment (an example is the hyaluronic capsule of Group A *Streptococcus*, whose adhesive properties help the pathogen to invade the host);
- other capsular polysaccharides prevent the activation of the alternative complement pathway;
- sometimes they mimic molecules produced by human cells so that the pathogen is not recognized as foreign by our immune system (serogroup B meningococcal capsular polysaccharide, hyaluronic acid).

Around 1930s the protective role of antibodies (Abs) induced by pneumococcal polysaccharide started to be investigated and in 1945 the first vaccine composed by purified polysaccharides from selected pneumococcal serotypes was tested in humans[6].

The research on vaccines development was subsequently slowed down by the introduction of antibiotics, however, with the emergence of drug resistant strains, the development of polysaccharide vaccines started again and a number of them have been studied in large clinical studies. Polysaccharide vaccines against meningococcus serogroup ACWY, *Streptococcus pneumoniae* and *Haemophilus influenzae* type b were licensed between the seventies and the eighties.[7,8] These bacteria possess polysaccharides which are either polymers formed by one monosaccharide unit (homopolymers) or more complex oligosaccharide repeats (heteropolymers), that can be charged or neutral.

Polysaccharide vaccines however did not completely solve the problem of bacterial diseases caused by encapsulated microorganisms. Being T-cell independent antigens, one of their main features which emerged from clinical trials, was their scarce immunogenicity in children less than two years of age.[9-10] As a consequence, polysaccharide vaccines can be used in adults, but not in infancy and elderly which are the most sensitive target populations.

1.3. Glycoconjugate vaccines

Glycoconjugate vaccines are among the safest and most efficacious vaccines developed during the last 30 years. They are a potent tool for prevention of life-threating bacterial infectious disease like meningitis and pneumonia.

The limitation of polysaccharides vaccines has been overcome by covalent conjugation to a carrier protein as source of T-cell epitopes. Since 1929, it has been demonstrated by Avery and Goebel that non-

immunogenic sugars after conjugation to a carrier protein become able to induce antibodies in animal model.[11] However the first application of this concept to a vaccine for human use started only in 1980 with the development of the first conjugate vaccine against *Haemophilus influenzae* type b (Hib) that was later on licensed between 1987 and 1990.[12-13]

Many other glycoconjugate vaccines have been developed against bacterial pathogens such as *Neisseriae meningitidis*, *Streptococcus pneumoniae* and Group B *Streptococcus*. Glycoconjugate vaccines are currently used in the immunization schedules of different countries like for example the United States (US) (Table 1.1).[14-20]

Table 1.1. Licensed glycoconjugate vaccines.

Vaccine indication	Type of conjugate	Manufacturer
Haemophilus influenzae type b	PRP-TT	Sanofi-Pasteur
	PRP-OMPC	Merck
	PRP-CRM_{197}	Pfizer
	Hib-CRM_{197}	GSK
Haemophilus influenzae type b/Neisseria meningitidis group C	MenC/Hib-TT	GSK
Neisseria meningitidis serogroups $ACW_{135}Y$	MenA-TT	Serum Institute India
	MenC-CRM_{197}	Pfizer, GSK
	MenC-TT	Baxter
	MenACWY-DT	Sanofi-Pasteur
	MenACWY-CRM_{197}	GSK
	MenACWY-TT	Pfizer
Streptococcus pneumoniae serotypes	7 valent-CRM197 (4, 6B, 9V, 14, 18C, 19F, 23F)	Pfizer
	13 valent-CRM197 (1, 3, 4, 5, 6A, 6B, 7F, 9V, 14, 18C, 19A, 19F, 23F)	Pfizer
	10 valent-DT/TT Protein D (1, 4, 5, 6B, 7F, 9V, 14, 18C, 19F, 23F)	GSK

Chemical conjugation of polysaccharides to protein carriers allows processing of the protein carrier by polysaccharide-specific B cells and presentation, on their surface, of the resulting peptides in association with MHC class II. Further interaction with carrier-specific cells then induces a TD response already early in life which leads to immunological memory and boosting of the response by further doses of the vaccine (Figure 1.1). Recently it has been proposed a novel mechanism according to which internalization of glycoconjugate and following proteolytic digestions generate glycopeptides which are re-exposed by MHC

class II (Figure 1.2). This model was confirmed by isolation of specific T-cell clones directed to the sugar. This observation proves that although glycoconjugates are safe and effective, their mechanism of function is still not totally understood.

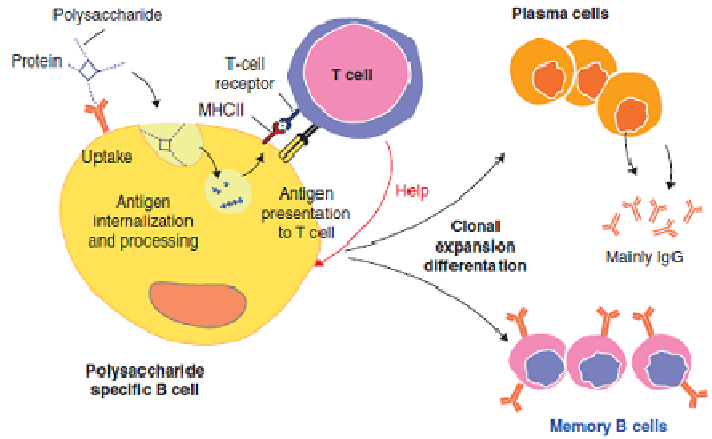

Figure 1.1. Mechanism of action of a glycoconjugate vaccine.[5]

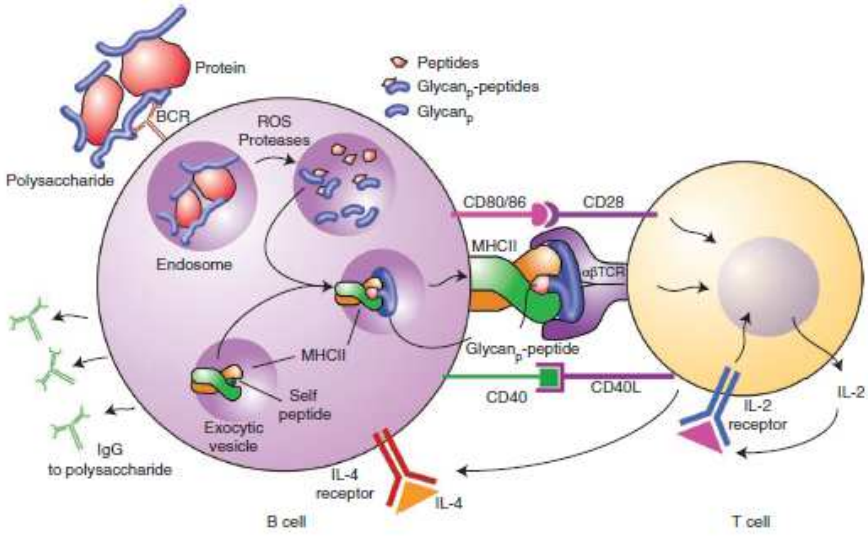

Figure 1.2. Recent working model of action of a glycoconjugate vaccine.[98]

To prepare glycoconjugate vaccines, two main approaches based on different chemistry of conjugation, have been used so far. One is based on the random chemical activation of the saccharide chain followed by covalent binding with the protein carrier obtaining a cross-linked structure between the polysaccharide and the protein. A second approach is based on the generation, by controlled fragmentation of the native polysaccharide, of appropriately sized oligosaccharides which are then activated at their terminal groups, usually with a linker molecule, and subsequently conjugated to the carrier protein obtaining a radial structure (Figure 1.3). Depending on the conjugation chemistry employed, a chemical spacer can be used in order to facilitate the coupling of the protein to the saccharide antigens and, in some cases, conjugation chemistry also requires prior derivatization of the protein carriers.

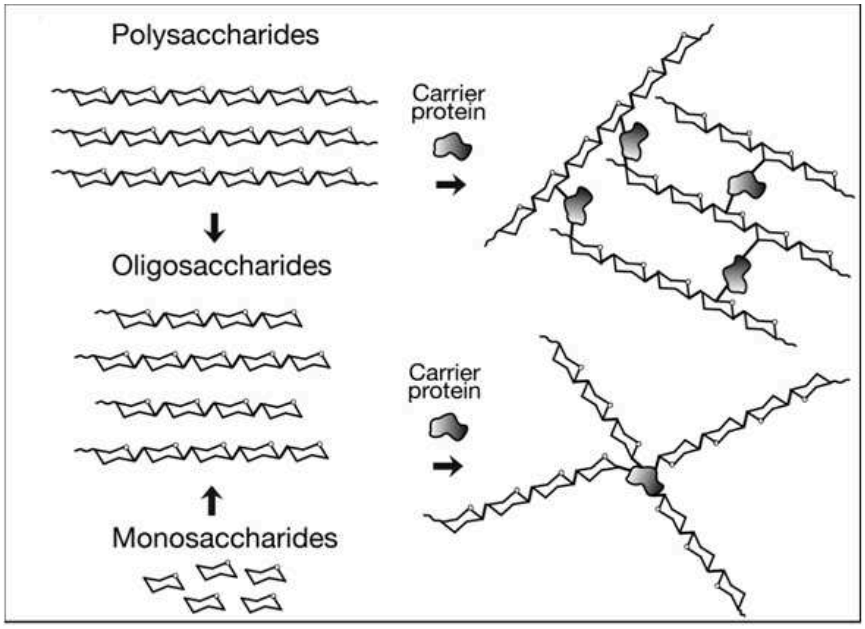

Figure 1.3. Structures of glycoconjugates.

In this second approach, utilization of chemically or chemo-enymatically synthesized carbohydrates, prepared starting from suitable monosaccharides, is increasingly attractive.[21-25] Synthetic oligosaccharides offer the advantage of being pure and well-defined molecules, tipically bearing at the terminal residue a linker for coupling to protein carriers.

A new approach called bioconjugation based on glyco-engineering the bacterial N-glycosylation pathway in bacteria such as *Escherichia coli* is also emerging. The polysaccharide, encoded by the inserted genes, is produced on a polyisoprenoid carrier and then is transferred to an asparagine residue of the carrier protein which has to contain at least one (native or engineered) N-glycosylation site. [26-29]

A chemistry which results in the formation of cross-linked structures was used for commercial Hib conjugate vaccines by Sanofi-Pasteur, Merck and Pfizer.

Novartis Vaccines (NVD, now GSK Vaccines) has instead developed a conjugation chemistry which provides conjugates having oligosaccharides oriented radially from the carrier protein.[5, 12]

In particular Hib and meningococcal NVD conjugate vaccines are made starting from purified capsular polysaccharides which have been size reduced by acid hydrolysis and fractionated to select an intermediate chain length population. The oligosaccharides were then derivatized at their reducing termini introducing first a primary amino group by reductive amination followed by a 6-carbon atom flexible hydrocarbon spacer having a terminal active ester ready for conjugation.[14,30-31] The same technology was used by NVD to develop its quadrivalent A, C, W135, Y anti-meningococcal conjugate vaccine.[32]

1.4. Variables influencing the immunogenicity and physicochemical properties of glycoconjugate vaccines

Many aspects can influence the immunogenicity of conjugate vaccines and the main variables investigated so far are the size of the saccharide moiety, the saccharide:protein ratio in the purified conjugate, the conjugation strategy, the nature of the spacer and the protein carrier.

Immunogenic epitopes involved in the interaction with specific antibodies usually comprise precise glycan structures, often not longer than six or eight sugar units (45 year-old paradigm established by Kabat).[33] An early study by Seppälä and Mäkelä investigated the effect of saccharide size and saccharide:protein ratio on the immunogenicity of dextrans-protein conjugates, and found that dextrans of low molecular weight conjugated to chicken serum albumin induced strong anti-dextran responses in mice, while increasing the dextrans size resulted in reduced immunogenicity.[34] Peeters et al. showed that a synthetic tetramer of Hib capsular polysaccharide repeating unit, conjugated to a protein carrier, induced in adult mice and non-human primates antibody levels comparable to a commercial Hib conjugate and higher than those induced by a trimer, indicating that for Hib a minimum of eight sugars is needed for a proper immunological response.[35] Laferriere et al. found little influence of the carbohydrate chain length on the immunogenicity of pneumococcal conjugate vaccines in mice.[36] Pozsgay et al. studied the immunogenicity in mice of synthetic *Shigella dysenteriae* type 1 LPS oligosaccharides conjugated to human serum albumin (HSA). The authors found that octa-, dodeca-, and hexadecasaccharide fragments induced high levels of lipopolysaccharide binding IgG antibodies in mice after three injections and were superior to a tetrasaccharide conjugate. The influence of the carbohydrate:protein ratio was different for the three conjugates. The octasaccharide-HSA conjugate with the highest density evoked a good immune response, while in the case of dodeca- and hexadecasaccharide conjugates, the median density was optimal.[37]

These studies suggest that oligosaccharide chain length and hapten loading are interconnected in determining the immunogenicity of glycoconjugate vaccines and are case antigen specific parameters.

The spacer is a short linear molecule that is generally linked to the polysaccharide chain or to the protein or to both moieties, depending on the chemistry, used to facilitate the coupling between the protein and sugar. There are evidences in the literature which suggest that rigid, constrained spacers, like cyclohexyl maleimide, elicit a significant amount of undesirable antibodies, with the risk of driving the immune response away from the targeted epitope on the hapten.[38, 39] The use of a flexible alkyl type maleimido spacer has been reported as a way to overcome the previous observed immunogenicity of cyclic maleimide linkers.[40]

A number of protein carriers have been used so far in preclinical and clinical evaluation of conjugate vaccines.[19, 41-46] Proteins such as diphtheria and tetanus toxoids, which derive from the respective toxins after chemical detoxification with formaldehyde, were initially selected as carriers because of the safety track record accumulated with tetanus and diphtheria vaccination. CRM_{197}, a non-toxic mutant of diphtheria toxin[47] which instead does not need chemical detoxification, has been extensively used as carrier for

licensed Hib, pneumococcal, meningococcal conjugate vaccines and for other vaccines being developed. An outer membrane protein complex of serogroup B meningococcus has been used by Merck as carrier for their Hib conjugate vaccine.[48] GSK in their multivalent pneumococcal conjugate vaccine introduced the use of the Hib-related protein D as carrier for most of the polysaccharides included into the vaccine.[49, 50] The team of John Robbins made extensive use of the recombinant non-toxic form of *Pseudomonas aeruginosa* exo-toxin as carrier for *Staphylococcus aureus* type 5 and 8 as well as for *Salmonella typhi* Vi conjugates.[51, 52]

A number of clinical trials have been conducted to compare the immunogenicity of different conjugate vaccines with different carrier proteins.[53-57]

It is however very difficult a direct comparison of the effect of different protein carriers, due to the coexistence of other variables as conjugation chemistry, saccharide chain length, adjuvant, formulation technology, and previous or concomitant vaccination with other antigens.

1.5. Chemical biology approaches to designing defined carbohydrate vaccines

As isolated polysaccharides are structurally complex, the corresponding glycoconjugates most likely contain the ‘‘right’’ B cell epitopes needed to confer protective immunity. Identification of the right epitope is a time-consuming step. Antigen design has traditionally been an iterative process. Understanding the structure of a protective B cell epitope is vital before immunization experiments are performed. The currently available tools to map carbohydrate epitopes can make use of small amounts of glycans for screening purposes.

B cell epitopes can be classified into two groups: sequential (continuous) epitopes and conformational (discontinuous) epitopes. A sequential B cell epitope is recognized as the primary structure of an antigen, while a conformational B cell epitope consists of residues that may be distantly separated in the primary structure and are recognized due to the close proximity within the folded 3D structure[58]. The nature of an epitope is of utmost importance during antigen design: conformational epitopes are associated with a distinct secondary structure of the glycan, a feat that may only be achieved in longer sequences comprising multiple repeating units. Thus, the synthetic effort compromises the applicability of these long glycans as synthetic antigens.

The implications of structural requirements are still poorly understood. In addition to glycan length, important determinants for the viability of a carbohydrate antigen comprise the stereochemistry of glycosidic linkages and the arrangement of individual glycan components within a repeating unit. In addition, the presence of branching points and different substituents like phosphates, acetates and pyruvates may be crucial for immunogenicity[59].

Recent progress in synthetic carbohydrate chemistry, bioinformatics and analysis of carbohydrate-protein interactions facilitates the 3D-structural interpretation of glycan-antibody complexes. Numerous methods are currently in practice that can aid the antigen design process. For instance, advancements in structural

methods, such as X-ray crystallography, NMR or small angle X-ray scattering (SAXS), are used to generate valuable information on the 3D structures of glycans and their interaction partners[60-62]. Information on the structural requirements of glycan recognition can form the basis of designing optimized carbohydrate vaccine candidates. Structural vaccinology is a newly emerging field and has already contributed significantly to the development of modern protein-based vaccines[63-64]. Adaptation of the structural vaccinology principles to saccharides may reveal the nature of glycotopes that are recognized by the host immune system, thereby facilitating the design of more efficient vaccines. For instance, structural understanding of the epitope helps to improve biochemical characteristics of vaccine antigens and to select the combination of glycan residues that are necessary to increase the breadth of the immune response. Recently, Bundle and coworkers used structural information to design a universal carbohydrate antigen based on the antigenic determinants of A-type and M-type O antigens of *Brucella*[65]. Studies on the nature of antigenic determinants recognized by monoclonal antibodies facilitated the design of one single oligosaccharide that may form the basis for the diagnosis of Brucellosis.

Structural information on the binding of epitopes may help in decoding the rules of immunodominance and provide the basis for manipulating the antigen structure to render protective epitopes immunodominant[64].

3D-structural information on oligosaccharide antigens is becoming increasingly available. NMR spectroscopy and X-ray crystallography are the most reliable techniques to reveal glycan-antibody interactions at the molecular level. However, typical Ka values of glycan-antibody interactions are weak, in the 10^2–10^6 M range, complicating the cocrystallization of both binding partners. In such instances, NMR is extremely useful to obtain insights into the solution structure and the dynamics of a ligand-antibody complex. However, due to the intrinsic complexity and flexibility of carbohydrates, a multidisciplinary strategy combining NMR parameters with molecular modeling protocols should be followed in order to generate reliable structural information[66].

In ligand-based structural glycobiology, changes in the parameters of the ligand are monitored upon passing from the free to the bound state[66]. Thereby, NMR techniques are often preferred over other biophysical methods.

NMR measurements can be employed to detect binding, to elucidate the bound conformation of the glycan, to map the bound epitope and to provide information on molecular dynamics[66]. Combinations of transferred nuclear Overhauser effect spectroscopy (TR-NOESY)[67] and saturation transfer difference (STD)[68-69] NMR experiments have been employed extensively to study the conformations of carbohydrates bound to antibodies and to define interacting epitopes[61, 70-73]. Seeberger group revealed the structural features of the interaction between a *Bacillus anthracis* tetrasaccharide containing three rhamnoses and a unique terminal anthrose unit and a monoclonal antibody by STD NMR. A combined approach involving glycan array screening, surface plasmon resonance (SPR) and STD NMR revealed structural insights into the molecular events of carbohydrate-antibody interactions. The use of several *B. anthracis* oligosaccharides demonstrated a crucial role of the anthrose residue in recognition[73].

A shortcoming of NMR-based epitope mapping is the restriction on certain tight kinetic requirements. Such methods work optimally when the off rate is fast in the relaxation time scale of the ligand. For slow dissociation kinetics, conventional NMR methods do not provide adequate information. Consequently, STD and TR-NOESY methods are not useful for dissociation constants in the low micromolar or nanomolar ranges[66] and the observation of the parameters associated with the receptor becomes the method of choice.

In a receptor-based approach, methods of structural biochemistry are employed to map the antigen combining sites or complementarity determining regions (CDRs) of an antibody. However, antibodies are large macromolecules and, due to their weaker interactions, gaining detailed structural information of a carbohydrate-antibody complex represents a real challenge.

X-ray crystallography would provide structural information on antigen combining sites with highest resolution. Despite the usefulness of this approach, only few crystal structures of carbohydrate-antibody complexes have been solved thus far. Due to the high polarity of the hydroxyl groups and flexibility of the carbohydrate structures[74], crystallization of carbohydrate-protein complexes is a challenging task. Infact for example, conformational and compositional heterogeneity in carbohydrate moieties of glycoconjugates is expected to interfere with crystallization, and deglycosylation has proved essential for heavily glycosylated proteins such as human chorionic gonadotropin[75].

Various studies have demonstrated that carbohydrate binding sites of an anti-glycan antibody can vary significantly in the epitope size they accommodate. Cocrystal structures of carbohydrate-bound antibodies reveal the span of the bound epitope and structural details of important residues that interact with antibody CDRs. Relatively small oligosaccharides occupy the binding site in reported structures[76-77], while few reports of larger epitopes exist[78]. In one special case, a (2/8)-polysialic acid apparently occupies an exceptionally long binding site[77]. Two key examples demonstrating the receptor based approach in carbohydrate antigen design involve *Vibrio cholerae* O1 antigen[76], where the epitope involves 2 consecutive residues in the terminal part of the molecule, and synthetic O antigen fragments from serotype 2a *Shigella flexneri*[62], where the epitope involves 6 out of 10 monosaccharides.

1.6. GBS

Streptococcus agalactiae, also known as Group B Streptococcus (GBS), is one of the major causes of sepsis, pneumonia and meningitis in neonatal and infants in the first three months after birth.[79] It is a Gram positive beta-hemolytic coccus which appears in pairs (Figure 1.4) or chains[80], that colonizes the urogenital and gastrointestinal tracts of more than 30% of the healthy population and, in particular, the vagina of 25-40% of healthy women.[81-83]

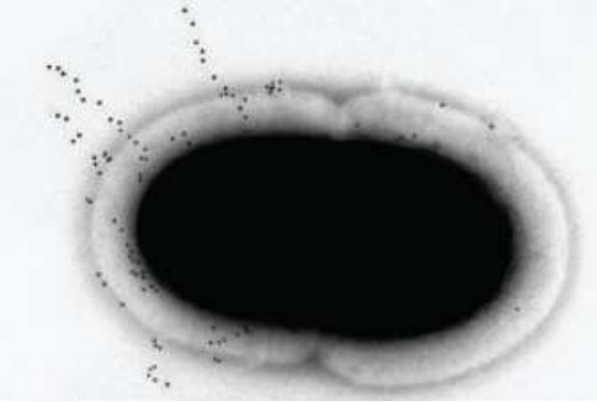

Figure 1.4. Immunogold Electron Microscopy of GBS strain CJB111.[99]

It was classified for the first time in 1930 by R. Lancefield and R. Hare during a serological differentiation study on human isolates and other groups of hemolytic streptococci.[84] It is included in the group B of "Lancefield System", where Streptococci are identified with alphabetical letters from A to O, based on capsular polysaccharide antigens and groups A, B and D are the most dangerous[85]. GBS clinical isolates are also classified into ten serotypes, according to the chemical nature of capsular polysaccharides (PS): Ia, Ib, II, III, IV, V, VI, VII, VIII and IX.[86-88] However around 8-14% of the clinical isolates in the Europe and USA are non-typeable strains because cannot be distinguished on the basis of PS antigenicity. All GBS serotypes contain, in different combinations, these carbohydrates: galactose, glucose, rhamnose, N-acetylglucosammine and sialic acid (N-acetylneuraminic acid) (Figure 1.5).

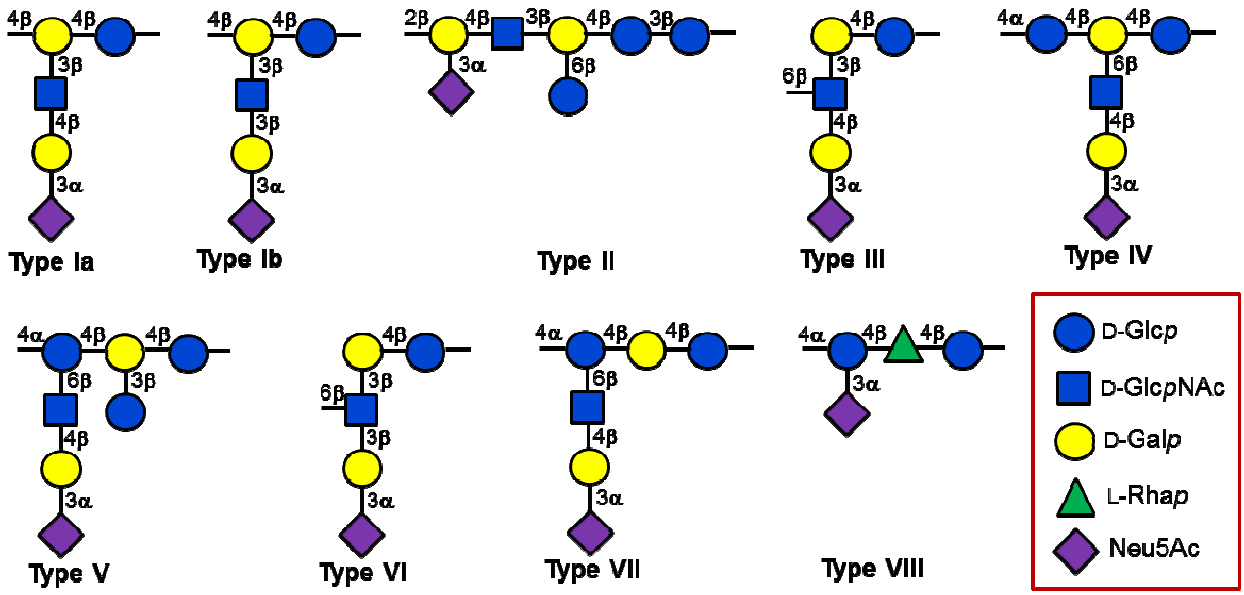

Figure 1.5. Chemical structures of isolated GBS serotypes.[100]

Streptococcus agalactiae is known as the most frequent cause of sepsis, pneumonia and meningitis in neonates within first months from birth.[82,89] It is an etiologic agent also in adults, in particular elderly persons, immunocompromised, diabetics and patients affected by others chronic pathology of liver and kidney. In the cellular hyper-trophism of vaginal epithelium, where it can adhere despite low values of pH[90], it forms a permanent colonization in more than 40% of women. During pregnancy, the uro-genital tract colonization is cause of severe infections/year, leading to chorioamnionitis, endometrial tenderness, tachycardia, cystitis and fever which make necessary antibiotic therapies also after delivery. GBS can also be cause of intrauterine death, aborts, prelabor rupture of the membranes, with preterm labor/delivery, causing the exposure of 90% of premature neonates to infection. In most cases infection is transferred vertically from asymptomatic mothers and, every year, only for US, 8000-12000 infected babies and 2000 deaths are recorded. Infection appears in uterus or at delivery for contact of throat, ear, nostril, umbilicus and respiratory ways with amniotic liquid or infected vaginal fluids. After the aspiration/ingestion of bacteria, neonatal lungs become the starting focus of infection. From here it can rapidly arrive to flow of blood, continue towards others tissues and organs like blood-brain barrier (Figure 1.6).

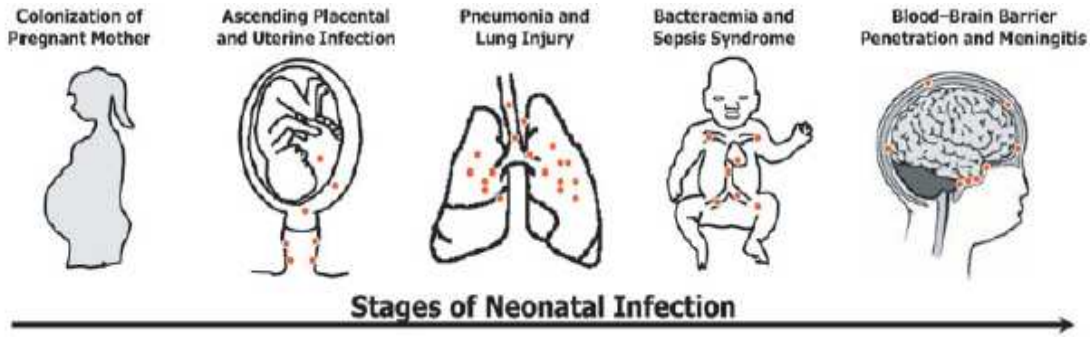

Figure 1.6. Stages of neonatal group B streptococcal (GBS) infection.[101]

Neonatal disease can occur in two different forms: the **Early-Onset Disease** (EOD) and the **Late-Onset Disease** (LOD).

EOD occurs during the first seven days of life, with the vast majority of cases (approximately 90%) present during the first 24 hours of life.[91] Neonates with EOD present respiratory disease (54%), sepsis without focus (27%) and meningitis (15%).[92]

LOD occurs beyond seven days of life and can develop up to three months of age. In 50% of the cases it has a maternal origin. Neonates with LOD present sepsis (46%), meningitis (37%), urinary infection (7%), osteoarthritis (6%), respiratory disease (4%) and cellulitis (4%). Over 20% of survivors of GBS meningitis have permanent sequelae, including hearing loss, mental retardation, cortical blindness and seizures (Table 1.2).

Table 1.2. Neonatal manifestation of group B streptococcal disease.[102]

	Early-onset disease	Late-onset disease
Onset	First week of life (usually within the first 24 h)	One week to 3 months of age
Clinical presentation	Respiratory distress Pneumonia Sepsis	Sepsis Meningitis Osteoarthritis
Incidence of prematury	Increased	No change
Maternal obstetrical complication	Frequent (70%)	Uncommon
Transmission	Vertical: acquired *in utero* or intrapartum	Usually horizontal transmission: can also be intrapartum
Predominant serotypes*	Ia, III, V	III, Ia, V

*In descending order of prevalence

Risk factors include non-white race and preterm birth, but most of time it is a horizontal transmission, after contact with sanitary staff or colonized mothers. LOD is basically due to serotype III strain, with an incidence until 60% depending on the geographic area. Studies performed on non-pregnant adults with GBS associated invasive disease revealed that GBS serotypes Ia, III and V accounted for more than two-third of cases. More than 25% of the subjects had invasive GBS disease caused by type V strains (Table 1.3).

Table 1.3. Serotype distribution of group B streptococcal isolates from non-pregnant adults with invasive GBS infection, 1992-1999.[103]

GBS serotype	N° (%) of subjects (n=589)
Ia	143 (24.3)
Ib	72 (12.2)
II	70 (11.9)
III	97 (16.5)
IV	2 (0.3)
V	162 (27.5)
VI	0
VII	0
VIII	1 (0.2)
Non-typeable	42 (7.1)

The clinical manifestations of GBS infection in elderly adults are: skin and soft-tissue infections (in these cases, cellulites is the most frequent clinical manifestation), urinary tract infections (bacteremic urinary tract infections account for 33.4% of the cases in adults >70 years of age), pneumoniae (only in older debilitated adults), bacteremia with no identified focus (in the 15% of non-pregnant adults affected by GBS invasive diseases), arthritis, osteomyelitis, meningitis (in only 2% of non-pregnant adults with GBS invasive disease) and endocarditis.

1.7. GBS Vaccine

Early in 1930s Rebecca Lancefield *et al.* demonstrated that polyclonal antibodies from rabbit sera, able to recognize PS epitopes, conferred protection against GBS infection in animal models. During the last two decades, plain GBS polysaccharides have been extensively studied as vaccines in preclinical and human clinical studies. However, the first human clinical trials conducted in the 1980s showed that the purified native PS from serotype III was not sufficient to induce a robust IgG response in adults and induced an insignificant response in neonates.

Subsequently, conjugation of PSs to immunogenic proteins, such as tetanus toxoid (TT) and mutated diphtheria toxoid (CRM_{197})[93-94], was shown to dramatically increase the immune response in children, eliciting the differentiation of memory cells associated to a long term protection. Following these findings, PS-TT conjugate vaccines based on nine GBS serotypes were produced and tested pre-clinically.[76] These studies, carried out in animal models, showed that conjugate antigens were able to induce functional PS-specific IgG that, in presence of complement, stimulate *in vitro* the opsonization and killing of GBS by human peripheral blood leukocytes. This success constituted the rationale to proceed with the clinical studies in human. Further studies demonstrated that glycoconjugate vaccines constituted by serotypes Ia, Ib, II, III, and V PS linked to TT were safe, well-tolerated and highly immunogenic in human adults[94], but cross-protection between serotypes was still lacking. Therefore a multivalent vaccine was required in order to obtain a broad coverage of the vaccine against the prevalent circulating GBS serotypes. A tetravalent combination of PS–TT conjugates (serotypes Ia, Ib, II, and III) was successfully tested in a mouse model and further human trials were performed using the combination of two PS TT-conjugates (serotypes II and III). Results showed that the combination had the same immunogenicity and reactogenicity of each monovalent PS vaccine.[94]

However, although recent epidemiological studies[95] suggest that a tetravalent combination of serotypes Ia, Ib, III and V would be sufficient to achieve a coverage against the majority of GBS strains circulating in Europe and North America, there are other geographical areas where such combination would be not be effective owing to a different serotypes distribution (i.e. VI and VIII, predominant in Japan). Moreover, the PS-conjugate vaccine would not protect against all the non-typeable isolates.

An additional obstacle to the licensure of vaccine against GBS is the difficulty of conducting clinical efficacy trials in human: large sample size would be required, but the use of IAP reduces the incidence of neonatal disease. A possible solution to overcome this difficulty came from the studies of Feng-Ying C. Lin and coworkers who carried out a prospective way to estimate the maternal GBS-PSs antibody levels needed to give protection to neonates from EOD. The amount of maternal antibodies against GBS-PSIa was measured by ELISA in 45 case patients (mothers whose neonates developed EOD) and 319 controls (mothers of neonates colonized by GBS-PSIa but without EOD). Distribution of maternal antibody concentrations showed that the probability of developing EOD declined with increasing maternal levels of anti-PSIa IgG[96]. This work demonstrated that it is possible to define thresholds of anti-GBS PSIa specific IgG levels in the mothers which are predictive for the protection of newborns.

More recently, thresholds have also been set for the levels of maternal anti GBS-PSIII IgGs required to protect newborns from EOD caused by GBS serotype III.[97] The results of Feng-Ying C. Lin suggested that complex clinical trials required for a GBS vaccine registration might be replaced with an *in vitro* correlate of protection based on the quantification of vaccine induced antibodies.

1.8. References

1. Cooper NR, Nemerow GR. The role of antibody and complement in the control of viral infections**.** *J. Invest. Dermatol.* **83***,* 121s–127s (1984).
2. Bacchetta R, Gregori S, Roncarolo MG. CD4+ regulatory T cells: mechanisms of induction and effector function. *Autoimmun. Rev.* **4**, 491–496 (2005).
3. Igietseme JU, Eko FO, He Q, et al. Antibody regulation of T cell immunity: implications for vaccine strategies against intracellular pathogens. *Expert Rev Vaccines* **3**, 23–34 (2004).
4. Hoebe K, Janssen E, Beutler B. The interface between innate and adaptive immunity. *Nat. Immunol.* **5**, 971–974 (2004).
5. Costantino P, Rappuoli R, Berti F. The design of semi-synthetic and synthetic glycoconjugate vaccines *Expert Opin. Drug Discov.* **6 (10)**, 1045-1066 (2011).
6. Macleod CM, Hodges RG, Heidelberg M, Bernhard WG. Prevention of pneumococcal pneumonia by immunization with specific capsular polysaccharides. *J. Exp. Med.* **82***,* 445-465 (1945).
7. Artenstein MS, Gold R, Zimmerly JG. Prevention of meningococcal disease by group C polysaccharide vaccine. *N. Engl. J. Med.* **282***,* 417-420 (1970).
8. Gold R, Artenstein MS. Meningococcal infections. 2. Field trial of group C meningococcal polysaccharide vaccine in 1969-70. *Bull World Health Organ.* **45***,* 279-282 (1971).
9. Peltola H, Makela H, Kayhty H. Clinical efficacy of meningococcus group A capsular polysaccharide vaccine in children three months to five years of age. *N. Engl. J. Med.* **297***,* 686-691 (1977).
10. Peltola H, Kayhty H, Sivonen A, Makela H. *Haemophilus influenzae* type b capsular polysaccharide vaccine in children: a double-blind field study of 100,000 vaccinees 3 months to 5 years of age in Finland. *Pediatrics* **60***,* 730-737 (1977).
11. Avery OT, Goebel WF. Chemo-immunological studies on conjugated carbohydrate-proteins : ii. Immunological specificity of synthetic sugar-protein antigens. *J. Exp. Med.* **50***,* 533-550 (1929).
12. Schneerson R, Barrera O, Sutton A, Robbins JB. Preparation, characterization, and immunogenicity of *Haemophilus influenzae* type b polysaccharide-protein conjugates. *J. Exp. Med.* **152***,* 361-376 (1980).
13. Anderson PW, Pichichero ME, Insel RA. Vaccines consisting of periodate-cleaved oligosaccharides from the capsule of *Haemophilus influenzae* type b coupled to a protein carrier:structural and temporal requirements for priming in the human infant. *J. Immunol.* **137***,* 1181-1186 (1986).
14. Costantino P, Viti S, Podda A. Development and phase 1 clinical testing of a conjugate vaccine against meningococcus A and C. *Vaccine* **10***,* 691-814 (1992).
15. Eby R. Pneumococcal conjugate vaccines. *Pharm. Biotechnol.* **6***,* 695-718 (1995).

16. Ravenscroft N, Averani G, Bartoloni A. Size determination of bacterial capsular oligosaccharides used to prepare conjugate vaccines. *Vaccine* **17**, 2802-2816 (1999).
17. Lakshman R, Finn A. Meningococcal serogroup C conjugate vaccine. *Expert. Opin. Biol. Ther.* **2**, 87-96 (2002).
18. Paoletti LC, Kasper DL. Glycoconjugate vaccines to prevent group B streptococcal infections. *Expert. Opin. Biol. Ther.* **3**, 975-984 (2003).
19. Snape MD, Perrett KP, Ford KJ. Immunogenicity of a tetravalent meningococcal glycoconjugate vaccine in infants: a randomized controlled trial. *JAMA* **299**,173-184 (2008).
20. Bardotti A, Averani G, Berti F. Physicochemical characterization of glycoconjugate vaccines for prevention of meningococcal diseases. *Vaccine* **26**, 2284-2296 (2008).
21. Verez-Bencomo V et al. A synthetic conjugate polysaccharide vaccine against *Haemophilus influenzae* type b. *Science* **305(5683)**, 522-525 (2004).
22. Seeberger PH. Automated oligosaccharide synthesis. *Chem. Soc. Rev.* **37**, 19-28 (2008).
23. Jaipuri FA, Pohl NL. Toward solution-phase automated iterative synthesis: fluorous-tag assisted solution-phase synthesis of linear and branched mannose oligomers. *Org. Biomol. Chem.* **6(15)**, 2686-2691 (2008).
24. Adamo R et al. Synthesis of laminarin fragments and evaluation of a β-(1, 3) glucan hexasaccaride-CRM197 conjugate as vaccine candidate against *Candida albicans*. *Journal of Carbohydrate Chemistry* **30(4-6)**, 249-280 (2011).
25. Adamo R, Romano MR et al. Phosphorylation of the synthetic hexasaccharide repeating unit is essential for the induction of antibodies to *Clostridium difficile* PSII cell wall polysaccharide. *ACS Chem. Biol.* **7(8)**, 1420-1428 (2012).
26. Szymanski CM et al. Evidence for a system of general protein glycosylation in *Campylobacter jejuni*. *Mol. Microbiol.* **32(5)**, 1022-1030 (1999).
27. Kelly J et al. Biosynthesis of the N-linked glycan in *Campylobacter jejuni* and addition onto protein through block transfer. *J. Bacteriol.* **188(7)**, 2427-2434 (2006).
28. Feldman MF et al. Engineering N-linked protein glycosylation with diverse O antigen lipopolysaccharide structures in *Escherichia coli*. *Proc. Natl. Acad. Sci. USA* **102(8)**, 3016-3021 (2005).
29. Ihssen J et al. Production of glycoprotein vaccines in *Escherichia coli*. *Microb. Cell. Fact.* **9**, 61 (2010).
30. Costantino P et al. Size fractionation of bacterial capsular polysaccharides for their use in conjugate vaccines. *Vaccine* **17(9-10)**, 1251-1263 (1999).
31. Matjila MJ et al. Safety and immunogenicity of two *Haemophilus influenzae* type b conjugate vaccines. *S. Afr. Med. J.* **94(1)**, 43-46 (2004).

32. Broker M et al. Chemistry of a new investigational quadrivalent meningococcal conjugate vaccine that is immunogenic at all ages. *Vaccine* **27(41)**, 5574-5580 (2009).
33. Kabat EA. The upper limit for the size of the human antidextran combining site. *J. Immunol.* **84**, 82–85 (1960).
34. Seppala I, Makela O. Antigenicity of dextran-protein conjugates in mice. Effect of molecular weight of the carbohydrate and comparison of two modes of coupling. *J. Immunol.* **143(4)**, 1259-1264 (1989).
35. Peeters CC et al. Synthetic trimer and tetramer of 3-beta-Dribose-(1-1)-D-ribitol-5-phosphate conjugated to protein induce antibody responses to *Haemophilus influenzae* type b capsular polysaccharide in mice and monkeys. *Infect. Immun.* **60(5)**, 1826-1833 (1992).
36. Laferrière CA et al. The synthesis of *Streptococcus pneumoniae* polysaccharide-tetanus toxoid conjugates and the effect of chain length on immunogenicity. *Vaccine* **15(2)**, 179-186 (1997).
37. Pozsgay V et al. Protein conjugates of synthetic saccharides elicit higher levels of serum IgG lipopolysaccharide antibodies in mice than do those of the O-specific polysaccharide from *Shigella dysenteriae* type 1. *Proc. Natl. Acad. Sci. USA* **96(9)**, 5194-5197 (1999).
38. Peeters JM et al. Comparison of four bifunctional reagents for coupling peptides to proteins and the effect of the three moieties on the immunogenicity of the conjugates. *J. Immunol. Methods* **120(1)**, 133-143 (1989).
39. Buskas T et al. The immunogenicity of the tumor-associated antigen Lewis(y) may be suppressed by a bifunctional cross-linker required for coupling to a carrier protein. *Chemistry* **10(14)**, 3517-3524 (2004).
40. Phalipon A et al. A synthetic carbohydrate-protein conjugate vaccine candidate against *Shigella flexneri* 2a infection. *J. Immunol.* **182(4)**, 2241-2247 (2009).
41. Pace D. Quadrivalent meningococcal ACYW-135 glycoconjugate vaccine for broader protection from infancy. *Expert Rev. Vaccines* **8(5)**, 529-542 (2009).
42. Ruggeberg JU, Pollard AJ. Meningococcal vaccines. *Paediatr. Drugs* **6(4)**, 251-266 (2004).
43. Hwang KW. *Haemophilus influenza* type b (Hib) vaccine and its carrier proteins. *Arch. Pharm. Res.* **33(6)**, 793-795 (2010).
44. Ostergaard L et al. Immunogenicity, reactogenicity and persistence of meningococcal A, C, W-135 and Y-tetanus toxoid candidate conjugate (MenACWY-TT) vaccine formulations in adolescents aged 15-25 years. *Vaccine* **27(1)**, 161-168 (2009).
45. Kabanova A, Margarit I, Berti F et al. Evaluation of a *Group A Streptococcus* synthetic oligosaccharide as vaccine candidate. *Vaccine* **29(1)**, 104-114 (2010).
46. Micoli F et al. Vi-CRM_{197} as a new conjugate vaccine against *Salmonella Typhi*. *Vaccine* **29(4)**, 712-720 (2011).

47. Giannini G et al. The amino-acid sequence of two non-toxic mutants of diphtheria toxin: CRM45 and CRM197. *Nucleic Acids Res 1984; 12(10):4063-4069*
48. Donnelly JJ et al. Immunogenicity of a *Haemophilus influenzae* polysaccharide-Neisseria meningitidis outer membrane protein complex conjugate vaccine. *J. Immunol.* **145(9)**, 3071-3079 (1990).
49. Prymula R, Schuerman L. 10-valent pneumococcal nontypeable *Haemophilus influenza* PD conjugate vaccine: Synflorix. *Expert Rev, Vaccines* **8(11)**, 1479-1500 (2009).
50. Forsgren A et al. Protein D of *Haemophilus influenzae*: a protective nontypeable *H. influenzae* antigen and a carrier for pneumococcal conjugate vaccines. *Clin Infect Dis* **46(5)**, 726-731 (2008).
51. Fattom A et al. Laboratory and clinical evaluation of conjugate vaccines composed of *Staphylococcus aureus* type 5 and type 8 capsular polysaccharides bound to *Pseudomonas aeruginosa* recombinant exoprotein A. *Infect. Immun.* **61(3)**, 1023-1032 (1993).
52. Szu SC et al. Vi capsular polysaccharide protein conjugates for prevention of typhoid fever. Preparation, characterization, and immunogenicity in laboratory animals. *J. Exp. Med.* **166(5)**, 1510-1524 (1987).
53. Decker MD et al. Comparative trial in infants of four conjugate *Haemophilus influenzae* type b vaccines. *J. Pediatr.* **120**, 184-189 (1992).
54. Granoff DM, Anderson EL, Osterholm MT et al. Differences in the immunogenicity of three *Haemophilus influenzae* type b conjugate vaccines in infants. *J. Pediatr.* **121(2)**, 187-194 (1992).
55. Halperin SA et al. Comparison of the safety and immunogenicity of an investigational and a licensed quadrivalent meningococcal conjugate vaccine in children 2-10 years of age. *Vaccine* **28(50)**, 7865-7872 (2010).
56. Southern J et al. Immunogenicity of a reduced schedule of meningococcal group C conjugate vaccine given concomitantly with the Prevenar and Pediacel vaccines in healthy infants in the United Kingdom. *Clin. Vaccine Immunol.* **16(2)**, 194-199 (2009).
57. Jackson LA et al. Phase III comparison of an investigational quadrivalent meningococcal conjugate vaccine with the licensed meningococcal ACWY conjugate vaccine in adolescents. *Clin. Infect. Dis.* **49(1)**, 1-10 (2009).
58. Arnon R, Van Regenmortel MHV. Structural basis of antigenic specificity and design of new vaccines. *FASEB J.* **6**, 3265–3274 (1992).
59. Anish C, Schumann B, Pereira CL, Seeberger PH. Chemical biology approaches to designing defined carbohydrate vaccines. *Chemistry and Biology* **21(1)**, 38-50 (2014).
60. Khan S, Rodriguez E, Patel R, Gor J, Mulloy B, Perkins SJ. The solution structure of heparan sulfate differs from that of heparin: implications for function. *J. Biol. Chem.* **286**, 24842–24854 (2011).

61. Rademacher C, Shoemaker GK, Kim HS, Zheng RB, Taha H, Liu C, Nacario RC, Schriemer DC, Klassen JS, Peters T, Lowary TL. Ligand specificity of CS-35, a monoclonal antibody that recognizes mycobacterial lipoarabinomannan: a model system for oligofuranosideprotein recognition. *J. Am. Chem. Soc.* **129**, 10489–10502 (2007).
62. Vulliez-Le Normand B, Saul FA, Phalipon A, Belot F, Guerreiro C, Mulard LA, Bentley GA. Structures of synthetic O-antigen fragments from serotype 2a *Shigella flexneri* in complex with a protective monoclonal antibody. *Proc. Natl. Acad. Sci. USA*. **105**, 9976–9981 (2008).
63. Dormitzer PR, Grandi G, Rappuoli R. Structural vaccinology starts to deliver. *Nat. Rev. Microbiol.* **10**, 807–813 (2012).
64. Schneewind O, Missiakas D. Structural vaccinology to thwart antigenic variation in microbial pathogens. *Proc. Natl. Acad. Sci. USA*. **108**, 10029–10030 (2011).
65. Guiard J, Paszkiewicz E, Sadowska J, Bundle DR. Design and synthesis of a universal antigen to detect brucellosis. *Angew. Chem. Int. Ed. Engl.* **52**, 7181–7185 (2013).
66. Marcelo F, Canada FJ, Jimenez-Barbero J. The interaction of saccharides with antibodies. A 3D view by using NMR. *In Anticarbohydrate Antibodies, P. Kosma and S. Muller-Loennies, eds. (Vienna: Springer)*. 385–402 (2012).
67. Ni F, Zhu Y. Accounting for ligand-protein interactions in the relaxation-matrix analysis of transferred nuclear Overhauser effects. *J. Magn. Reson. B*. **103**, 180–184 (1994).
68. Mayer M, Meyer B. Characterization of ligand binding by saturation transfer difference NMR spectroscopy. *Angew. Chem. Int.* **38**, 1784–1788 (1999).
69. Mayer M, Meyer B. Group epitope mapping by saturation transfer difference NMR to identify segments of a ligand in direct contact with a protein receptor. *J. Am. Chem. Soc.* **123**, 6108–6117 (2001).
70. Clement MJ, Fortune A, Phalipon A, Marcel-Peyre V, Simenel C, Imberty A, Delepierre M, Mulard LA. Toward a better understanding of the basis of the molecular mimicry of polysaccharide antigens by peptides: the example of *Shigella flexneri* 5a. *J. Biol. Chem.* **281**, 2317–2332 (2006).
71. Herfurth L, Ernst B, Wagner B, Ricklin D, Strasser DS, Magnani JL, Benie AJ, Peters T. Comparative epitope mapping with saturation transfer difference NMR of sialyl Lewis(a) compounds and derivatives bound to a monoclonal antibody. *J. Med. Chem.* **48**, 6879–6886 (2005).
72. Maaheimo H, Kosma P, Brade L, Brade H, Peters T. Mapping the binding of synthetic disaccharides representing epitopes of chlamydial lipopolysaccharide to antibodies with NMR. *Biochemistry* **39**, 12778–12788 (2000).
73. Oberli MA, Tamborrini M, Tsai YH, Werz DB, Horlacher T, Adibekian A, Gauss D, Moller HM, Pluschke G, Seeberger PH. Molecular analysis of carbohydrate-antibody interactions: case study using a *Bacillus anthracis* tetrasaccharide. *J. Am. Chem. Soc.* **132**, 10239–10241 (2010).

74. Bush CA, Martin-Pastor M. Structure and conformation of complex carbohydrates of glycoproteins, glycolipids, and bacterial polysaccharides. *Annu. Rev. Biophys. Biomol. Struct.* **28**, 269-293 (1999).
75. Lustbader JW, Birken S, Pileggi NF, Gawinowicz MA, Pollak S, Cuff ME, Yang W, Hendrickson WA, Canfield RE. Crystallization and characterization of human chorionic gonadotropin in chemically deglycosylated and enzymatically desialylated states. *Biochemistry.* 9239–9243 (1989).
76. Villeneuve S, Souchon H, Riottot MM, Mazié JC, Lei P, Glaudemans CPJ, Kovac P, Fournier JM, Alzari PM. Crystal structure of an anti-carbohydrate antibody directed against *Vibrio cholerae* O1 in complex with antigen: molecular basis for serotype specificity. *Proc. Natl. Acad. Sci. USA*. **97**, 8433–8438 (2000).
77. Evans SV, Sigurskjold BW, Jennings HJ, Brisson JR, To R, Tse WC, Altman E, Frosch M, Weisgerber C, Kratzin HD et al. Evidence for the extended helical nature of polysaccharide epitopes. The 2.8 Å resolution structure and thermodynamics of ligand binding of an antigen binding fragment specific for alpha-(2—>8)-polysialic acid. *Biochemistry*. **34**, 6737–6744 (1995).
78. Nagae M, Ikeda A, Hane M, Hanashima S, Kitajima K, Sato C, Yamaguchi Y. Crystal structure of anti-polysialic acid antibody single chain Fv fragment complexed with octasialic acid: insight into the binding preference for polysialic acid. *J. Biol. Chem.* **288**, 33784–33796 (2013).
79. Lauer P, Rinaudo CD, Soriani M, Margarit I, Maione D, Rosini R, Taddei AR, Mora M, Rappuoli R, Grandi G, Telford JL. Genome analysis reveals pili in Group B *Streptococcus*. *Science* **309(5731)**, 105 (2005).
80. Facklam R. What happened to Streptococci: overview of taxonomic and nomenclature changes. *Clin. Microb. Rev.* **15(4)**, 613–630 (2002).
81. Dillon HC, Gray E, Pass MA and Gray BM. Anorectal and vaginal carriage of Group B *Streptococci* during pregnancy. *J. Infect. Dis.* **145(6)**, 794-799 (1982).
82. Schuchat A. Epidemiology of Group B Streptococcal disease in the United States: shifting paradigms. *Clin. Microb. Rev.* **11(3)**, 497-513 (1998).
83. Hansen S, Uldbjerg N, Kilians M, Sorensen UBS. Dynamics of *Streptococcus agalactiae* colonization in women during and after pregnancy and in their infants. *J. Clin. Microb.* **42(1)**, 83–89 (2004).
84. Lancefield RC. A serological differentiation of specific types of *Bovine Hemolytic Streptococci* (Group B). *J. Exp. Med.* **59**, 441-458 (1934).
85. Lancefield RC, Hare R. The serological differentiation of pathogenic and non-pathogenic strains of hemolytic Streptococci from parturient women. **61(3)**, 335–349 (1935).
86. Wagner M, Wagner B, Kubin V. Immunoelectron microscopic study of the location of group-specific and type-specific polysaccharide antigens on isolated walls of Group B *Streptococci*. *J. Gen. Microb.* **120**, 369-376 (1980).

87. Kong F, Gowan S et al. Serotype Identification of Group B *Streptococci* by PCR and sequencing. *J. Clin. Microb.* **40(1)**, 216-226 (2002).

88. Slotved HC, Kong F et al. Serotype IX, a proposed pew *Streptococcus agalactiae* serotype. *J. Clin. Microb.* **45(9)**, 2929–2936 (2007).

89. McCracken GH. *Group B streptococci*: the new challenge in neonatal infections. *J. Pediatr.* **82(4)**, 703-706 (1973).

90. Tamura GS, Kuypers JM et al. Adherence of Group B *Streptococci* to cultured epithelial cells: roles of environmental factors and bacterial surface components. *Infection and Immunity.* **62(6)**, 2450-2458 (1994).

91. Garland S. Early onset neonatal *Group B Streptococcus* infection: associated obstetric risk factors. *Aust. N. Z. J. Obstet. Gynaecol.* **31(2)**, 117-118 (1991).

92. Yagupsky P, Menegus MA, Powell KR. The changing spectrum of Group B Streptococcal disease in infants: an eleven-year experience in a tertiary care hospital. *Pediatr Infect Dis J.* **10(11)**, 801-8 (1991).

93. Paoletti LC, Wessels MR, Michon F, Difabio J, Jennings HJ, Kasper DL. Group-B *Streptococcus* type-II polysaccharide-tetanus toxoid conjugate vaccine. *Infect. Immun.* **60**, 4009-4014 (1992).

94. Paoletti LC, Peterson DL, Legmann R, Collier RJ. Preclinical evaluation of group B streptococcal polysaccharide conjugate vaccines prepared with a modified diphtheria toxin and a recombinant duck hepatitis B core antigen. *Vaccine* **20**, 370-376 (2001).

95. Harrison LH, Elliott JH et al. Serotype distribution of invasive Group B Streptococcal isolates in Maryland: implications for vaccine formulation. *J. Infect. Dis.* **177(4)**, 998-1002 (1998).

96. Lin FY, Philips JB 3rd, Azimi PH, Weisman LE, Clark P, Rhoads GG, Regan J, Concepcion NF, Frasch CE, Troendle J, Brenner RA, Gray BM, Bhushan R, Fitzgerald G, Moyer P, Clemens JD. Level of maternal antibody required to protect neonates against early-onset disease caused by Group B *Streptococcus* type Ia: a multicenter, seroepidemiology study. *J. Infect. Dis.* **184(8)**, 1022-1028 (2001).

97. Lin FY, Weisman LE, Azimi PH, Philips JB 3rd, Clark P, Regan J, Rhoads GG, Frasch CE, Gray BM, Troendle J, Brenner RA, Moyer P, Clemens JD. Level of maternal IgG anti-Group B *streptococcus* type III antibody correlated with protection of neonates against early-onset disease caused by this pathogen. *J Infect Dis.* **190(5)**, 928-34 (2004).

98. Avci FY, Kasper DL. How bacterial carbohydrates influence the adaptive immune system. *Annu. Rev. Immunol.* **28**, 107-10 (2010).

99. Rosini R, Rinaudo CD, et al. Identification of novel genomic islands coding for antigenic pilus-like structures in *Streptococcus agalactiae*. *Mol. Microbiol.* **61(1)**, 126-141 (2006).

100. Berti F, Adamo R. Recent mechanistic insights on glycoconjugate vaccines and future perspectives. *ACS Chem. Biol.* **8**, 1653−1663 (2013).

101. Doran KS, Nizet V. Molecular pathogenesis of neonatal group B streptococcal infection: no longer in its infancy. *Mol. Microbiol.* **54(1)**, 23-31 (2004).

102. Shet A, Ferrieri P. Neonatal & maternal group B streptococcal infections: a comprehensive review. *Indian J. Med. Res.* **120(3)**, 141-150 (2004).

103. Edwards MS, Baker CJ. Group B streptococcal infections in elderly adults. *Clin. Infect. Dis.* **41(6)**, 839-847 (2005).

CHAPTER 2: MATERIALS AND METHODS

2.1. Isolation and purification of the type III capsular polysaccharide

GBS strain COH1 was used for preparation of PSIII from 1L of bacterial culture grown to exponential phase in Todd Hewitt broth. The purification process was based on previously described procedures[1]. Briefly, the bacterial pellet was recovered by centrifugation at 4000 rpm for 20 min and incubated with 0.8 N NaOH at 37 °C for 36h. After centrifugation at 4000 rpm for 20 min, 1M Tris buffer (1:9, v/v) was added to the supernatant and diluted with 1:1 (v/v) HCl to reach a neutral pH. To further purify PSIII, 2 M $CaCl_2$ (0.1 M final concentration) and ethanol (30% (v/v) final concentration) were added to the solution. After centrifugation at 4000 × g for 20 min, the supernatant was subjected to tangential flow filtration with a 10 kDa-molecular weight cutoff (Hydrosart Sartorius) against 14 volumes of 50 mM Tris, 500 mM NaCl pH 8.8 and 7 volumes of 10mM sodium phosphate pH 7.2.

2.2. Fragments of type III polysaccharides prepared by deamination

Native type III PS was partially de-N-acetylated as follows: the polysaccharide was dissolved at 2 mg/mL in 0.5 M NaOH, heated at 70°C for 2-4h, and then chilled in an ice-water bath. Glacial acetic acid was added to the sample to bring the pH to 4.5. The partially de-N-acetylated product was deaminated by the addition of 200µL of 5% (w/v) $NaNO_2$ and stirred at 4°C for 2h. The material was purified by a G25 column eluting with water.

To reconstitute full N-acetylation of sialic acid residues, a 1:1 diluted solution of 4.15µL/mL acetic anhydride in ethanol was added, and the reaction was incubated at room temperature for 2h. The material was purified by a G25 column eluting with water.

2.3. Purification of oligosaccharides

The fragments of different length were separated by anion exchange chromatography using a semi-preparative HPLC with a Mono Q column. Increasing the NaCl percentage of the elution buffer with a staircase gradient, it was possible to isolate oligosaccharides with a difference in chain length in the range of 1-2 repeating units.

2.4. MALDI analysis

MALDI-TOF mass spectra were recorded by UltraFlex III MALDI-TOF/TOF instrument (Bruker Daltonics) in linear mode and with negative ion detection. The samples for analysis were prepared by mixing 2.5µL of

product (~10µM) and 2.5µL of Super DHB matrix. 2.5µL of each mixture were deposited on samples plate, dried at room temperature for 10 min and subjected to the spectrometer.

2.5. HPAEC-PAD analysis for revealing Gal, Glc and GlcNAc

Standard samples of GBS PSIII at five increasing concentrations ranging between 0.5 and 10.3µg/mL were prepared to build the calibration curve. GBS PSIII samples were prepared targeting the calibration curve midpoint. The reference and analytical samples were prepared in 4 M trifluoroacetic acid, incubated at 100°C for 3h, dried under vacuum (SpeedVac Thermo), and suspended in water. All analytical samples were filtered with 0.45 µm Phenex-NY (Phenomenex) filters before analysis. HPAEC-PAD analysis was performed with a Dionex ICS-3000 equipped with a CarboPac PA1 column (4 × 250 mm; Dionex) coupled with a PA1 guard to column (4 × 50 mm; Dionex). Samples (50 µL injection volume) were run at 1mL/min, using isocratic elution with 14 mM NaOH, followed by a washing step with 0.5 M NaOH.

2.6. HPAEC-PAD analysis for revealing NeuNAc

The calibration curve was prepared with five increasing concentrations of NeuNAc ranging between 1.0 and 10.0 µg/mL (as saccharide powder/mL). GBS PSIII samples were prepared targeting the calibration curve midpoint. The reference and analytical samples were prepared in 50 mM HCl, incubated at 75°C for 1h, and treated with 62.5 mM NaOH after chilling at +4°C. All analytical samples were filtered with 0.45 µm Phenex-NY (Phenomenex) filters before analysis. HPAEC-PAD analysis was performed with a Dionex ICS-3000 equipped with a CarboPac PA20 Fast Sialic Acid column (3 × 30 mm; Dionex), 5µL injection volume and 0.5mL/min flow, using elution from 30 mM to 500 mM sodium acetate.

2.7. HPAEC-PAD data acquisition and analysis

In both HPAEC-PAD analyses, the effluent was monitored using an electrochemical detector in the pulse amperometric mode with a gold working electrode and an Ag/AgCl reference electrode. A quadruple-potential waveform for carbohydrates was applied. The resulting chromatographic data were processed using Chromeleon software 6.8 (Dionex). Gal, Glc, GlcNAc and NeuNAc concentration were determined and converted in µmol/mL to estimate the relative mol/mol ratio.

2.8. CRM_{197} conjugation of PSIII oligosaccharides obtained by chemical depolymerization

For the conjugation reaction to CRM_{197}, purified oligosaccharides from chemical depolymerization were dissolved in 100 mM sodium phosphate buffer at pH 7.2. CRM was added to the solution with an active ester to protein molar ratio varying from of 10:1 to 70:1 and a final concentration of 10mg/mL in protein. Then, $NaBCNH_3$ was added to the solution (saccharide:$NaBCNH_3$ 1:1 w/w) and incubated ON at 37°C. Conjugation was monitored by SDS-PAGE 4–12% of polyacrylamide in MOPS. The conjugates were purified from the unreacted saccharide on a CHT hydroxyapatite column, using for elution 2 mM sodium phosphate/300mM NaCl at pH 7.2 (20mL, 1mL/min), followed by 400 mM sodium phosphate at pH 7.2 (40mL, 1mL/min). When unreacted CRM_{197} was present, the conjugate was purified by CHT hydroxyapatite column chromatography using a 4 step elution program: 2 mM sodium phosphate/300mM NaCl at pH 7.2 (20 mL, 1 mL/min), 10 mM sodium phosphate at pH 7.2 (20mL, 1mL/min), 35 mM sodium phosphate at pH 7.2 (20mL, 1mL/min), and 400 mM sodium phosphate at pH 7.2 (40mL, 1mL/min). The conjugate was detected by measuring UV absorption at 215, 254 and 280 nm. Protein content in the purified glycoconjugates was determined by micro-BCA (Thermo-scientific). Saccharide content was estimated by HPAEC-PAD analysis.

2.9. CRM_{197} conjugation of synthetic DP1s

A solution of di-N-hydroxysuccinimidyl adipate (10 eq) and triethylamine (0.2 eq) in DMSO was added to the pentasaccharide **1**-**3**. The reaction was stirred for 3h, then the product was precipitate at 0°C by adding ethyl acetate (9 volumes). The solid was washed 10 times with ethyl acetate (2 volumes each) and lyophilized. The activated sugar was conjugated to CRM_{197} in sodium phosphate 100 mM at a protein concentration of 5mg/ml, using a ratio of 50-100:1 mol saccharide/mol protein.

2.10. SDS-PAGE analysis

Sodium Dodecyl Sulfate- Polyacrilamide gel electrophoresis (SDS-PAGE) was performed on 4-12% pre-casted polyacrylamide gel (NuPAGE®Invitrogen) using MOPS 1x as running buffer (NuPAGE®Invitrogen). 5µg of protein were loaded for each sample. After electrophoretic running with a voltage of 150V for about 45 minutes, the gel was stained with blue coomassie.

2.11. Desialylation of PSIII-CRM_{197} conjugates

3mg of PSIII-CRM_{197} as saccharide content (Saccharide Concentration 984.6 µg/mL, Protein Concentration 757.4 µg/mL, Glycosylation Degree 1.30) were dried under vacuum (Genevac EZ-2 Plus) and re-dissolved

in 3mL of deuterated sodium acetate 50 mM at pH 4.75; the mixture was reacted at 80°C and monitored by ^{1}H NMR to estimate the de-sialylation percentage of each sample.

The conjugates were purified by dialysis against 10 mM sodium phosphate pH 7.2 and characterized for their Gal content, protein concentration and integrity (SDS-Page analysis and Capillary Electrophoresis analysis).

2.12. Immunogenicity of conjugates in mice

Two groups of eight female BALB/c mice were immunized by intraperitoneal injection of different doses in saccharide content of each prduced glycoconjugate using alum hydroxide as an adjuvant. Alum hydroxide and CRM-PSIII were used as controls. Mice received the vaccines at days 1, 21 and 35. Sera were bled at days 1, 21, 35 and 49.

2.13. ELISA analysis using GBS PS III conjugated to human serum albumin (HSA) as coating reagent

Microtiter plates (96 wells, NUNC, Maxisorp) were coated with 100 µL of 1µg/mL of GBS PSIII conjugated to HSA *via* the spacer adipic acid dihydrazide in Phosphate Buffered Saline (PBS) pH 7.4. Plates were incubated overnight at 2-8°C, washed three times with PBST (0.05% Tween-20 in PBS pH 7.4) and saturated with 250 µL/well of PBST-B (2% Bovine Serum Albumin-BSA in PBST) for 90 min at 37°C. The plates were then aspirated to remove the solution. Two-fold serial dilutions of test and standard sera in PBST-B were added to each well. Plates were then incubated at 37°C for 1h, washed with PBST, and then incubated for 90 min at 37°C with anti-mouse IgG-alkaline phosphatase (Sigma) diluted 1:2000 or anti-rabbit IgG-alkaline phosphatase diluted 1:1000 in PBST-B. After washing, the plates were developed with a 4 mg/mL solution of p-Nitrophenyl Phosphate (pNPP) in 1 M diethanolamine (DEA) pH 9.8, at room temperature for 30 min. After blocking with 7% EDTA, the absorbance was measured using a SPECTRAmax plate reader with wavelength set at 405 nm. IgG concentrations were expressed as relative ELISA Units/mL (EU/mL) and were calculated by interpolating the absorbance values of serial sample dilutions on the standard calibration curve (Reference line method). The murine standard consists of a pool of hyperimmune sera obtained from animals immunized with 3 doses of GBS PS III-CRM conjugate vaccines adjuvanted with Alum.

ELISA inhibition experiments were performed following the same procedure but pre-incubating sera with one or more concentrations of the inhibitor for 20 min at room temperature.

2.14. ELISA analysis using unconjugated PSIII or Pn14 as coating reagent

Microtiter plates (96 wells, NUNC, Maxisorp) were coated with 100 µL of unconjugated PS III or Pn14 in PBS pH 7.4 (35µg/mL), followed by overnight incubation at 2-8°C. After washing three times with PBST, a PBS solution containing 2% BSA and sucrose (51 mg/mL) was added (250 µL/well), and plates were incubated 90 min at 37°C, and then aspirated to remove the solution. Two-fold serial dilutions of test and standard sera in PBST-B were added to each well. Plates were then incubated at 37°C for 2 hours, washed with PBST, and incubated for 2 additional hours at 37°C with either anti-mouse IgG-alkaline phosphatase (Sigma) diluted 1:2000 or anti-rabbit IgG-alkaline phosphatase diluted 1:1000 in PBST-B. After washing, the plates were developed with pNPP and the absorbance values measured with a SPECTRAmax plate reader as reported in the previous section. IgG concentrations were calculated as reciprocal serum dilution giving OD of 1.0.

2.15. Opsonophagocytosis Killing Assay (OPKA)

Functional activity of anti-GBS antibodies was estimated by Opsono Phagocytic Killing Assay (OPKA) using differentiated HL-60 cells and strains COH1-III[2]. The percent of killing was calculated as (mean Colony Forming Units at T0 - mean CFU at T60)/(mean CFU at T0). OPK titers were expressed as the reciprocal serum dilution mediating 50% bacterial killing, estimated through piecewise linear interpolation of the dilution-killing OPK data. The Lower Limit of Detection was 1:30 and the assay coefficient of variation was approximately 30%.

OPK inhibition experiments were performed following the same assay but pre-incubating sera with one or more concentrations of the inhibitor for 20 min at room temperature.

2.16. Preparation of anti-PSIII rabbit monoclonal antibody

The clone producing the rabbit monoclonal antibody anti-PSIII NVS-1-19-5 was obtained using hybridoma technology by EPITOMICS Inc. (California). Rabbits were immunized five times with GBS PSIII-CRM conjugate. At the time of each injection, the antigen aliquot was thawed and combined with Complete Freund's Adjuvant (CFA) (for the first injection) or with incomplete Freund's Adjuvant (IFA) for the subsequently injections. The injection route was subcutaneous (SC). The serum titer against PSIII was evaluated and one rabbit was chosen. After splenectomy two hundred million lymphocyte cells were fused with 100 million fusion partner cells and plated on 20x 96-well plates respectively. Cell growth was examined 2-3 weeks after fusion. Supernatants were screened by ELISA against PSIII-HSA and 9 positive multiclone supernatants were analyzed by OPK assay for the functional activity. 3 clones were sub-cloned and supernatants analyzed as described above. From the selected hybridoma clone IgG heavy and light chain

cDNA was amplified, cloned into proprietary mammalian expression vector and sequenced. Then, transient expression of recombinant antibody in HEK-293 derived cell line was performed and the recombinant rabbit mAb obtained was purified using protein A from the transfection supernatant. Rabbit mAb obtained was analyzed by ELISA against PSIII-HSA to confirm specific binding and by OPK assay for functional activity.

2.17. Fab production

Fab was prepared from the mAb using a "Fab Preparation Kit" (Pierce). mAb was digested into Fab by incubation overnight in a buffer containing immobilized papain in a hot room at 37°C. The resultant soluble Fab, Fc fragments and undigested IgG were separated from the immobilized papain gel by a separator tube. Then the Fab was separated from the Fc and undigested IgG by using a protein A column. Fab solution was exchanged using Zeba Spin Desalting column in PBS pH 7.2.

2.18. Surface Plasmon Resonance (SPR) analysis

Binding kinetics and affinities were determined by SPR using a BIACORE X100 system. Glycoconjugates of PSIII and its fragments were immobilized on research grade CM5 sensor chips (Biacore) using the amine coupling kit supplied by the manufacturer (Biacore). Immobilizations were conducted in 10-20mM sodium acetate (pH 4-5) at sugar concentrations of 2-4µg/mL. The immobilized surface density was ~50 resonance units in each instance. Measurements were conducted in 10 mM HEPES (pH 7.2), 150mM NaCl, 3mM EDTA, 0.005% Tween20 at 25°C and at a flow rate of 45µL/min. Following mAb or Fab binding, conjugate surfaces were regenerated with 3.5M $MgCl_2$ and a contact time of 120s. Sensorgram data were analyzed using BIAevaluation software (Biacore).

2.19. SPR Fab binding inhibition

Inhibition assays were performed following the SPR procedure as described above using a CM5 sensor chip with immobilized HSA-PSIII. Binding analysis was performed with samples of Fab at a fixed concentration pre-incubated with PSIII or its fragments serially diluted (2x) starting from a concentration of 2mg/mL.

2.20. STD NMR experiments

NMR experiments were carried out on a Bruker 500 MHz NMR instrument equipped with a TBI cooled probe at controlled temperature (± 0.1 K). Data acquisition and processing were performed using TOPSPIN 1.3 and 3.1 software, respectively. Suppression of water signal was achieved by excitation sculpting (2 msec

selective square pulse). Proton-Carbon Saccharides resonances were assigned collecting both 1D (^{1}H and ^{13}C) and 2D (TOCSY, NOESY, HSQC, HSQC-TOCSY) experiments, using standard pulse sequences. STD-NMR experiments were acquire with 96 scans over 96 accumulations and spectral width of 8000 Hz (12 ppm) at 298 K; a saturation transfer of 2/4 sec. were applied to enhance the saturation transfer effect, irradiating at a frequency of 8.0, -1.0 and -2.0 ppm (3 different spectra recorded for each sample). No differences were observed in the STD spectra irradiating at 8.0 or -1.0 or -2.0 ppm (4000, -500 and -1000 Hz respectively) for all samples, confirming that the saturation transfer effect was not irradiation dependent. To avoid pitfalls in the interpretation of STD-NMR spectra, a negative control spectrum was always recorded in absence of mAb (ligand and buffer) at the very same condition (concentration and pH) of the mAb-saccharide samples. The STD negative controls were always subtracted to the relative mAb-saccharide STD spectrum, obtaining the STDD experiments. For branched pentasaccharide [α-NeuNAc-(2→3)-β-Gal-(1→4)-β-GlcNAc-(6→1)-β-Glc-(4→1)-β-Gal] increasing saturation times from 0.5 up to 5.0 sec were applied to avoid overseeing of possible bias in the calculation of STD effects due to the different proton longitudinal relaxation times (T_1), as well as the intramolecular spin diffusion within the bound state.

2.21. NMR sample preparation

mAb were exchanged in the working buffer (Tris d-11 50 mM in D_2O at pH 8.0 +/- 0.1) through 2mL Zeba Spin desalting column saturated with 3 cycles of working buffer, mAb were finally eluted at the same starting concentration of 1mg/ml. The 100% of recovery was assessed through microBCA spectrophotometric assay. All saccharides used [DP3, DP2, fragments **1-3** or desialylated pentasaccharide (DP1)] were desalted, quantified, dried and then dissolved in the working buffer too. mAb final concentration in the NMR tube was of 4uM. Ligand (saccharides): mAb ratios were set from 1:15 up to 1:100 mol/mol, depending on samples.

2.22. Protein crystallization

Rabbit Fab NVS-1-19-5 was purified in 20 mM Tris·HCl, 150mM NaCl, pH 8.0, and concentrated to 20 mg/mL using centrifugal filter devices with a 10 kDa cutoff membrane (Amicon Ultra; Millipore). The complex of DP2 oligosaccharide with the Fab NVS-1-19-5 was prepared by incubation at RT with a molar ratio saccharide/Fab 10:1. Crystallization experiments were performed using a sitting-drop vapor-diffusion format at 295 K, by mixing equal volumes (200 nL) of the complex with crystallization reservoir solutions using a Crystal Gryphon liquid handling robot (Art Robbins Instruments). Crystals were obtained after 48 hours using a reservoir made of 0.1 M Cadmium chloride hemi (pentahydrate), 30% (v/v) PEG 400, and 0.1 M sodium acetate, pH 4.6 (Structure Screen 1 & 2 HT-96; Molecular Dimensions). All crystals were mounted in cryoloops, and flash-cooled in liquid nitrogen for subsequent data collection at 100 K.

2.23. Structure determination

X-ray diffraction data were collected at the ESRF (Grenoble, France), on beamline ID30A-1 (MASSIF-1), and using a Pilatus 2M detector. Data were indexed and processed using XDS[3], and the CCP4 program suite[4]. Crystals belonged to space group $C222_1$, with the asymmetric unit containing two Fab-DP2 complexes. The structure of the complex was determined by molecular replacement in Phaser[5], using as template model coordinates the structure of rabbit Fab R56 (PDB code 4JO1). Refinement and manual model building were performed using Phenix[6], BUSTER[7] and COOT[8]. Structure quality was assessed using Molprobity[9]. Figures were generated using PyMOL (http://www.pymol.org). Data collection and refinement statistics are reported in Table 5.5.

2.24. References

1. Wessels MR, et al. Immunogenicity of a polysaccharide-protein conjugate vaccine against type III Group B *Streptococcus. J. Clin. Invest.* **86**, 1428-1433 (1990).
2. Fabbrini M et al. A new flow-cytometry-based opsonophagocytosis assay for the rapid measurement of functional antibody levels against Group B Streptococcus. *J. Immunol. Methods.* **378(1-2)**, 11-19 (2012)
3. Kabsch W. XDS. *Acta Crystallogr. D Biol. Crystallogr*. **66(2)**, 125–132 (2010).
4. Collaborative Computational Project, Number 4. The CCP4 suite: programs for protein crystallography. *Acta Crystallogr D Biol Crystallogr.* **50(5)**, 760–763 (1994).
5. McCoy AJ et al. Phaser crystallographic software. *J. Appl. Cryst.* **40(4)**, 658–674 (2007).
6. Adams PD et al. PHENIX: a comprehensive Python-based system for macromolecular structure solution. *Acta Crystallogr. D. Biol. Crystallogr.* **66(2)**, 213–221 (2010).
7. Bricogne G, Blanc E, Brandl M, Flensburg C, Keller P, Paciorek W, Roversi P, Sharff A, Smart OS, Vonrhein C, Womack TO. BUSTER v.2.11.4. Cambridge: Global Phasing Ltd. (2011).
8. Emsley P, Cowtan KCoot: Model-building tools for molecular graphics. *Acta Crystallogr. D Biol. Crystallogr.* **60(12-1)**, 2126–2132 (2004).
9. Chen VB et al. MolProbity: all-atom structure validation for macromolecular crystallography. *Acta Crystallogr. D Biol. Crystallogr.* **66(1)**, 12–21 (2010).

CHAPTER 3: PREPARATION OF SYNTHETIC GBS TYPE III FRAGMENTS

3.1. Synthesis of Group B *Streptococcus* type III polysaccharide fragments

A [2 + 3] convergent approach leading to the repeating units **1**-**3** (called linear, branched and Y-shape DP1, respectively) with the end terminal sugar bearing a linker for possible conjugation has been established[1].

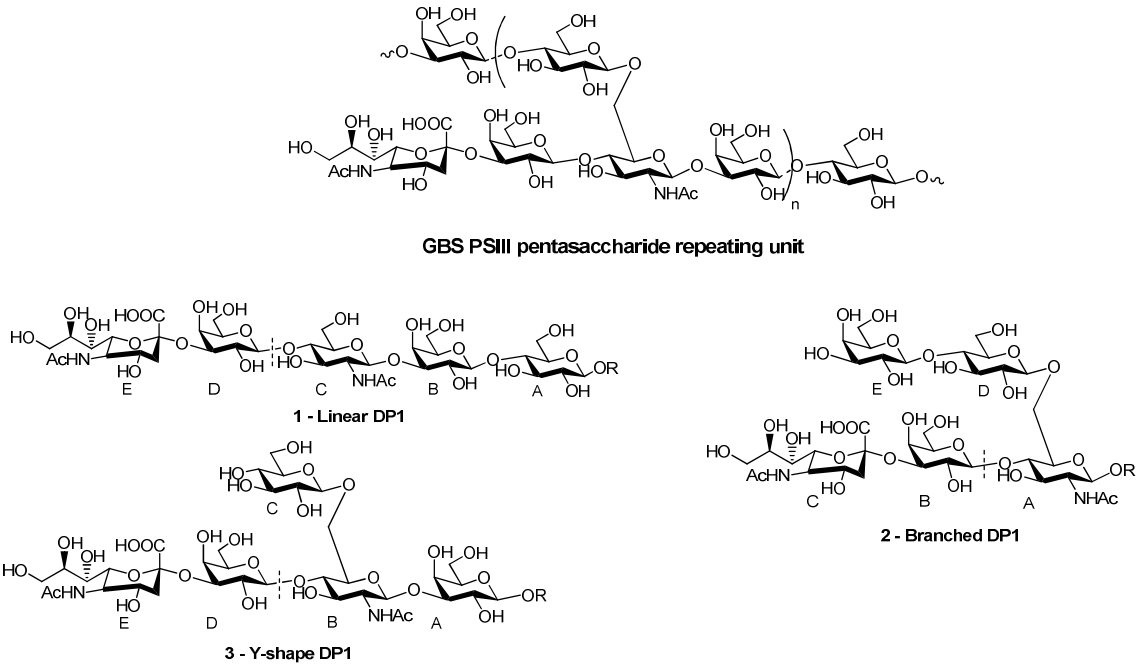

Figure 3.1. Chemical structure of PSIII and related repeating unit sequences 1-3 (linear, branched and Y-shape DP1, respectively). In our approach R was a linker suited for conjugation ($CH_2CH_2NH_2$). A [2 + 3] convergent approach was envisaged for the synthesis of these fragments.

Table 3.1. Chemical shift (ppm) of ^{1}H and ^{13}C NMR signals and 3J H_1-H_2 scalar coupling costants of linear, branched and Y-shape DP1 in D_2O[a]

		1- Linear DP1		2- Branched DP1		3- Y-shape DP1		PSIII[c]	
Residue		**^{1}H**	**^{13}C**	**^{1}H**	**^{13}C**	**^{1}H**	**^{13}C**	**^{1}H**	**^{13}C**
Gal	1	4.43 *J* 8.2 Hz	103.77	4.45 *J* 7.8 Hz	103.28	4.39 *J* 8.0 Hz	103.72	4.43	103.90
	2	3.57	70.68	3.55	71.58	3.57	70.49	3.59	70.82
	3	3.72	82.85	3.68	73.18	3.72	83.08	3.73	83.32
	4	4.16	69.05	3.93	69.48	4.16	69.16	4.17	69.06
	5	3.66	75.10	3.68	72.96	3.69	75.70	3.71	75.78
	6	3.65	63.16	3.71	61.58	3.73	62.35	3.74	61.87
	6'	3.88		3.76		3.76		3.79	
GlcNAc	1	4.69 *J* 8.2 Hz	103.72	4.52 *J* 7.8 Hz	101.98	4.71 *J* 8.0 Hz	103.63	4.70	103.97
	2	3.81	55.89	3.75	55.68	3.80	56.08	3.83	56.01
	3	3.73	72.82	3.72	74.23	3.73	73.40	3.73	72.85
	4	3.76	78.50	3.86	77.98	3.88	78.28	3.91	77.40
	5	3.72	75.69	3.72	76.02	3.73	74.38	3.73	73.90
	6	3.95	68.18	4.00	68.18	3.97	68.51	3.98	68.22
	6'	3.95		4.31		4.30		4.29	
Glc	1	4.50 *J* 8.5 Hz	102.74	4.55 *J* 7.8 Hz	103.00	4.52 *J* 8.0 Hz	103.66	4.54	103.44
	2	3.32	73.51	3.37	73.35	3.31	73.88	3.36	73.42
	3	3.64	75.38	3.67	75.15	3.52	76.78	3.67	75.12
	4	3.65	78.58	3.67	78.75	3.40	70.78	3.67	79.23
	5	3.66	75.38	3.68	75.54	3.53	76.58	3.67	75.53
	6	3.81	60.62	3.84	60.73	3.73	61.38	3.81	60.86
	6'	3.96		3.99		3.93		4.00	
Gal_s[b]	1	4.56 *J* 9.0 Hz	103.00	4.61 *J* 7.6 Hz	102.78	4.62 *J* 7.8 Hz	102.95	4.62	102.87
	2	3.57	70.22	3.56	69.89	3.57	70.28	3.57	70.23
	3	4.12	76.18	4.10	75.93	4.10	76.48	4.10	76.59
	4	3.92	68.78	3.96	68.27	3.97	68.40	3.97	68.43
	5	3.71	75.56	3.67	75.33	3.70	76.08	3.69	75.85
	6	3.74	61.85	3.71	61.80	3.73	61.78	3.74	61.76
	6'	3.71		3.75		3.76		3.77	
NeuNAc	3	2.76	40.35	2.76	40.36	2.76	40.38	2.76	40.47
	3'	1.80		1.83		1.82		1.82	
	4	3.68	69.05	3.67	69.30	3.68	69.38	3.69	69.21
	5	3.85	52.36	3.85	52.34	3.85	52.58	3.86	52.50
	6	3.62	73.70	3.63	73.60	3.64	74.05	3.66	73.80
	7	3.65	68.78	3.60	69.05	3.60	69.25	3.31	68.82
	8	3.87	72.59	3.87	72.45	3.88	72.70	3.89	72.65
	9	3.88	63.27	3.86	63.18	3.87	63.54	4.43	63.41
	9'	3.65		3.66		3.66		3.59	

a. NMR experiments were carried out on a Bruker 500 MHz NMR instrument equipped with a TBI cooled probe at controlled temperature (± 0.1 K). Data acquisition and processing were performed using TOPSPIN 1.3 and 3.1 software, respectively.

b. Gal_s refers to the residue linked to NeuNAc.

c. These values were taken from ref 2.

As shown in Table 3.1, the ^{1}H and ^{13}C chemical shifts for the signals of the synthesized fragments were in excellent agreement with literature NMR data for PSIII and different length fragments[2].

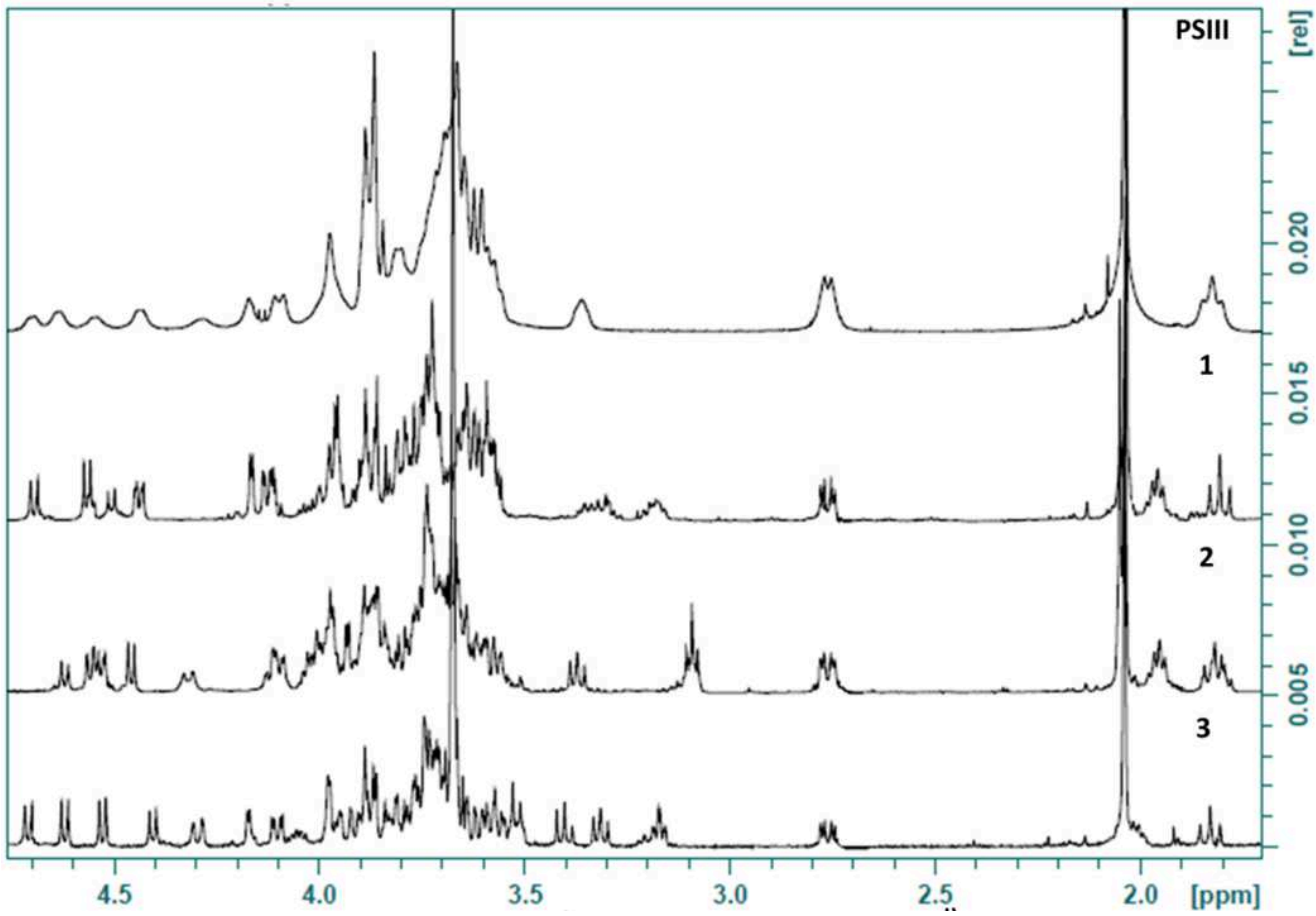

Figure 3.2. ^{1}H NMR spectra of pentasaccharides 1-3 in comparison to PSIII in Tris buffer pH 7 (D_2O, 500MHz, 298 k)

Antibody recognition of linear, branched and Y-shape DP1 by ELISA

To confirm that the synthesized fragments could be used to study the interactions with PSIII specific mAbs, reactivity to the fragments with polyclonal anti-PSIII Abs was confirmed. To this end, linear, branched and Y-shape DP1 were first conjugated to CRM_{197}, by treatment with an excess di-N-hydroxysuccinimidyl adipate (Figure 3.3)[3]. The isolated half esters were incubated with the protein in sodium phosphate buffer at

pH 7.2. The amount of coupled glycan was proportional to the active ester used in conjugation (Table 3.2). Thus the use of 15 equivalents led to incorporation of an average of 3 glycan moieties; when 75 equivalents were used the level of carbohydrate incorporation was increased to 24-27 mol/mol of protein.

After purification by dialysis against sodium phosphate buffer, the glycoconjugates **35-37** were characterized by 4-12% sodium dodecylsulfate polyacrylamide gel electrophoresis (SDS-PAGE) and MALDI TOF MS for the estimation of the carbohydrate/protein molar ratio (Figure 3.4a,b and Table 3.2), and by microBCA for the protein content quantification. The degree of carbohydrate incorporation was corroborated by quantification of Gal present in the conjugated saccharide through high-performance anion-exchange chromatography coupled with pulsed amperometric detection (HPAEC-PAD)[4].

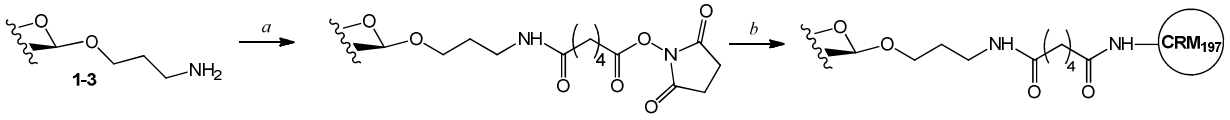

Figure 3.3. Reagents and conditions. *a*. Di-N-hydroxusuccinimidyl adipate, triethylamine, DMSO; *b*. 100mM sodium phosphate pH 7.2.

Table 3.2. Attributes of the synthesized glycoconjugates.

Glycoconjugate	mol NHS/ mol protein	Protein conc. (µg/mL)	Sacch. conc. (µg/mL)	Average n° of saccharide chains per protein
CRM_{197}-DP1 linear **35**	15:1	1428	75	3.1
CRM_{197}-DP1 branched **36a**	15:1	1268	64	3.0
CRM_{197}-DP1 branched **36b**	75:1	1035	409	23.0
CRM_{197}-DP1 Y-shape **37**	75:1	1518	700	26.9

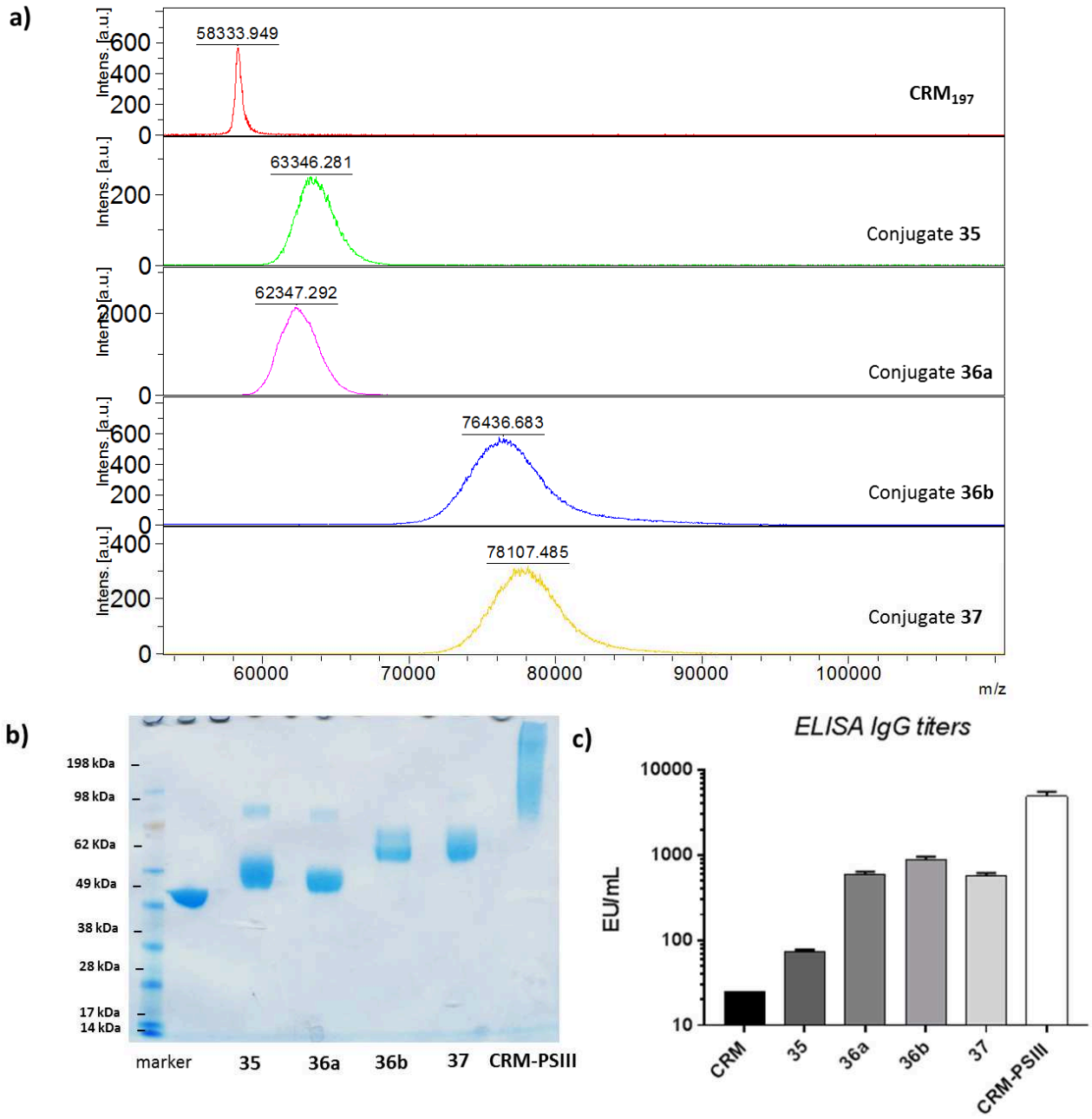

Figure 3.4. **a)** MALDI TOF spectra of synthesized glycoconjugates **35-37**; **b)** SDS-PAGE gel electrophoresis of glycoconjugates **35-37** and **c)** anti-PSIII IgG titers measured by ELISA using glycoconjugates **35-37** for coating. Anti-PSIII murine serum was raised with the polysaccharide conjugated to a GBS pilus protein; CRM_{197} and PSIII-CRM_{197} conjugate were the controls.

Next, the glycoconjugates were used to measure by ELISA specific antibodies present in the anti-PSIII murine serum generated by immunization with the polysaccharide conjugated to a GBS pilus protein (Figure 3.4c). The conjugated compounds of branched and Y-shape DP1 (**36-37**), presenting a Glc residue β-(1,6) linked to GlcNAc, exhibited the highest binding. The recognition of branched DP1 appeared independent from its level of incorporation in the obtained glycoconjugates **36a,b**. On the opposite, the conjugated linear DP1 **35** was recognized ~10-fold lower than branched and Y-shape, and only slightly better than the

negative control CRM_{197}. As expected, the highest level of anti-PSIII antibodies was detected for the positive control PSIII-CRM_{197} (6-10-fold higher than **36**-**37**). In sum, these data indicated that the presence of the branch is a structural relevant motif for the recognition of anti-PSIII antibodies.

3.3. References

1. Cattaneo V, Carboni F, Oldrini D, De Ricco R, Donadio N, Margarit I, Berti F, Adamo R. Synthesis of *Group B Streptococcus* type III polysaccharide fragments for evaluation of their interactions with monoclonal antibodies. *Pure and Applied Chemistry (waiting for publication).*
2. Brisson JR, Uhrinova S, Woods R, van der Zwan JM, Jarrell HC, Paoletti LC, Kasper DL, Jennings HJ. NMR and molecular dynamics studies of the conformational epitope of the type III *Group B Streptococcus* capsular polysaccharide and derivatives. *Biochemistry* **36**, 3278-3292 (1997).
3. Adamo R, Romano MR, Berti F, Leuzzi R, Tontini M, Danieli E, Cappelletti E, Cakici OS, Swennen E, Pinto V, Brogioni B, Proietti D, Galeotti CL, Lay L, Monteiro MA, Scarselli M, Costantino P. Phosphorylation of the synthetic hexasaccharide repeating unit is essential for the induction of antibodies to *Clostridium difficile* PSII cell wall polysaccharide. *ACS Chem. Biol.* **17**, 1420–1428 (2012).
4. A Nilo, L Morelli, I Passalacqua, B Brogioni, M Allan, F Carboni, A Pezzicoli, D Maione, M Fabbrini, MR Romano, QY Hu, I Margarit, F Berti, R Adamo. Anti-*Group B Streptococcus* glycan-conjugate vaccines using pilus protein GBS80 as carrier and antigen: comparing lysine and tyrosine-directed conjugation. *ACS Chem. Biol.* **10**, 1737–1746 (2015).

CHAPTER 4: PREPARATION OF SEMI-SYNTHETIC GBS TYPE III FRAGMENTS

4.1 Depolymerization and activation of native GBS type III

For the production of GBS III oligosaccharides, the depolymerization approach reported in the paper of Michon of 2006[1] has been used (Figure 4.1).

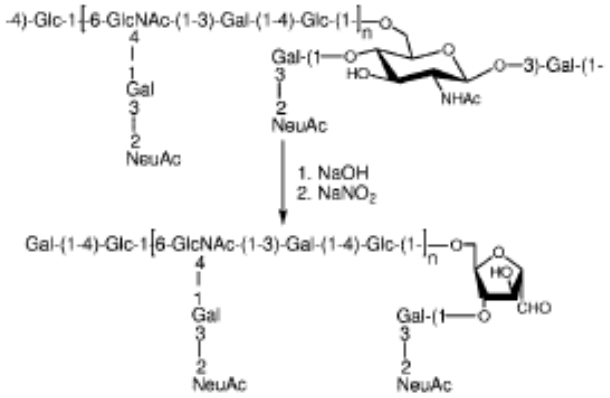

Figure 4.1. Deaminative cleavage of GBS type III polysaccharide[1].

The polysaccharide was partially N-deacetylated in 0.5M NaOH at 70°C. The resulting N-deacetylated glucosamine residues in the backbone were then susceptible to nitrosation with nitrous acid and acetic acid to form an unstable N-nitrosoamine. The subsequent deaminative cleavage resulted in the production of fragments having terminal aldehyde groups. Smaller fragments could be obtained by increasing the time of the N-deacetylation reaction.

N-reacetylation of the fragment was carried out to ensure that all the sialic acid residues were acetylated at the end of the depolymerization.

In order to obtain oligosaccharides with defined composition, an ionic exchange chromatography method was developed. Taking advantage of the negative charge of NeuNAc moities, a semi-preparative HPLC with a MonoQ column was used. Increasing the sodium chloride concentration in the elution buffer, using a staircase gradient, fragments of different length were resolved. As shown in Figure 4.2, each peak of the chromatogram corresponded to a subpopulation of saccharides, the shortest fragments of which were eluted first.

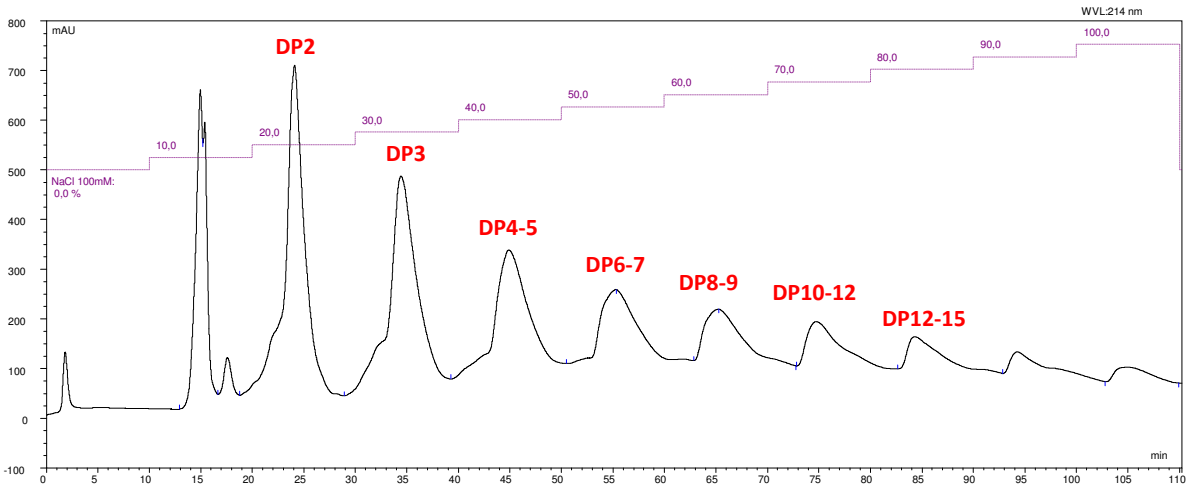

Figure 4.2. Purification of different length oligosaccharides. Mono Q anion-exchange column chromatography of depolymerized GBS PS III

Comparison of the 500 MHz ^{1}H NMR spectra of the type III fragments with those of the native GBSIII polysaccharide indicated that no structural change had occurred during the chemical processes and, most importantly, that terminal sialic acid residues had been preserved during the nitrosation treatment process.
The length of the purified oligosaccharides was determined by integrating NMR analysis, HPLC-HPAED and MALDI TOF MS. The aldheyde proton signal at 5.10 ppm (highlighted in Figure 4.3B), that appears in the form of emiacetal in the NMR spectrum of depolymerized GBSIII, can be diagnostic to determine the ratio of the terminal 2,5-anhydro-D-mannose residue (blue in Figure 4.3A), generated during the depolymerization reaction, compared to the other sugars of the saccharide. In particular, the H-3e (i.e. equatorial) position of NeuNAc at 2.75ppm and the H-2 position of Glc at 3.35ppm were preferred for oligosaccharide length determination due to their higher resolution in respect to other carbohydrate signals.

A

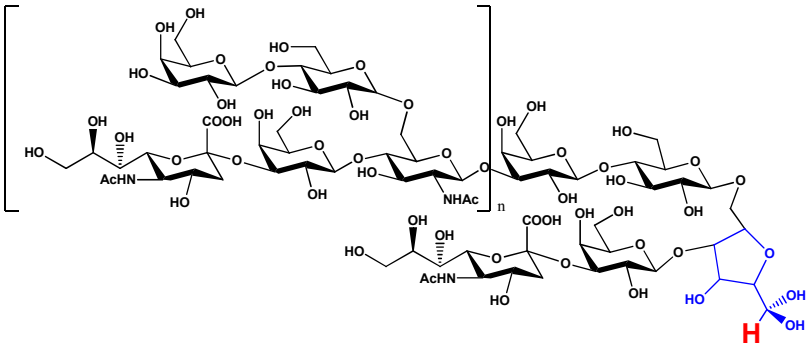

B

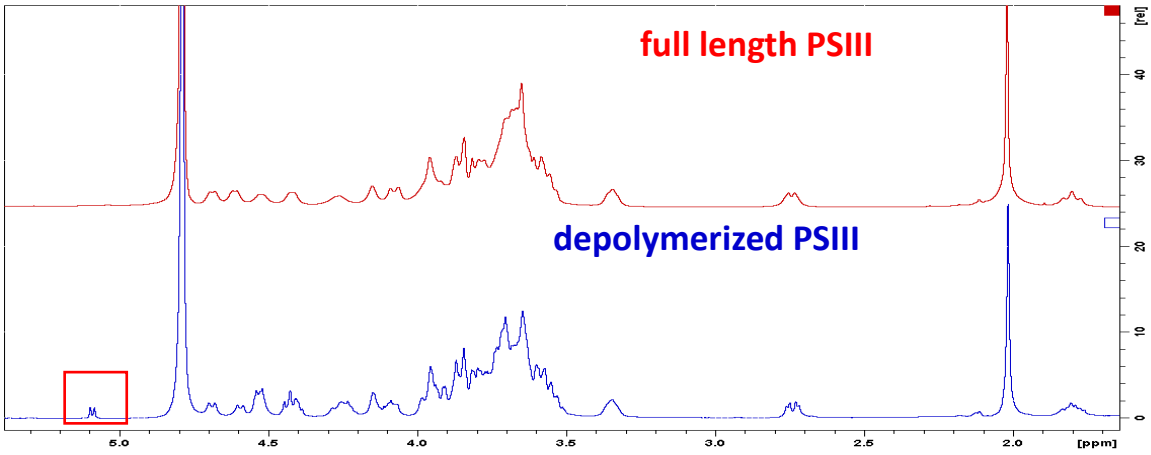

Figure 4.3. Assessment of PSIII depolymerization. (A) Chemical structure of GBSIII fragments. The 2,5-anhydri-D-mannose residue obtained during the chemical depolymerization of PSIII is indicated in blue. (B) NMR spectra of the full length (in red) and depolymerized (in blue) PS III.

Based on these data, generated fragments were called DP2 (Degree of Polymerization 2), DP3, etc. To clarify what it means Degree of Polymerization for the obtained oligosaccharides, it should be highlighted that all the fragments obtained using this degradative procedure contained complete RUs of GBSIII, plus an appendage consisting of a terminal modified RU. Then, i.e. DP2 (Figure 4.4) contains 1 complete RU (highlighted by a red box) and 1 modified RU (the remained five sugars).

A

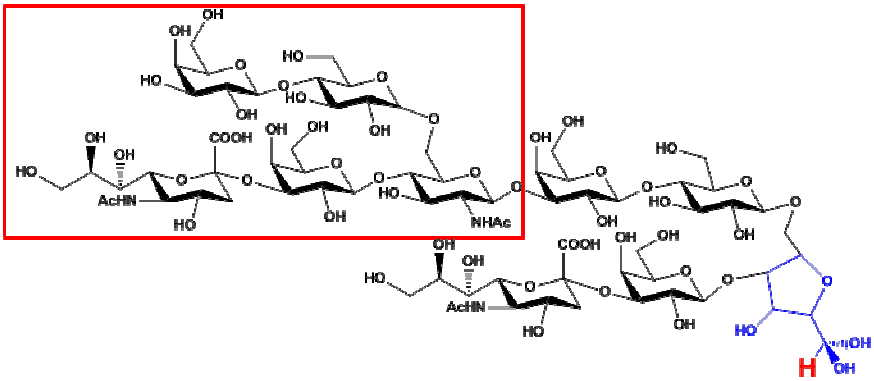

B

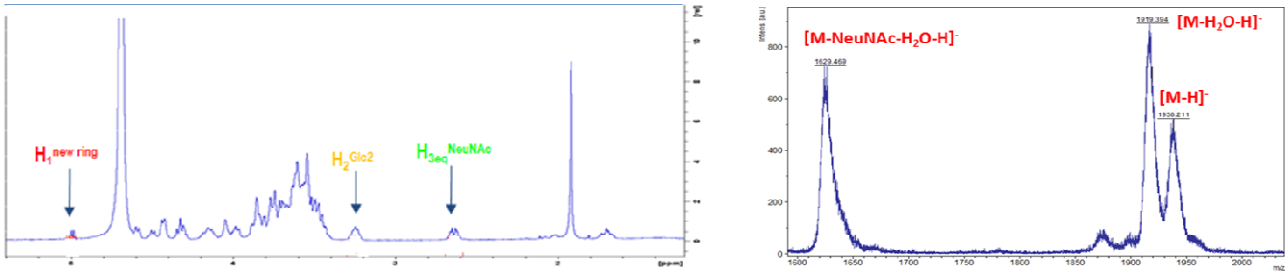

Figure 4.4. GBSIII DP2 oligosaccharide. (A) Chemical structure of DP2 with the complete repeating unit within the red box. (B) Length determination of DP2 by NMR and MALDI-TOF (in negative mode) spectra.

To determine the mass of the first eluted peak and assess the homogeneity of this sample, MALDI-TOF MS has been used. Sialic acid is preferentially lost during mass spectrometric investigations[2-3]. 2,5-Dihydroxybenzoic acid has been reported to be preferable to α-cyano-4-hydroxycinnamic acid as matrix in the analysis of gangliosides, because it minimizes loss of sialic acid[4]. Analysis of DP2 (Figure 4.4B) and DP3 with this matrix were performed in negative mode, and the OSs length previously obtained by NMR was confirmed. The MS spectrum of DP2 is shown in Figure 4.4B: mass peaks correspond to the entire saccharide and to a fragment deriving from the loss of one water molecule and one sialic acid residue.

MS analysis proved that DP2 and DP3 are homogeneous fragments, whereas for longer OSs no proof of homogeneity was achieved. Therefore these OSs are indicated as average Degree of Polymerization (avDP). Due to the progressive overlapping of the peaks in the chromatography profile, it has been assumed that the sample homogeneity decreases as the size of the fragments increases.

To corroborate the integrity of the obtained DP2 and DP3 observed by NMR analysis, HPAEC-PAD analysis was performed with a Dionex ICS3000 equipped with a CarboPac PA1 column. PSIII was used as control. The relative ratio of the different sugars composing the polymer was determined (Table 4.1), indicating that no significant loss of sialic acid during the depolymerization was produced. Considering that

one GlcNAc residue was lost in the entire molecule (the one that was become a 2,5-anhydro-D-mannose residue during the reaction), the length of the oligosaccharide was estimated using the formula:

$$DP = [X] / ([X]-[GlcNAc])$$

where [X] represents the concentration of Glc or half of the concentration of Gal. DPs estimated (Table 4.1) by this method were in good agreement with the length assessed through NMR and MS analysis.

Table 4.1. **HPAEC-PAD quantification of monosaccharide components and relative length estimation.**

Sample	GlcNAc µmol/mL	Glc µmol/mL	Gal µmol/mL	NeuNAc µmol/mL	DP calculated by GlcNAc
DP2	7.71	13.79	30.75	12.91	2.1
DP3	9.81	14.86	29.46	14.31	3.0
PSIII	5.86	5.97	12.06	5.83	n.a.

4.2. Conjugation of GBSIII fragments to CRM_{197}

The aldehyde group in the resulting 2,5-anhydro-D-mannose residue formed following deamination at the reducing end of the polysaccharide fragment represents a useful handle for conjugation and was utilized, without further chemical manipulation, for reductive amination with the amines of the CRM_{197}. The resulting glycoconjugates contained saccharide chains attached radially to the carrier protein through the end terminal residue. This conjugation chemistry was different from that used for the native PSIII where 20% of sialic acid residues were chemically activated by $NaIO_4$ oxidation of the glycerol side chain before the reductive amination to the carrier, resulting in a cross-linked structure (Figure 4.5).

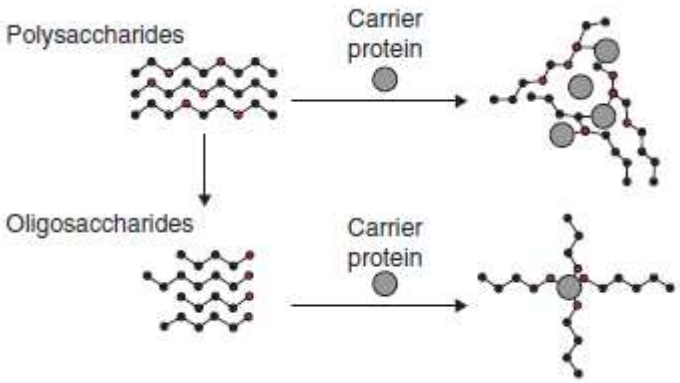

Figure 4.5. Schematic representation of different poly/oligosaccharide-protein chemical couplings[5].

Purification of the final glycoconjugates was performed by chromatography on hydroxyapatite, and tuning of the phosphate buffer concentration used for elution enabled the separation of the glycoconjugate from the unconjugated polysaccharide and protein. Saccharide and protein concentration were obtained by HPAEC-PAD and BCA analysis respectively. The biochemical characteristics of a series of such type III single-ended oligosaccharide glycoconjugates varied in the size of their oligosaccharide and in the saccharide:protein ratio (average number of saccharide chains per protein or glycosylation degree) as it can be seen in Table 4.2.

Table 4.2. Biochemical characteristics of GBS type III conjugate vaccines.

	Name	Protein concentration (µg/mL)	Sacch. Concentration (µg/mL)	Average n° of saccharide chains per protein
1	**CRM-DP2**	1122	140	3.5
2	**CRM-DP2**	535	160	9.0
3	**CRM-DP3**	383	44	2.0
4	**CRM-DP3**	484	130	4.5
5	**CRM-DP5**	639	159	3.0
6	**CRM-DP5**	349	161	5.5
7	**CRM-DP6,5**	456	79	1.5
8	**CRM-DP6,5**	289	110	3.5
9	**CRM-DP11**	531	235	2.3

The conjugates were controlled before and after the purification step through SDS-PAGE analysis.

For some glycoconjugates (n°1, 3, 4, 5, 8 in Table 4.2), the glycosylation degree was confirmed by mass spectrometry analysis at MALDI-TOF instrument (Figure 4.6). The average molecular weight obtained by

MS fits perfectly with the estimated number of saccharide chains per protein. It has been unfeasible to analyze by MS glycoconjugates obtained with longer structures.

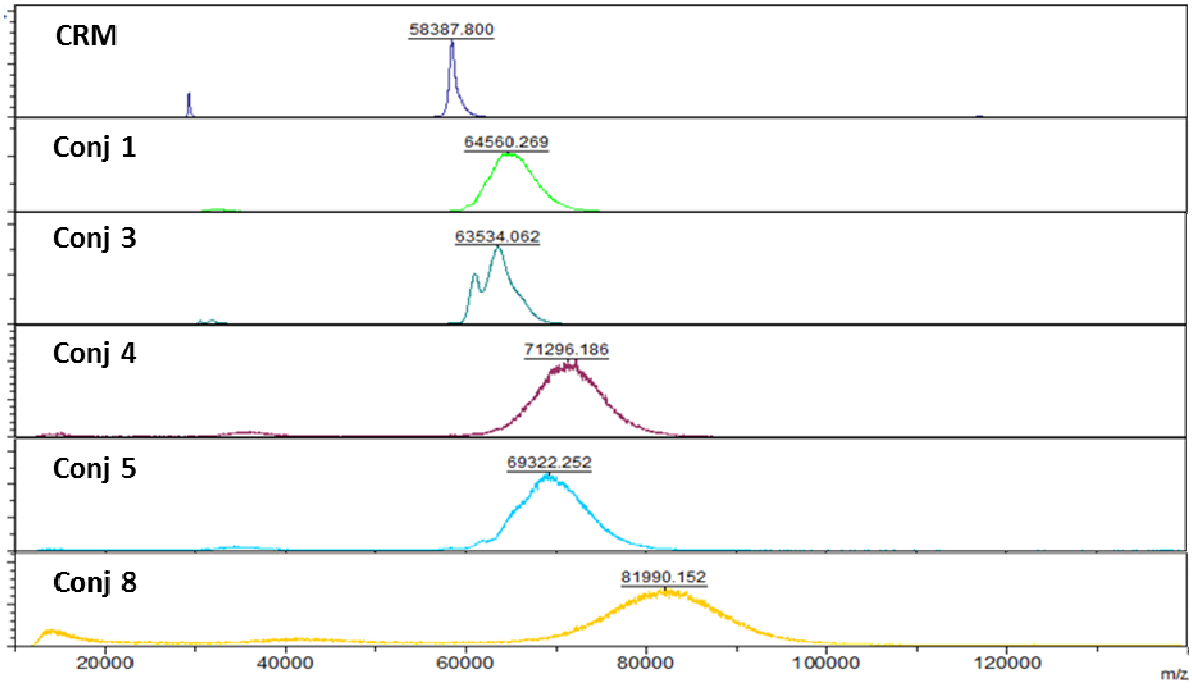

Figure 4.6. Characterization of the GBS type III conjugate vaccines. MALDI TOF spectra of some CRM conjugates

4.3. References

1. Michon F et al. Group B Streptococcal type II and III conjugate vaccines: physicochemical properties that influence immunogenicity. *Clin. Infect. Dis.* **13**, 936–943 (2006).
2. Tsarbopoulos A, Bahr U, Pramanik BN, Karas M. Glycoprotein analysis by delayed extraction and post-source decay MALDI-TOF-MS. *Int. J. Mass Spectrom. Ion Processes* **169/170**, 251-261 (1997).
3. Harvey D. Matrix-assisted laser desorption/ionization mass spectrometry of carbohydrates. *J. Mass Spectrom. Rev.* **18**, 349-451 (1999).
4. Sugiyama E, Hara A, Uemura K,Taketomi T. Application of matrix-assisted laser desorption ionization time-of-flight mass spectrometry with delayed ion extraction to ganglioside analyses. *Glycobiology* **7(5)**, 719-724 (1997).
5. Costantino P, Rappuoli R, Berti F. The design of semi-synthetic and synthetic glycoconjugate vaccines *Expert Opin. Drug Discov.* **6 (10)**, 1045-1066 (2011)

CHAPTER 5

Revisiting the concept of conformational epitope of Group B *Streptococcus* type III capsular polysaccharide

Filippo Carboni, Roberto Adamo, Monica Fabbrini, Riccardo De Ricco, Vittorio Cattaneo, Barbara Brogioni, Daniele Veggi, Vittoria Pinto, Irene Passalacqua, Davide Oldrini, Rino Rappuoli, Enrico Malito, Immaculada Margarit y Ros, Francesco Berti

5.1. Introduction

Bacterial cell surface carbohydrates are the interface of multiple host interactions and have been targeted to develop highly efficacious glycoconjugate vaccines against severe infections caused by *Streptococcus pneumoniae*, *Haemophilus influenzae* type b and *Neisseria meningitidis*[1,2]. Glycoconjugate vaccines against other important pathogens are under clinical or pre-clinical development[2].

Mapping of the epitopes recognised by functional antibodies mediating protection from infection is crucial for understanding the mechanism of action of this type of vaccines, as well as for antigen optimization and for the development of immunochemical assays. In many cases the antigenic portion responsible for the immunological properties of the polysaccharide (PS) and the structural details of the minimal epitope targeted by specific functional antibodies are unknown[3].

Minimal epitopes can be composed of short defined glycans comprising 2-3 monosaccharides, as for the β-(1→2) mannans from *Candida albicans* cell wall, *V. Cholerae* O1[4] or *Shighella flexeneri* variant Y[5] and *Salmonella*[6] O-antigens, up to a tetrasaccharide, as for the repeating unit of *Streptococcus pneumoniae* type 14 PS (Pn14),[7,8] and even six sugar residues, as in the case of *Shighella flexneri* serotype 2a O-antigen[33]. In contrast, the type III polysaccharide of *Streptococcus agalactiae* (Group B *Streptococcus*,'GBS') has been proposed as a prototype of a unique length-dependent conformational epitope[9].

GBS is an encapsulated Gram-positive β-hemolytic pathogen causing neonatal sepsis and meningitis, particularly in infants born to mothers carrying the bacteria[10]. The GBS capsular PS is constituted by multiple repeating units (RU, from about 50 to 300 per polymer) of four to seven monosaccharides shaped to form a backbone and one or two side chains. Ten serotypes presenting a unique pattern of glycosidic linkages have been identified and their structures elucidated[10,11]. Three monosaccharides (i.e. β-D-glucopyranose (β-D-Glc*p*), β-D-galactopyranose (β-D-Gal*p*), and α-D-N-acetylglucosamine (β-D-Glc*p*NAc)) are present in all the described serotypes, and sialic acid (α-N-acetyl-Neuraminic acid, NeuNAc) is always found at the terminus of one chain[10,11]. Maternal concentrations of antibodies directed to the different GBS capsular serotypes inversely correlate with the risk of newborn infection[12], suggesting that antibodies able to cross the placenta confer serotype-specific infant protection[13]. PS conjugates of different serotypes elicit

antibodies which mediate the GBS serotype specific opsonophagocytic killing in functional assays and protection against GBS challenge in neonate mice [14-18]. Furthermore, Ia, Ib, III, II and V monovalent vaccines, as well as a trivalent combination against types Ia, Ib and III, proved to be safe and immunogenic in non-pregnant and pregnant women, and maternal antibodies were transferred to neonates[19-21].

GBS strains belonging to the serotype III (GBSIII) are epidemiologically the most relevant in neonatal infections[22]. Pioneering immunological studies aimed at elucidating type III specific antigenic determinants indicated the presence of the terminal NeuNAc residue as essential for the elicitation of protective antibodies[23]. Subsequent studies revealed that sera from rabbits immunized with GBSIII bacteria and from humans vaccinated with PSIII conjugates contained two types of anti-carbohydrate antibodies, i.e. a major population recognizing the native polysaccharide but not its incomplete core antigen derivative lacking sialic acid (corresponding to the Pneumococcus PS Pn14), plus a variable population reacting with both the native PSIII and the core antigen[24,25]. Remarkably, both types of human PSIII-induced antibodies were shown to mediate GBSIII opsonophagocytic killing (OPK), while antibodies elicited by Pn14 (desialylated PSIII) did not recognize GBSIII bacteria and therefore did not mediate GBS killing[21].

Subsequent ^{13}C NMR spectroscopy studies highlighted ring-linkage signal displacements in the core versus the native PS, suggesting that NeuNAc residues exert a specific conformations over the native polysaccharide[24,26]. Molecular dynamics simulations confirmed a more flexible and disordered structure for desialylated PSIII, and suggested that native PSIII could form extended helical structures whose turn was made by more than four RUs[27-29]. PSIII fragments smaller than four RUs appeared as weak inhibitors of the binding of native PSIII to its specific antibodies, and failed to elicit an efficient immune response following conjugation[30].

Based on the above observations, it was concluded that the native PSIII forms a sialic acid-dependent conformational epitope that is essential for the elicitation and recognition of functional antibodies; the length dependency of this conformational epitope was ascribed to its localization on extended helices within a random coil structure[30]. According to the proposed model, the side chain NeuNAc moiety would exert a remote control over immunological determinants of the PS backbone, without being a direct part of the epitope[31].

A structural glycobiology approach of bacterial oligosaccharides in complex with functional monoclonal antibodies (mAbs) able to protect against the target pathogen, could represent the most direct methodology to gain information on PS immunological determinants at atomic level. However, due to the high polarity of the hydroxyl groups and flexibility of the carbohydrate structures[32], crystallization of carbohydrate-protein complexes is a challenging task. To date only a very limited number of carbohydrate antigen-Fab complexes have been resolved by X-ray crystallography[4-6,33]. As alternative, a combination of different techniques (NMR, Surface Plasmon Resonance (SPR), Isothermal Titration Calorimetry (ITC), glycoarray, competitive ELISA) is typically used to gain insights on carbohydrate-protein interactions and to map the binding regions[3,34-36].

In the present study we used STD-NMR and X-ray crystallography to investigate the interaction of GBSIII oligosaccharides obtained by synthetic and depolymerization procedures, with a protective monoclonal antibody.

5.2. Results

5.2.1. Selection and immunochemical characterization of a functional anti-PSIII rabbit monoclonal antibody

To investigate the binding of GBS PSIII to functional antibodies at atomic level and further decipher the role of the NeuNAc moiety, we first generated a rabbit anti-PSIII monoclonal antibody (mAb) capable of mediating GBS opsonophagocytic killing. Similarly to a previous report[20], rabbits immunized with native PSIII conjugated to genetically detoxified Diphteria Toxin (CRM_{197}) developed two types of antibodies differing in their capacity to bind the PSIII desialylated core antigen in addition to the native polysaccharide. Indeed, inhibition ELISA experiments showed that binding of IgG from rabbit sera to immobilized PSIII unconjugated (Figure 5.1) or conjugated to HSA[37] (Figure 5.2a) could be partially blocked by pre-incubation with soluble Pn14 or desialylated PSIII. Pn14 also partially inhibited antibody-mediated GBSIII OPK (Figure 5.2b), confirming functional activity of both types of NeuNAc dependent and independent rabbit antibodies. Similar results were described previously in the case of human responses to GBSIII[21].

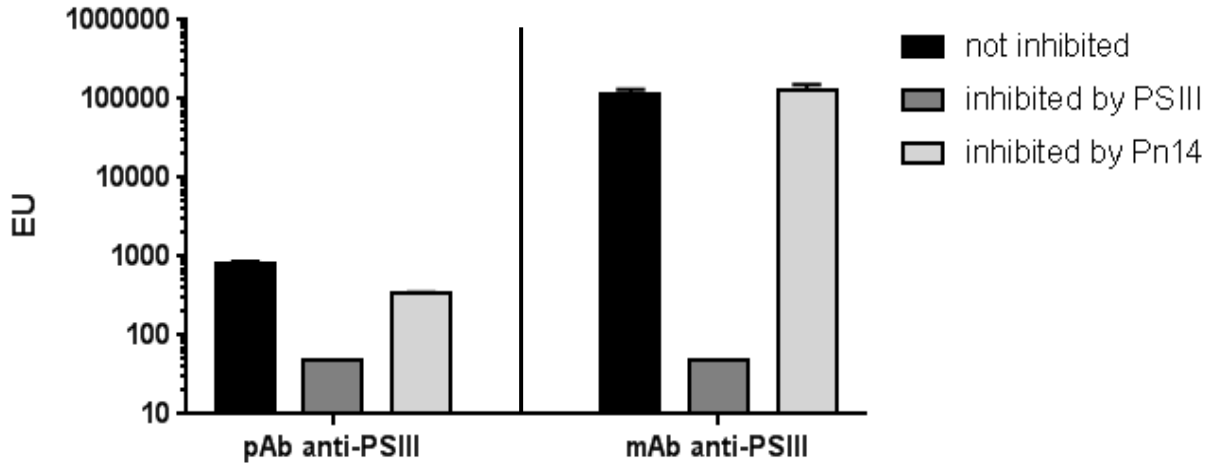

Figure 5.1. Antibody specificity toward PSIII. Inhibition ELISA binding of rabbit sera to immobilized PSIII unconjugated by pre-incubation with PSIII and Pn14.

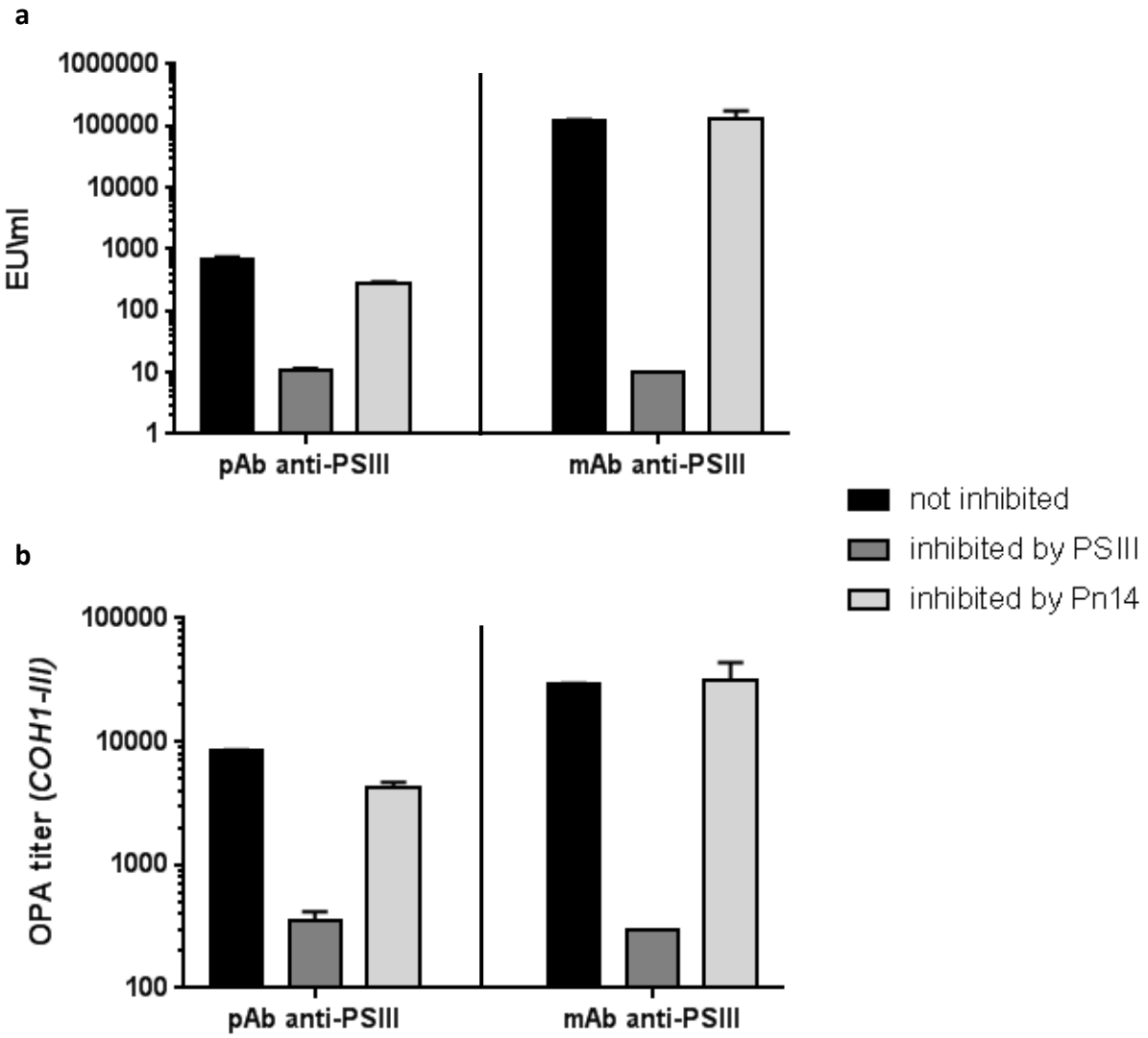

Figure 5.2. Antibody specificity toward PSIII. Inhibition experiments with PSIII and Pn14 of rabbit anti-PSIII pAb and anti-PSIII mAb in (a) ELISA binding immobilized PSIII conjugated to HSA and (b) OPK.

An IgG1 mAb was selected by hybridoma cell line technology (NVS-1-19-5), for which functional activity was ascertained by OPKA (OPK titer: 1.03µg/mL). Complete inhibition by native PSIII and absence of inhibition by Pn14 in ELISA and OPKA experiments (Figure 5.2a and 5.2b) confirmed that the epitope recognized by this mAb was sialic acid-dependent. A Fab fragment of mAb NVS-1-19-5 was then prepared by papain proteolytic cleavage, and high affinity binding towards the GBS PSIII was measured by SPR (K_D estimated with the Fab 6×10^{-8} M).

The NeuNAc-Gal covalent link in the lateral chain of the PSIII repeating unit is the more chemically labile glycosidic bond within the polysaccharide, and complete loss of NeuNAc residues or reduction of their carboxylic groups results in polysaccharide structures incapable of inducing functional antibodies[24]. To investigate the potential of the obtained mAb for probing the integrity of the PSIII antigen, we subjected

PSIII-CRM$_{197}$ to mild acid hydrolysis for different incubation times and obtained conjugates with decreasing sialylation levels of 100, 60-70, 20-30 and <5%, as estimated by NMR analysis (Figure 5.3 and Table 5.1).

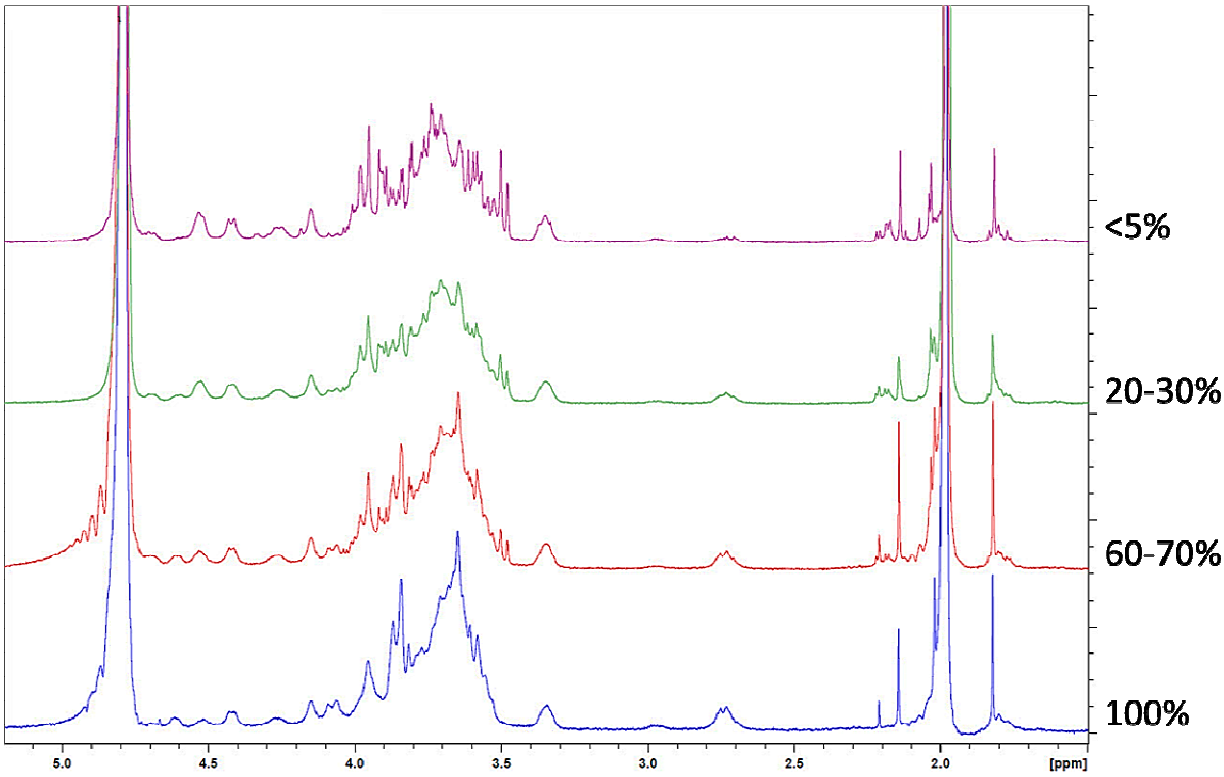

Figure 5.3. Estimation of desialylation level. ^{1}H NMR spectra of PSIII-CRM$_{197}$ at different reaction times (Table 5.1).

Table 5.1. Percentage of bound sialic acid content estimated by ^{1}H NMR.

Reaction Time (h)	0	6	24	72
% NeuNAc$^{\text{in chain}}$	100	60-70	20-30	<5.0

The resulting glycoconjugates were characterized for their structural integrity and saccharide/protein content (Figure 5.4 and Table 5.2).

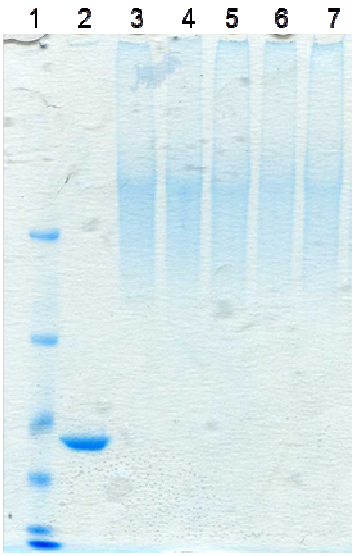

SDS-Page 3-8%

1. MW
2. CRM_{197}
3. CRM_{197}-III Ref. Vaccine
4. CRM_{197}-III 100%
5. CRM_{197}-III 70-80%
6. CRM_{197}-III 20-30%
7. CRM_{197}-III <5%

Figure 5.4. Gel electrophoresis of CRM_{197} PSIII conjugates. SDS-Page 3-8% Tris acetate gel of desialylated PSIII-CRM_{197} at different reaction times (Table 5.1).

Table 5.2. Saccharide and protein content in PSIII-CRM_{197} conjugates selected for immunization.

Sample (% bound NeuNAc)	Protein (µg/mL)	Sacch. (Gal-based) (µg/mL)	Sacch./Prot. (w/w)
PSIII-CRM_{197} 100%	695.7	837.7	1.2
PSIII-CRM_{197} 60-70%	884.6	930.2	1.1
PSIII-CRM_{197} 20-30%	785.5	768.1	1.0
PSIII-CRM_{197} <5.0%	872.0	703.8	0.8

ELISA experiments using immobilized native PSIII and, as competitor, soluble native or partially desialylated PSIII-CRM_{197} showed decreasing binding of the mAb to conjugates with increasing desialylation levels (Figure 5.5a). The capital role of the NeuNAc in elicitation of functional antibodies was confirmed by immunizing female mice with three doses of the different glycoconjugates, followed by sera analysis by ELISA for quantification of anti-PSIII and anti-Pn14 antibodies, and by OPKA to assess antibody functional activity. Lower levels of sialylation resulted in decreased recognition of HSA-conjugated native PSIII (Figure 5.5b-d), higher recognition of Pn14, and decreasing *in vitro* killing of GBS bacteria.

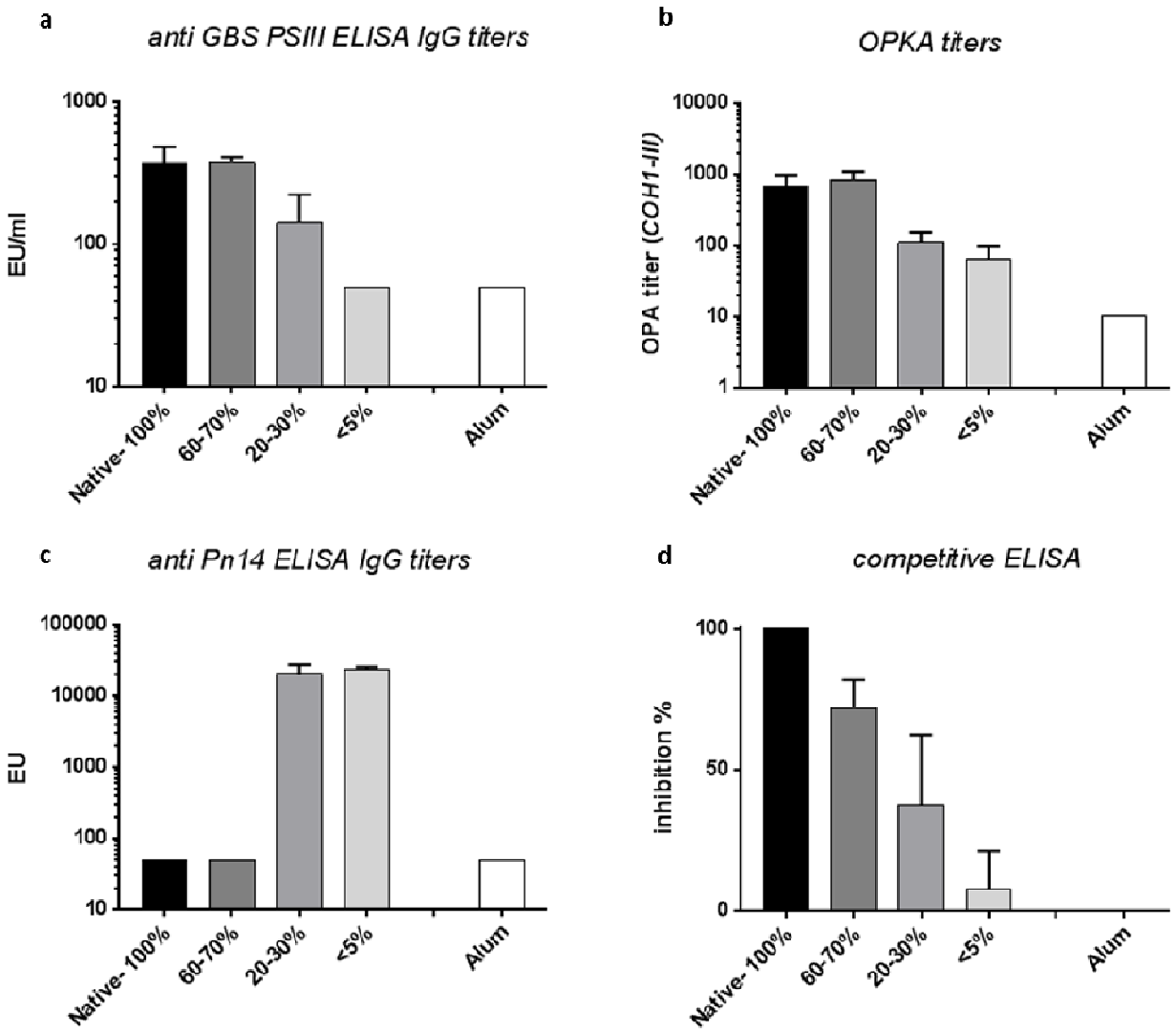

Figure 5.5. Effect of desialylation on the immunogenicity of PSIII conjugates. (a) anti-GBS PSIII IgG titers (EU/ml) for groups of eight mice vaccinated with i.p. injection of glycoconjugate with different level of sialic acid. Sera were analyzed after the third immunization. Alum was used as negative control. Mean (red columns) and standard deviations (black bars) are reported; (b) OPK titers measured testing the sera at different serial dilutions. Reported OPK titers correspond to the serum dilution inducing 50% bacteria killing, as described in literature; (c) anti-Pn14 IgG titers (EU) calculated as the dilution giving OD of 1.0 in ELISA plates coated with Pn14-HAS; (d) inhibition percentage of mAb NVS-1-19-5 binding to ELISA plates coated with PSIII conjugated to HSA using, as competitors, glycoconjugates containing different percentages of sialic acid.

5.2.2. Selection of the glycan fragments for structural studies

Antibodies elicited in mice by PSIII have been shown to bind oligosaccharide fragments in a length dependent manner[30,31]. Using a competitive ELISA assay, it was demonstrated that at least 2 unmodified repeating units (2 RU) were necessary for suboptimal binding to a GBSIII-specific mouse mAb, while inhibition with 3 to 7 RUs moderately increased and became much higher above this number of RU[27]. SPR experiments using a Fab fragment of the same mAb confirmed that the affinity (K_D) was comparable between 2 and 6-7 RUs, it increased by 3-fold from 6-7 RU to 20 RUs, and remained constant beyond this point[30].

To investigate more in detail the epitope recognized by the selected functional mAb, we generated a set of PSIII oligosaccharide fragments by partial de-N-acetylation followed by nitrosation[38]. Improvements in the purification described by Paoletti et al.[39], by using an anionic exchange HPLC in place of a size exclusion chromatography, allowed the isolation of fragments with a degree of polymerization (DP) in the range of 2-15 with a defined composition (Figure 4.2). These fragments were composed of a modified RU and a variable number of unmodified RUs (Figure 5.6).

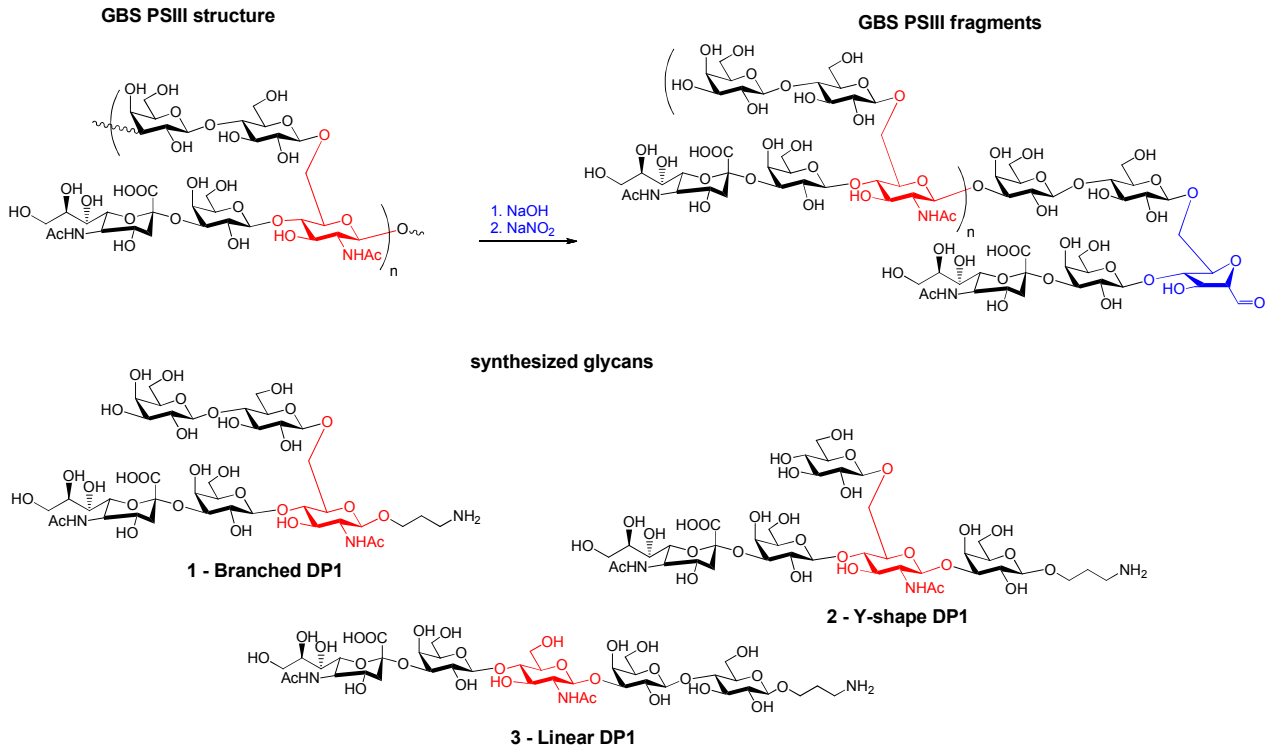

Figure 5.6. Chemical structure of GBS PSIII and glycan probes used in this study. The red highlighted GlcNAc residue is used as reference monosaccharide to outline the three possible sugar sequences related to PSIII repeating unit. The 2,5-anhydri-D-mannose residue obtained during the chemical depolymerization of PSIII is indicated in blue.

Length dependent recognition of the different fragments was firstly confirmed by competitive ELISA with the selected rabbit mAb NVS-1-19-5 (Figure 5.7)[30].

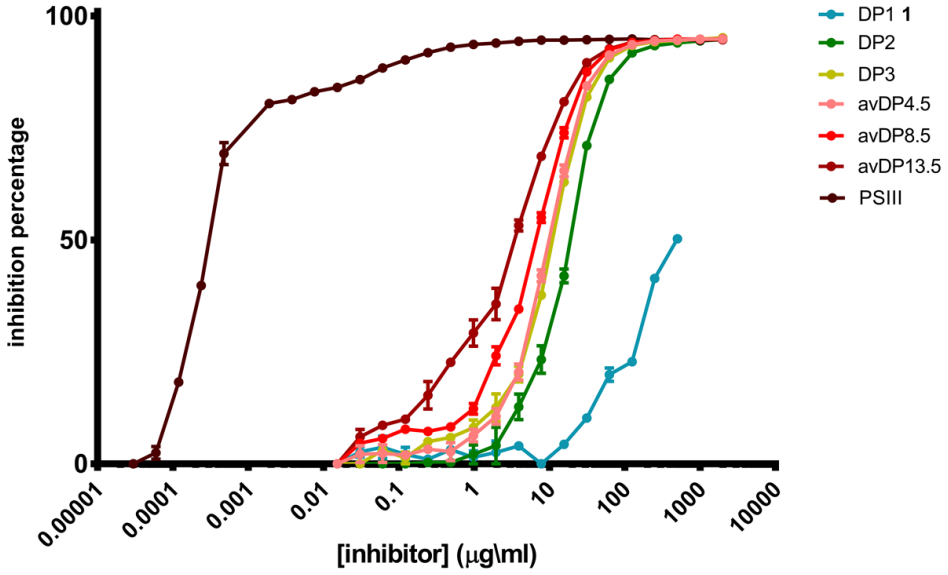

Figure 5.7. Specific length dependent recognition of rabbit mAb. Inhibition curves derived from ELISA inhibition data on the binding PSIII-HSA to rabbit mAb NVS-1-19-5 using PSIII and its fragments as inhibitors.

As expected, this difference slightly increased from DP2 to 11 up to 1-log and became 5-log higher when PSIII was used as inhibitor[26]. To exclude the effect of the bivalent interaction of mAb on the avidity, we performed a competitive SPR assay where different oligosaccharide fragments (DP1-13 range) were tested as competitors for the binding of soluble Fab fragment to PSIII conjugated to Human Serum Albumin (HSA) immobilized on the chip. Two major populations of inhibitors, DP≥2 and DP<2, were differentiated (Figure 5.8 and Table 5.3).

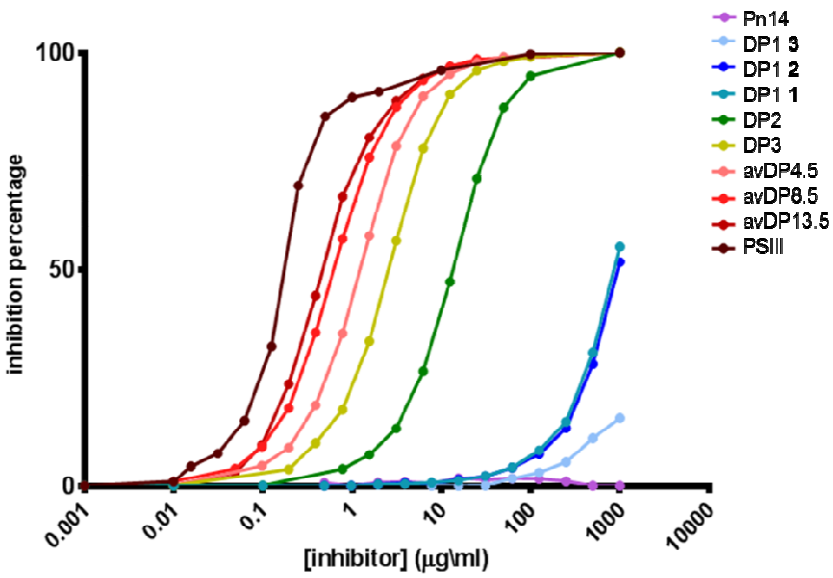

Figure 5.8. Competitive SPR of the binding between the rabbit Fab and PSIII. Different length fragments were used as inhibitors. PSIII and the Pn14 PS (i.e. PSIII fully desialylated) were the positive and negative control, respectively.

Table 5.3. IC_{50} for different length glycans

Glycan	IC_{50} (µg/ml)
DP1 linear -**3**	3119.00
DP1 Y-shape -**2**	1233.00
DP1 branched -**1**	1118.00
DP2	14.29
DP3	2.59
avDP4.5	1.23
avDP8.5	0.64
avDP13.5	0.46
PSIII	0.17
Pn14	nd

DP≥2 oligosaccharides showed asymptotically increasing affinity up to the native PSIII, with only 2-log difference between native PSIII and DP2. Concerning the single RUs, a 2-log difference was observed between DP2 and the synthetic branched and Y-shape (**1** and **2**) DP1 having a β-Glc-(1→6)-β-GlcNAc branching; conversely, a very weak inhibition was detected with the linear structure (**3**), suggesting that the arrangement of sugars in the RU impacts Ab recognition and the ramification point is relevant for binding. The binding affinities of the native PSIII and the DP2 fragment to the rabbit Fab were also compared by conjugating the two polysaccharide structures to CRM_{197} and immobilizing them on a SPR chip. The two binding constants determined according to a 1:1 fitting model differed by less than 10 fold (Figure 5.9 and Table 5.4)[40,41].

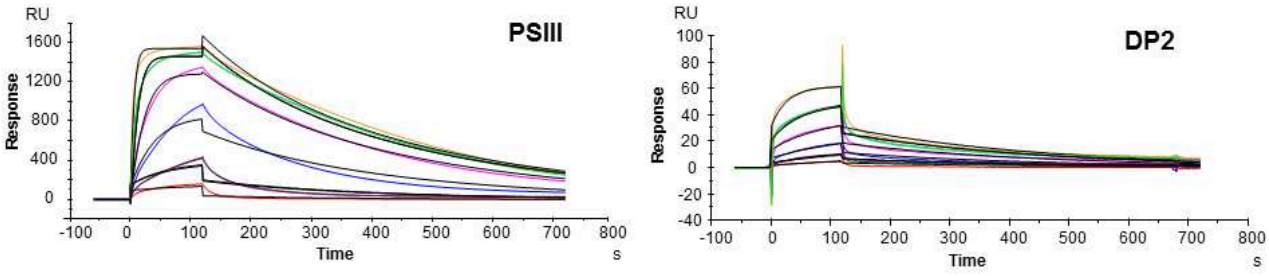

Figure 5.9. Binding kinetics and affinities of PSIII and DP2. Fitting to a 1:1 interaction model of Fab NVS-1-19-5 binding to the PSIII-CRM or DP2-CRM surfaces. Both surface density were 250 resonance units.

Table 5.4. Kinetic and affinity constants for Fab NVS-1-19-5 binding to PSIII or DP2 CRM-conjugates.

	K_a ($M^{-1}s^{-1}$)	K_d (s^{-1})	K_d (M)
PSIII	1.0×10^{5} (±1.7)[a]	3.7×10^{-3} (±3.9)	$\mathbf{3.6 \times 10^{-8}}$
DP2	2.4×10^{4} (±1.9)	3.0×10^{-3} (±2.7)	$\mathbf{2.6 \times 10^{-7}}$

[a] Numbers in parentheses are % SE

Overall, this preliminary analysis confirmed a length-dependent affinity of anti-PSIII GBS antibody but also indicated that DP2 contains the PSIII portion necessary for high affinity antibody binding and could be used for further structural analysis.

5.2.3. Identification of the PSIII antigenic determinant by STD NMR

To map the interactions of PSIII fragments with the protective mAb, Saturation Transfer Difference NMR (STD NMR) studies were undertaken[42,43].

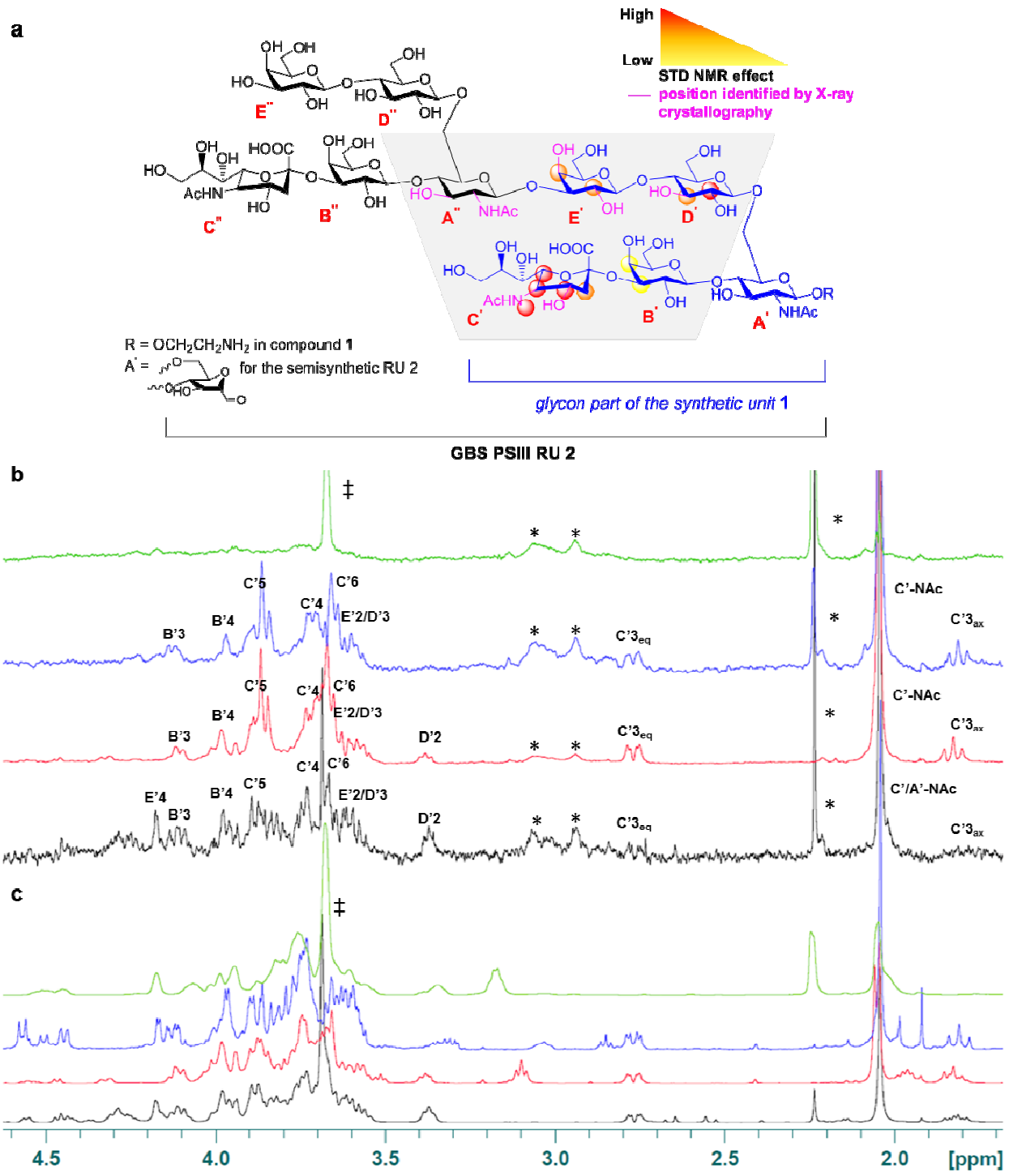

Figure 5.10. GBS PSIII epitope mapping. (**a**) Protons interacting with the mAb identified by STD NMR and X-ray crystallography; (**b**) STDD and (**c**) related ^{1}H NMR spectra of the desialylated tetrasaccharide (β-Gal-(1→4)-β-GlcNAc-(1→3)-β-Gal-(1→4)-α/β-Glc in green), the linear **3** (blue) and branched **1** (red) repeating units, and the DP2 fragment (black). Proton positions receiving saturation after irradiation of the protein are indicated. ‡ indicates the CH_2 signal of the Tris buffer; * refers to signals related to the protein.

STDD NMR spectra were derived by subtracting the STD NMR spectrum of the glycan in the bound state with the mAb (ligand/protein 15-50:1 molar ratio) to the reference spectrum in the unbound state. The DP3 STDD spectrum was super-imposable to the one obtained for the DP2-mAb complex (Figure 5.11), highlighting that the mAb was recognizing identical regions in the two fragments. Due to their higher affinity constants and larger size, experiments carried out on longer fragments (5.5 and 8 RUs) resulted in lower signal intensities that did not allow unequivocal detection of saturation transfer effects.

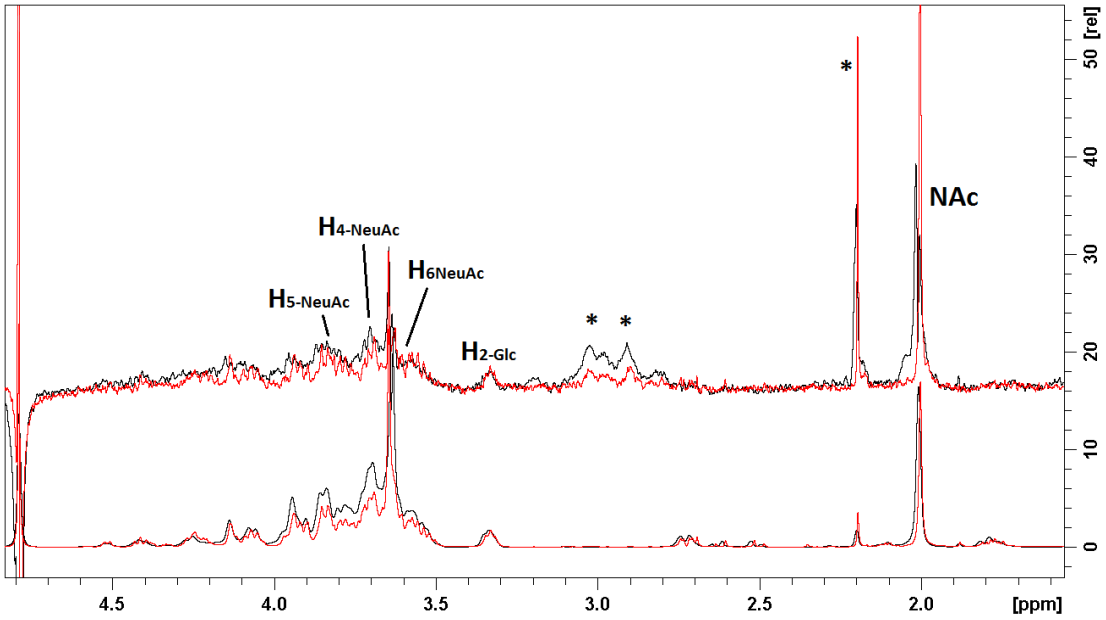

Figure 5.11. Comparison of DP2 and DP3 mapping. ^{1}H (bottom) and STDD-NMR (top) comparison of DP2-DP3–mAb complexes (Black lines DP3, red lies DP2).* labeled resonances match to mAb signals/impurities.

Notably, most of the ^{1}H NMR resonances that could unequivocally be assigned to the DP2-mAb complex were related to the α-NeuNAc-(2→3)-β-Gal^{B}-(1→4) residues (Figure 5.10a), indicating a direct involvement of this branch, in addition to the Glc and Gal residues of the backbone. In the DP2 oligosaccharide it was not possible to differentiate the NAc group of NeuNAc and GlcNAc. To better discriminate the exact positions engaged in antibody interaction, the synthesized DP1 was complexed with the mAb and analyzed by STDD NMR. As shown in Figure 5.10b-c, well recognizable resonances of the branched repeating unit **1** were recovered in the STDD spectrum with medium-high saturation intensity (>50%). The highest transfer of saturation was observed for the H-5 (3.85 ppm), H-4 (3.70 ppm), H-3 (2.76 and 1.82 ppm for equatorial and axial, respectively) and H-6 (3.65 ppm) of NeuNAc (Figure 5.10b), confirming that NeuNAc is the major anchoring site for mAb interaction. A similar pattern of signals related to the NeuNAc was obtained with linear and Y-shape DP1 (Figure 5.12). Further, the involvement of the NeuNAc N-acetyl group, not clearly distinguishable from the one of GlcNAc residue in the DP2, was unveiled in the synthetic probes at 2.0 ppm.

When the desialylated tetrasaccharide [β-Gal-(1→4)-β-GlcNAc-(1→3)-β-Gal-(1→4)-α/β-Glc] was analyzed in presence of the mAb, no transfer of saturation was observed.

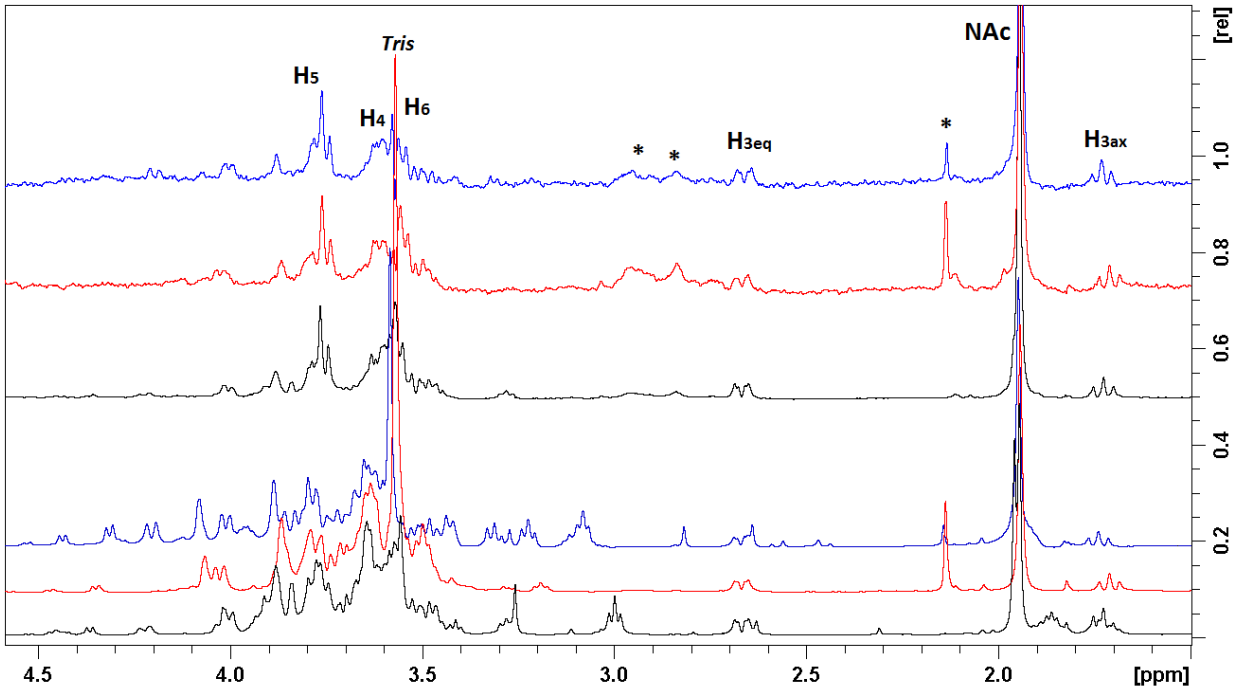

Figure 5.12. Comparison of synthetic DP1 glycans mapping. Comparison of mAb-DP1 STDD NMR spectra (top) and of ^{1}H NMR spectra (bottom) of DP1 branched (black lines), DP1 linear (red lines) and DP1 Y-shape (blue lines).* labeled resonances match to mAb signals/impurities, while assignments are referred to NeuNAc resonances.

A high STD signal was observed for the Glc H-2 position at 3.37 ppm in the DP2, the branched and Y-shape DP1 repeating units (Figure 5.12) in complex with the mAb, whereas no recovery was seen for this position in the linear repeating unit **3** where the Glc moiety is located far from the NeuNAc (Figure 5.10b-c). Previous conformational studies have revealed that the orientation of Glc backbone residue in the backbone was affected by removal of sialic acid, indicating the spatial proximity of the two residues[20]. The transfer of saturation to the H-2 of Glc indicated that the mAb binding of this residue is determined by its intrinsic location in the sugar sequence[29].

Owing to the better resolution of the STD NMR spectra of the synthetic glycans, the saturation transfer was more precisely quantified for some of the protons involved in binding. Experiments at increasing saturation times from 0.5 up to 5.0 sec were performed to avoid possible bias in the calculation of STD effects due to different proton longitudinal relaxation times (T_1), or intramolecular spin diffusion within the bound state (Figure 5.13). In the branched synthetic glycan **1** an STD effect of 100, 96 and 70% was measured for H-5, H-3_{eq} signals of NeuNAc and H-2 of Glc, respectively.

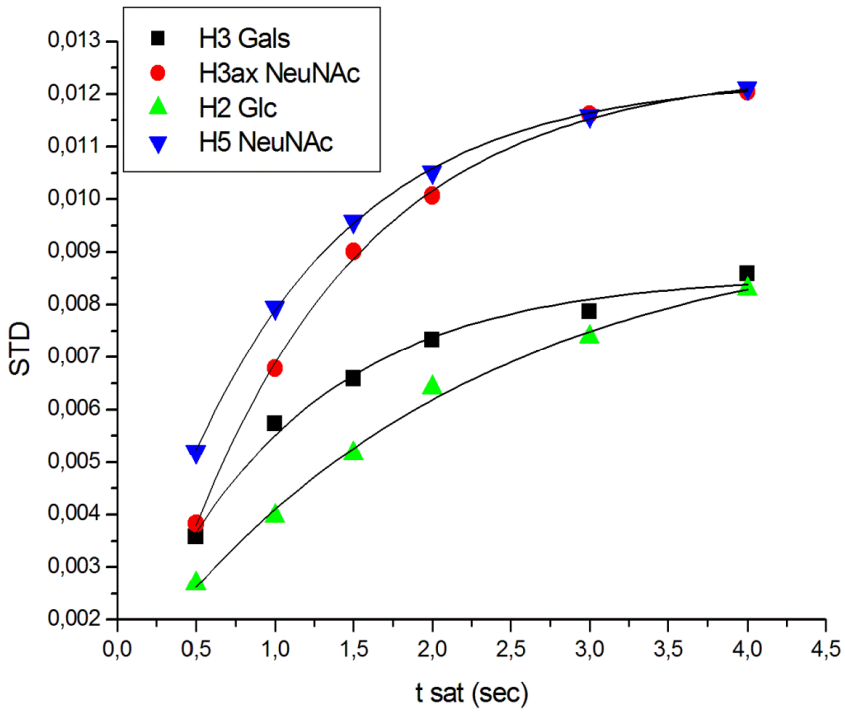

Figure 5.13. STD amplification factor as a function of saturation time. Data were fitted to the monoexponential equation $STD = STD_{max}\ [1 - \exp(-k_{sat}t)]$.

Taken together, these results unambiguously showed that the side chain NeuNAc and Gal residues, together with the Gal and Glc backbone sugars of the RU, directly interact with the mAb.

5.2.4. Structural studies of the PSIII-Fab complex by X-ray crystallography

To further elucidate the basis for the interaction of PSIII and the mAb at atomic level, we used X-ray crystallography to determine the three-dimensional structure of DP2 in complex with the NVS-1-19-5 Fab fragment. Crystals of this complex, belonging to space group $C222_1$ and containing two copies of a 1:1 DP2-Fab complex in the asymmetric unit (ASU), diffracted up to a resolution of 2.7 Å. The structure was solved by molecular replacement, using as template input model the coordinates of a rabbit Fab (PDB 4JO1) with which Fab NVS-1-19-5 shares 79% sequence identity. Excellent electron densities allowed the modeling of residues Gln20-Ser245 of the heavy (H) chain and Val24-Cys238 of the light (L) chain of the Fab, as well as the full DP2 oligosaccharide. The final coordinates of the complex were refined with R_{work}/R_{free} values of 21/27% (Table 5.5). Structural superimposition of the two copies of the Fab present in the ASU resulted in very low carbon alpha root mean square deviation (Cα rmsd) values (~0.5 Å; the two structures are essentially identical), and their bound DP2 conformations were also highly similar; therefore, one copy will be used for description of the structure.

Table 5.5. **Data collection and refinement statistics**.

	GBS DP2-Fab NVS-1-19-5
Data collection	
Wavelength (Å)	0.966
Resolution range (Å)	46.43 - 2.74 (2.838 - 2.74)
Space group	$C\ 2\ 2\ 2_1$
Unit cell *a, b, c* (Å)	135.34 142.23 144.73
Total reflections	164737 (14300)
Unique reflections	36702 (3512)
Multiplicity	4.5 (4.1)
Completeness (%)	99 (96)
Mean I/sigma(I)	12.12 (1.45)
Wilson B-factor (Å^2)	67.72
R_{merge}	0.08093 (0.7761)
R_{meas}	0.09201 (0.8913)
R_{pim}	0.04278 (0.428)
CC1/2	0.998 (0.649)
CC*	0.999 (0.887)
Refinement	
Reflections used in refinement	36701 (2864)
Reflections used for R-free	1834 (130)
R_{work}	0.2008
R_{free}	0.2503
Number of non-hydrogen atoms	7064
macromolecules	6479
ligands	316
solvent	269
Protein residues	879
RMS(bonds) (Å)	0.01
RMS(angles) (°)	1.29
Ramachandran favored (%)	92.3
Ramachandran outliers (%)	1.1
Rotamer outliers (%)	9.6
Clashscore	5.92
Average B-factor (Å^2)	74.21
macromolecules	73.51
ligands	98.29
solvent	62.97
PDB ID	5M63

Statistics for the highest-resolution shell are shown in parentheses.

$R_{work} = \Sigma||F_{(obs)}|- |F_{(calc)}||/ \Sigma|F_{(obs)}|$

$R_{free} = R_{work}$ but calculated for 5 % of the total reflections, chosen at random and omitted from refinement.

The Fab fragment binds the glycan with an extended interface (577 $Å^2$) formed by two adjacent pockets that are located between the light and the heavy chain of the Fab (Figure 5.14a-b). Most of the observed contacts are related to a single PS repeating unit, whereas the sugar residues of the consecutive RU depart from the binding pockets, with the exception of GlcNAc-A" which is directly bound to the Fab. The larger pocket hosts the NeuNAc of the RU branch that interacts with multiple hydrophilic residues of the CDRs from both the heavy and the light chains. Specifically, Arg56 of the light chain forms a hydrogen bond with the N-acetyl group of NeuNAc-C' and His127 interacts with its O-4. Additional weaker interactions of NeuNAc-C' occur through water molecule bridges, as observed for the carboxylic group of the sugar and Asn 74 of the H chain, and the CH-π interaction between Tyr52 of the L chain and the sialic NAc methyl group (Figure 5.14c).

The GlcNAc-A" residue appears involved in the binding to the smaller anchoring pocket of the Fab through at least two hydrogen bonds formed by the L chain Arg56 and Lys74 with the NAc group and the O-3 position of the sugar, respectively. The NAc group is stabilized by a CH-π interaction with Tyr126 and by water molecules trapped in the cavity by a network of H-bonds. Interestingly, the guanidine group of Arg56 is located within H-bond distance from the NAc carbonyl groups of both NeuNAc-C' and GlcNAc-A", whose methyl groups are at the same time favorably oriented to make CH-π interactions with the phenyl rings of Tyr52 of the L chain and Tyr126 of the H chain, respectively. This arrangement allows for a peculiar symmetric network of interactions involving the NeuNAc of one RU and the GlcNAc of a consecutive unit (Figure 5.14d). Complete de-N-acetylation of these residues resulted in loss of Fab recognition as demonstrated by Competitive SPR (Figure 5.15).

Inspection of the glycan structure revealed how Gal-E', though positioned outside of the two binding pockets, interacts with side chain atoms of Asn53 of the L chain and of Tyr126 of the H chain. The side chain of Tyr126 seems also favorably positioned to engage H-bond mediated interactions with the O-3 position of Glc-D'. Interestingly, GlcNAc-A' that was modified into 2,5-anhydro-D-mannose during the depolymerization reaction appears to be far from the anchoring pocket, hence its chemical manipulation during depolymerization did not interfere with the binding to the Fab.

The DP2-Fab complex crystal structure also reveals how NeuNAc-C' and Glc-D' appear to be in close contact, with a calculated distance between the O-9 atom of NeuNAc and the O-6 of Glc of 2.8Å. This suggests that hydrogen bonds between these two positions might be further stabilized upon binding to the Fab (Figure 5.14c). In summary, our structure clearly showed that the side chain NeuNAc and the backbone Gal and Glc of the first RU, as well as the backbone GlcNAc of the consecutive RU interact with multiple hydrophilic residues of the CDRs from both the heavy and the light chain while the NeuNAc glycerol moiety is involved in internal interactions rather than in direct binding to the Fab.

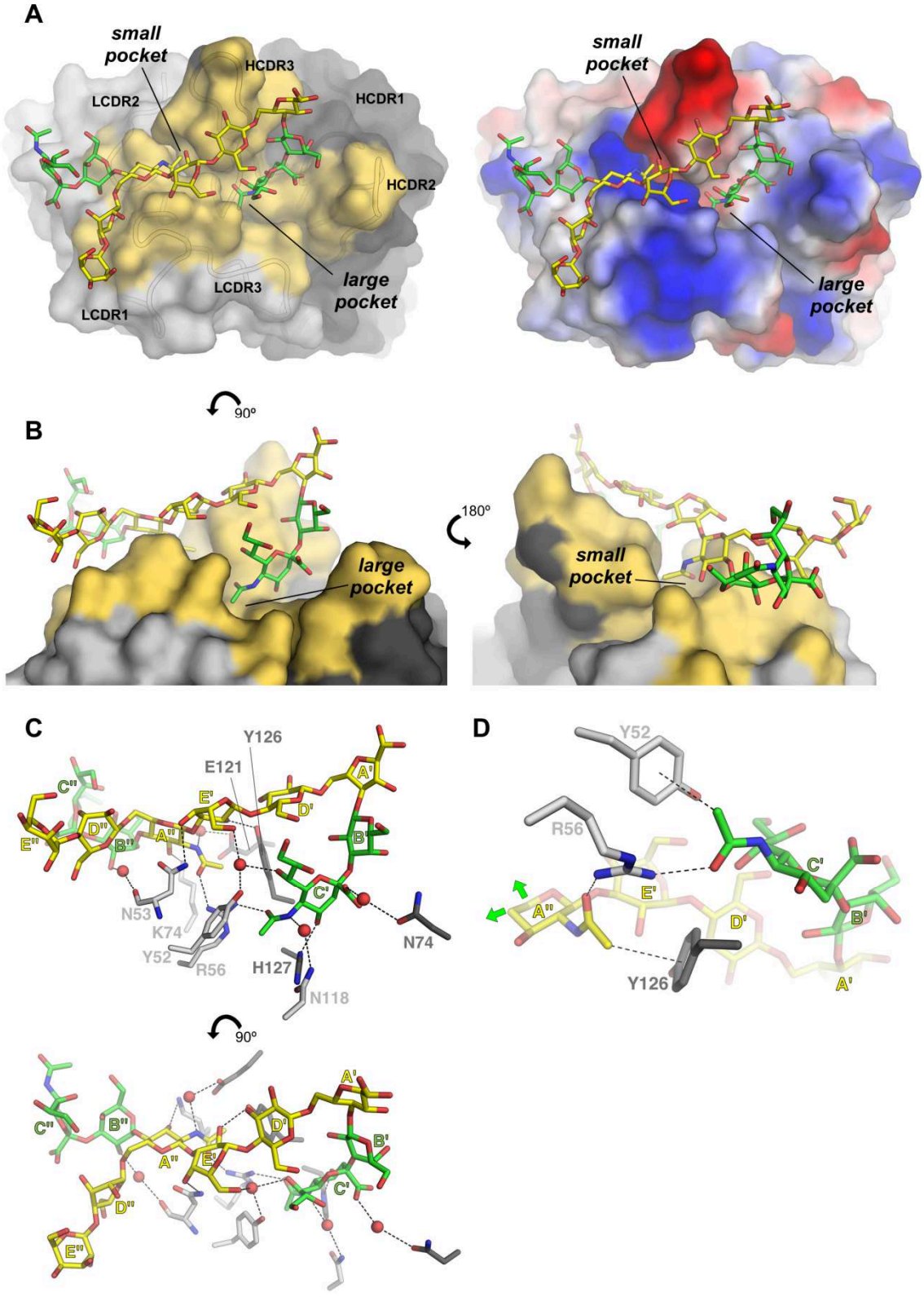

Figure 5.14. Crystal structure of DP2 bound to Fab NVS-1-19-5. (**A-left**) The Fab is depicted with surfaces, while DP2 with sticks. Fab residues involved in direct binding with DP2 (the paratope) are colored in yellow on the left. Binding pockets are shown with arrows and labelled. (A-right) Surface electrostatic

distribution of the Fab; (**b**) Fab-DP2 complex with light chain in light grey and heavy chain in dark grey; (**c**) Direct interactions between and the Fab. Carbon atoms of the DP2 backbone are colored in yellow, and those belonging to the branches are in green, while carbon atoms of the Fab are colored in light and dark gray for the L and H chain, respectively. Nitrogen and oxygen atoms are colored in blue and red, respectively, and water molecules are shown as red spheres. (**d**) Zoom into the interactions between the Fab and the NAc groups of NeuNAc-C' and GlcNAc-A", showing hydrogen bonds between the NAc carbonyl moieties and the guanidinium group of Arg56, and the CH-π interactions between the NAc methyl groups and the phenol of Tyr52 of the L chain and Tyr126 of the H chain. Hydrogen bonds in panels c+d are depicted with black dashes.

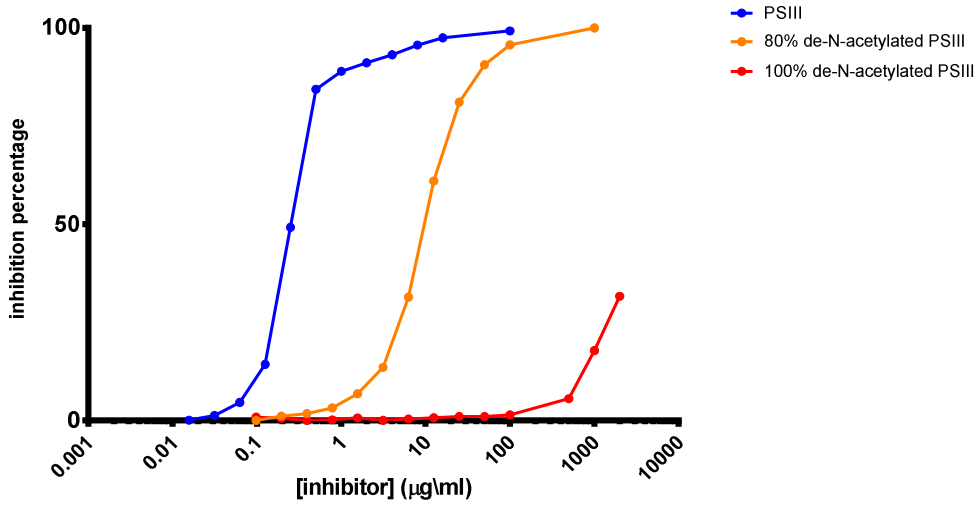

Figure 5.15. mAb recognition of de-N-acetylated PSIII. Competitive SPR of the binding between the rabbit Fab NVS-1-19-5 and PSIII conjugated to HSA, using PSIII at different percentage of de-N-acetylation. PSIII was the positive control.

5.3. Discussion

The definition and characterization at atomic level of polysaccharide epitopes targeted by protective antibodies is relevant for the design, description and even registration of glycoconjugate vaccines.

In this study we aimed to characterize the antigenic determinant of the capsular polysaccharide from the clinically relevant serotype III of GBS, a pathogen for which a vaccine is under evaluation in clinical trials. A GBS vaccine is expected to improve the overall coverage of protection against Early Onset neonatal disease, currently only partially achieved with IAP prophylaxis, and to fill an important medical gap by targeting prevention of late-onset GBS disease (LOD), stillbirths, miscarriages and prematurity.

The GBS polysaccharide III has been considered as a conformational epitope prototype, based on NMR simulation studies indicating the formation of one of several potential helical structures[27,29], where sialylated

side chains are arranged on the exterior surface of the helix. The PSIII helix is thought to be stabilized by the presence of a) specific interactions between the side chain sialic acid and the backbone glucosyl and galactosyl residues, influencing the orientation of the side chain and stabilizing the conformation of the backbone, and b) a carbohydrate chain length of at least 4 pentasaccharide RUs which introduces a conformational epitope equivalent to one present in the native PSIII. Shorter carbohydrate chains are subjected to conformational changes and in absence of specific interactions the overall helical structure collapses[27]. The need for a helical epitope for antibody recognition was hypothesised also considering that, similarly to other polysaccharides including serogroup B *Neisseria meningitidis* CPS, GBS PSIII showed a length dependent binding of specific monoclonal IgGs[30]. Zou et al. observed that K_D measured by SPR for monovalent binding remained virtually constant from 2 to 7 RUs which demonstrated that the epitope optimization was occurring from 2 to 7 RUs, while beyond 20 RUs this phenomenon would overlap with the multivalent exposition of stabilized epitopes. Moreover, Johnson et al. showed by STD NMR experiments that NeuNAc was not involved in the binding to a monoclonal IgM[44].

Further molecular dynamics (MD) simulation confirmed the role of sialic acid in maintaining the helical structure and how preponderant is this conformation of the polysaccharide prior to antibody binding[27]. However a question was not addressed: Is the helical conformation pivotal for binding of PSIII to antibodies?

We undertook a structural glycobiology approach to deeply investigate this intriguing feature, and further define the relevance of the NeuNAc residue in PSIII immunogenicity. Preliminary results obtained with mice immunized with PSIII-CRM_{197} conjugates with different levels of sialylation confirmed that the presence of NeuNAc is determinant to generate protective antibodies and that native PSIII GBS elicits two types of antibodies differing in sialic acid dependency[24,25].

A rabbit functional monoclonal IgG belonging to the major PSIII-specific sialic-acid dependent population was selected for structural analysis. This mAb also provides a useful analytical tool for discriminating sialylated (native) and partially desialylated PSIII GBS during the isolation, purification and conjugation steps for vaccine antigen production.

A set of oligosaccharides of different length was prepared by semisynthetic and synthetic methods. By using these fragments we first confirmed by competitive ELISA the length dependency of mAb binding to GBS PSIII oligosaccharides[30]. The difference in affinity among the fragments remarkably decreased from 5 to 2 log fold, when bivalent binding of the mAb was avoided by the use of a Fab fragment. The increase of affinity with growing saccharide lengths was progressive and no major difference in this trend was observed above 4-5 RUs. In addition, SPR binding affinity of the Fab to DP2-CRM and native PSIII-CRM conjugates varied within a narrow range (10-100 nM). Based on the above data, we assumed that the Fab binding to PSIII would presumably involve no more than 2 RUs, and the observed rise in affinity with fragments of increasing length could be justified by multivalency effects rather than the need for a helical conformation.

To demonstrate this hypothesis, we performed STD NMR and X-ray crystallography experiments using the Fab and DP≤2 RU. The information obtained by these two techniques was in good agreement, and is summarized in Figure 5.10a. STD NMR unequivocally showed that NeuNAc in the branch and Gal and Glc residues in the backbone of the RU are the structural motifs that are recognized by the antibody. Furthermore, the branched DP1-**1** contains most of the structural elements for mAb interaction. Ring protons of NeuNAc were shown not to receive STD effect in a carbohydrate-IgM complex analyzed by STD NMR, although saturation was transferred to an N-propionyl group used in replacement of the NAc[44]. One possible explanation of the difference with our results could be that the isolated protective IgM was directed to the second type of antibodies cross-reactive with Pn14 present in anti-PSIII sera.

X-ray crystallography data confirmed the interactions for NeuNAc-C', Glc-D' and Gal-E' residues. Additionally, it showed that the GlcNAc-A' residue is outside the Fab binding pocket and not involved in the recognition, while the GlcNAc-A" of a proximal RU contributes to the stabilization of the interaction with the Fab. This result could explain the difference in binding affinity between DP1 and DP2 observed by competitive SPR. With the exception of GlcNAc-A", the consecutive repeating unit is exposed externally to the binding area, therefore longer structures would likely not be accommodated by the Fab. STD NMR revealed an interaction involving the Gal-B' of the branch, which did not appear in the crystal structure. This could be ascribed to higher flexibility of the α-NeuAc-(2→3)-β-Gal^{B}-(1→4) branch in the liquid solution compared to crystallography which facilitates transfer of saturation to the Gal residue.

Intramolecular interactions between NeuNAc and Glc have been long debated, as oxidation of the glycerol side chain is typically used in the preparation of glycoconjugate vaccines. The proximity of these residues has been suggested by a chemical shift of Glc related signals in NMR spectra after modification of H8-H9 positions[24,29]. Torsion angles distribution for NeuAc and the interactions of this residue with Glc have been used as paramaters to build the helical model[39]. On the other hand, *in silico* studies suggested no hydrogen bonding formation between NeuNAc and Glc[27]. STD NMR and X-ray data confirmed the structural proximity of NeuAc and Glc, facing each other in the Fab complex independently from the presentation in a helical structure. The glycerol group appeared engaged in H-bond formation with Glc. Acetylation of positions C-7, -8 and -9 was found in various clinical isolates including PSIII expressing strains[45], although this feature was demonstrated not to be relevant to elicit functional antibodies[46]. Furthermore, moderate oxidation of the C-9 position is known to be well tolerated for PSIII conjugation to carrier protein[16]. Therefore the H-bond interaction of the glycerol moiety with Glc might not have an impact on the immunogenicity.

In summary, the glycan epitope for GBS PSIII is composed of five non-consecutive residues highlighted by the trapezoidal area (Figure 5.10a), and it would involve an additional GlcNAc residue of the vicinal repeating unit, as demonstrated by exploring the branched glycan **1** containing the additional a GlcNAc-A" residue. It is worth of note that, the β-Glc-(1→6)-β-GlcNAc linkage creates a ramification in the carbohydrate structure that is discriminant for mAb affinity and recognition.

This creates a spatially defined but discontinuous motif which involves sugars from the branch and the backbone of the polysaccharide, and that can be defined as a *conformational epitope*. Indeed, this type of epitope is a distinctive motif compared to the linear epitopes involving 2-3 consecutive residues that were so far mapped by structural studies for *V. Cholerae* O1[4], *Shighella flexeneri* variant Y and *Salmonella* O-antigens[5,6], while it seems more similar to *Shighella flexneri* serotype 2a O-antigen[33], where an epitope involving 6 out of 10 monosaccharides from 2 RUs is recognized by Fab. Importantly, the described PSIII epitope is totally independent from the existence of a helical structure whereas it appears generated by the presence of branches in the polysaccharide.

Carbohydrates present a higher level of complexity compared to other classes on natural biopolymers such as polypeptides or polynucleotides, because of the presence of α- or β-glyocosidic bonds and the occurrence of connections at different positions of the ring which create ramifications. These unique features would result into spatial motifs that would be relevant for antibody recognition and specificity even in the presence of a limited number of sugar residues, as it has been demonstrated here for GBS PSIII. In this manner, the need for the human immune system to recognize GBS PS by means of their length dependent helical structures in order to avoid recognition of self-antigens containing sialic acid would need to be reconsidered[31].

The finding that the PSIII epitope is defined within a limited number of sugars confirms our initial hypothesis that differences in affinity to the Fab with increasing fragment lengths could be explained based on the *statistical rebinding* of the Fab to consecutive defined epitopes as displayed on the SPR chip. The rabbit anti-PSIII mAb studied here provides a useful analytical tool for discriminating sialylated (native PSIII) and desialylated (equivalent to Pn14) PSIII GBS.

New approaches for the preparation of glycoconjugate vaccines which eliminate the fermentation of pathogens and deliver more defined products are emerging. These include the use of synthetically made oligosaccharide[47], the *in vivo E. coli* expression of glycoproteins[48] or *in vitro* polysaccharide production[49]. The existence of helical conformational epitopes which would imply the necessity of using long polysaccharide antigen has been considered a challenge to apply these technologies to certain pathogens.

The elucidation and understanding of the structural bases for the immune recognition of carbohydrate epitopes reported here paves the way to the design of glycoconjugate vaccines, as well as contributes to accelerating the development of modern vaccines based on chemoenzymatic or bioengineering methods.

5.4. References

1. Avci FY, Kasper DL. How bacterial carbohydrates influence the adaptive immune system. *Annu. Rev. Immunol.* **28**, 107-10 (2010).
2. Costantino P, Rappuoli R. Berti F. The design of semi-synthetic and synthetic glycoconjugate vaccines. *Expert Opin. Drug Disc.* **6**, 1045-1067 (2011).
3. Anish C, Schumann B, Lebev Pereira C, Seeberger PH. Chemical biology approaches to designing defined carbohydrate vaccines. *Chem. Biol.* **21**, 38-50 (2014).
4. Villeneuve S, et al. Crystal structure of an anti-carbohydrate antibody directed against Vibrio cholerae O1 in complex with antigen: molecular basis for serotype specificity. *Proc. Natl. Acad. Sci. USA* **97**, 8433-8 (2000).
5. Vyas NK, et al. Molecular recognition of oligosaccharide epitopes by a monoclonal Fab specific for *Shigella flexneri* Y lipopolysaccharide: X-ray structures and thermodynamics. *Biochemistry* **41**, 13575-13586 (2002).
6. Cygler M, Wu S, Zdanov A, Bundle DR, Rose DR. Carbohydrates, shapes and biological Recognition. *Bioche. Soc. Trans.* **21**, 437-441 (1999).
7. Safari D, et al. Identification of the smallest structure capable of evoking opsonophagocytic antibodies against *Streptococcus pneumoniae* type 14. *Vaccine* **76**, 4615-4623 (2008).
8. Safari D, et al. The immune response to Group B *Streptococcus* type III capsular polysaccharide is directed to the -Glc-GlcNAc-Gal- backbone epitope. *Glycocon. J.* **28**, 557-562 (2011).
9. Jennings HJ. The role of sialic acid in the formation of protective conformational bacterial polysaccharide epitopes. In Anticarbohydrate Antibodies, P. Kosma and S. Muller-Loennies, eds. (Vienna: Springer), 55-73 (2012).
10. Nuccitelli A, Rinaudo CD, Maione D. Group B *Streptococcus* vaccine: state of the art. *Ther Ad.v Vaccines* **3**, 76-90 (2015).
11. Berti F, et al. Structure of the type IX Group B *Streptococcus* capsular polysaccharide and its evolutionary relationship with types V and VII. *J. Biol. Chem.* **289(34)**, 23437-23448 (2014).
12. Kasper DL, Baker CJ. Correlation of maternal antibody deficiency with susceptibility to neonatal group B streptococcal infection. *N. Engl. J. Med.* **294**, 753-756 (1976).
13. Munoz FM, Ferrieri P. Group B *Streptococcus* vaccination in pregnancy: moving toward a global maternal immunization program. *Vaccine* **31S**, D46- D51 (2013).
14. Paoletti LC, et al. Effects of chain length on the immunogenicity in rabbits of Group B *Streptococcus* type III oligosaccharide-tetanus toxoid conjugates. *J. Clin. Invest.* **89**, 203-209 (1992).
15. Paoletti LC, Kennedy RC, Chanh TC, Kasper DL. Immunogenicity of Group B *Streptococcus* type III polysaccharide-tetanus toxoid vaccine in baboons. *Infect. Immun.* **64**, 677–679 (1996).

16. Wessels MR, et al. Immunogenicity in animals of a polysaccharide-protein conjugate vaccine against type III Group B *Streptococcus*. *J. Clin. Invest.* **86**, 1428-1433 (1990).
17. Kasper DL, Baker CJ, Galdes B, Katzenellenbogen E, Jennings HJ. Immunochemical analysis and immunogenicity of the type II Group B streptococcal capsular polysaccharide. *J. Clin. Invest.* **72**, 260-269 (1983).
18. Baker CJ, Rench MA, Paoletti LC, Edwards MS. Dose–response to type V Group B streptococcal polysaccharide–tetanus toxoid conjugate vaccine in healthy adults. *Vaccine* **25**, 55–63 (2007).
19. Edwards MS. Group B streptococcal conjugate vaccine: a timely concept for which the time has come. *Hum. Vaccin.* **4**, 444-448 (2008).
20. Donders GG, et al. Maternal immunization with an investigational trivalent Group B streptococcal vaccine: a randomized controlled trial. *Obstet. Gynecol.* **127**, 213-221 (2016).
21. Clarke ET, et al. Polysaccharide-Specific memory B cells generated by conjugate vaccines in humans conform to the $CD27^{+}IgG^{+}$ Isotype–switched memory B cell phenotype and require contact-dependent signals from bystander T cells activated by bacterial proteins to differentiate into plasma cells. *J. Immunol.* **191**, 6071-6083 (2013).
22. Edmond KM, et al. Group B streptococcal disease in infants aged younger than 3 months: systematic review and meta-analysis. *Lancet.* **379**, 547-556 (2012).
23. Kasper DL, et al. Immunodeterminant specificity of human immunity to type III Group B *Streptococcus*. *J. Exp. Med.* **149**, 327-339 (1979).
24. Jennings HJ, Lugowski C, Kasper DL. Conformational aspects critical to the immunospecificity of the Type III Group B streptococcal polysaccharide. *Biochemistry* **20**, 4512-4518 (1981).
25. Guttormsen HK, et al. Type III Group B streptococcal polysaccharide induces antibodies that cross-react with *Streptococcus pneumoniae* type 14. *Infect. Immun.* **70**, 1724–1738 (2002).
26. Jennings HJ, et al. Structure, Conformation and immunology of sialic acid containg polysaccharides of human pathogenic bacteria. *Pure & Appl. Chem.* **56**, 893-905 (1984).
27. González-Outeirino J, Kadirvelraj R, Woods RJ. Structural elucidation of type III Group B *Streptococcus* capsular polysaccharide using molecular dynamics simulations: the role of sialic acid. *Carbohydr. Res.* **340**, 1007-1018 (2005)
28. Woods R, Yongye A. Computational techniques applied to defining carbohydrate antigenicity. In Anticarbohydrate Antibodies. Edited by P. Kosma and S. Müller-Loennies, eds. (Vienna: Springer), pp. 361-383 (2012).
29. Brisson JR, et al. NMR and Molecular Dynamics studies of the conformational epitope of the type III Group B *Streptococcus* capsular polysaccharide and derivatives. *Biochemistry* **36**, 3278-3292 (1997).
30. Zou W, et al. Conformational Epitope of the Type III Group B *Streptococcus* Capsular Polysaccharide. *J. Immunol.* **163**, 820-825 (1999).

31. Zou W, Jennings HJ. The conformational epitope of type III Group B *Streptococcus* capsular polysaccharide. *The Molecular Immunology of Complex Carbohydrates-2,* Edited by Albert M. Wu, Accademic/plenum Publishers, 473-484 (2001).

32. Bush CA, Martin-Pastor M. Structure and conformation of complex carbohydrates of glycoproteins, glycolipids, and bacterial polysaccharides. *Annu. Rev. Biophys. Biomol. Struct.* **28**, 269-293 (1999).

33. Vulliez-Le Normand B, et al. Structures of synthetic O-antigen fragments from serotype 2a *Shigella flexneri* in complex with a protective monoclonal antibody. *Proc Natl Acad Sci U S A.* **105**, 9976-9981 (2008).

34. Geissner A, Pereira CL, Leddermann M, Anish C, Seeberger PH. Deciphering antigenic determinants of *Streptococcus pneumoniae* serotype 4 capsular polysaccharide using synthetic oligosaccharides. *ACS Chem. Biol.* **11**, 335−344 (2016).

35. Oberli MA, et al. Molecular analysis of carbohydrate-antibody interactions: case study using a *Bacillus anthracis* tetrasaccharide. *J. Am. Chem. Soc.* **132**, 10239-102419 (2010).

36. Coelho H, et al. The quest for anticancer vaccines: deciphering the fine-epitope specificity of cancer-related monoclonal antibodies by combining microarray screening and Saturation Transfer Difference NMR. *J. Am. Chem. Soc.* **137**, 12438-12441 (2015).

37. Bhushan R, Anthony BF, Frasch CE. Estimation of Group B *Streptococcus* type III polysaccharide-specific antibody concentrations in human sera is antigen dependent. *Infect. Immun.* **66**, 5848-5853 (1998).

38. Michon F, et al. Group B streptococcal Type II and III conjugate vaccines: physicochemical properties that influence immunogenicity. *Clin. Infect. Dis.* **13**, 936–943 (2006).

39. Paoletti LC, et al. An oligosaccharide-tetanus toxoid conjugate vaccine against type III Group B *Streptococcus*. *J. Biol Chem.* **265**, 8278-18283 (1990).

40. Pieters RJ. Maximising multivalency effects in protein–carbohydrate interactions. *Org. Biomol. Chem.* **7**, 2013-2025 (2009).

41. Gestwicki JE, Cairo CW, Strong LE, Oetjen KA, Kiessling LL. Influencing receptor-ligand binding mechanisms with multivalent ligand architecture. *J. Am. Chem. Soc.* **124**, 14922-14933 (2002).

42. Mayer M, Meyer B. Group epitope mapping by Saturation Transfer Difference NMR To identify segments of a ligand in direct contact with a protein receptor. *J. Am. Chem. Soc.* **123**, 6108-6117 (2001).

43. Meyer B, Peters T. NMR spectroscopy techniques for screening and identifying ligand binding to protein receptors. *Angew. Chem. Int. Ed.* **42**, 864-890 (2003).

44. Johnson MA, et al. NMR studies of carbohydrates and carbohydrate-mimetic peptides recognized by an anti-Group B *Streptococcus* antibody. *J. Biol. Chem.* **278**, 24740–24752 (2003).

45. Lewis AL, Nizet V, Varki A. Discovery and characterization of sialic acid O-acetylation in Group B *Streptococcus*. *Proc Natl Acad Sci U S A.* **101**, 11123–11128 (2004).

46. Pannaraj PS, et al. Group B Streptococcal conjugate vaccines elicit functional antibodies independent of strain O-acetylation. *Vaccine* **16**, 4452-4456 (2009).
47. Verez-Bencomo V, et al. A Synthetic conjugate polysaccharide vaccine against *Haemophilus influenzae* type b. *Science* **305**, 522–525 (2004).
48. Kowarik M, et al. N-linked glycosylation of folded proteins by the bacterial oligosaccharyltransferase. *Science* **314**, 1148-1150 (2008).
49. Fiebig T, et al. Functional expression of the capsule polymerase of *Neisseria meningitidis* serogroup X: A new perspective for vaccine development. *Glycobiology* **24**, 150-158 (2014).

CHAPTER 6

Determining the minimal epitope of GBS PSIII and the effect of its multivalent presentation onto the carrier protein on the immunogenicity

6.1. Introduction

Since the beginning of XIX century, vaccines have become a hugely important and successful countermeasure to the threat of infectious disease[1]. Vaccines provide protection by inducing humoral and/or cellular immunity to disease-causing pathogens. The dense surface distribution of often unique glycan structures on diverse pathogens and on malignant cells makes carbohydrates attractive vaccine targets[2]. The surface of bacterial pathogens is covered with a dense array of polysaccharide that is a unique feature of not only the particular species, but also the strain of bacteria considered. Carbohydrate-specific antibodies are predominantly responsible for protection against bacteria with either a capsule or lipopolysaccharide on their surfaces. People lacking these antibodies, for example the elderly and neonates, are at high risk of developing infections. With the increasing prevalence of antibiotic-resistant bacterial strains, the proven track record of capsular polysaccharide-based vaccines has encouraged the development of these types of vaccines against a broader range of pathogens. For many bacterial infections, glycoconjugate vaccines have been made based on fragments of their capsular polysaccharides, for example *Streptococcus pneumoniae*, *Neisseria meningitides* and *Haemophilus influenzae*[3].

Administration of capsular polysaccharides (PS) has been part of routine vaccinations against a variety of pathogenic bacteria for many years, but it is effective only in the adult population[4]. This major limitation of plain polysaccharide vaccines can be overcome by chemical conjugation to a carrier protein as T-cell helper, such as the chemically detoxified diphtheria and tetanus toxoid (DT and TT, respectively) or the genetically detoxified diphtheria toxin (CRM_{197}). The covalent linkage renders poorly immunogenic sugars potent antigens capable of evoking a T-cell memory response[5-6]. Thereby, glycoconjugation represents the key to render vaccination with carbohydrates efficacious in children, ensuring memory response and boost the response to the vaccine.

The immunogenicity of carbohydrate-based vaccines is influenced by a series of interconnected variables, including the saccharide length, the saccharide:protein ratio in the purified conjugate, the conjugation strategy and the nature of the spacer. The molecular size of the carbohydrate antigen is a major concern in designing optimal glycoconjugates[7-9]. Large polysaccharides and their conjugates may have the undesirable property of insolubility. Size-unconstrained antigens may yield heterogeneous conjugates with the potential for immunogenic inconsistency[10-11]. Glycoconjugates constituted from size-specific antigens are thus particularly attractive. Although bacterial polysaccharides are usually made up of hundreds to thousands of

repeating oligosaccharides, their antigenic structural determinants consist not of the entire polymer but rather of specific oligosaccharide fragments[12-13]. One hypothesis is that oligosaccharides containing complete antigenic epitopes are optimal in vaccines; however, the exploration of vaccines containing antigenic oligosaccharides or shorter-length polysaccharides derived from bacterial capsular polysaccharides has been hindered until recently by technical difficulties in chemical preparation of oligosaccharides[14-15].

There is now ample evidence that short defined carbohydrates varying from two sugar residues, as in the case of β-mannans from *Candida albicans*[16], up to the tetrasaccharide repeating unit of *S. pneumoniae* type 14[17] or even to an pentasaccharide in the case of *Shighella* serotype 2a can elicit robust production of functional antibodies[18].

Gram-positive *Streptococcus agalactiae* or G*roup B Streptococcus* (GBS) is a leading cause of invasive infections in pregnant women, newborns, and elderly people[19]. Most GBS strains possess a capsular polysaccharide (PS) on their surface which is a major virulence factor. Ten different PS serotypes have been characterized, five of which are responsible for the vast majority of the disease in North America and Europe[20]. GBS infection can be contracted by neonates from the maternal genital tract and can result in prematurity or newborn bacteremia, pneumonia, and/or meningitis. Therefore, vaccination of pregnant women represents the best strategy for prevention of GBS infection in newborns[21-22]. Early in the 1930s, Lancefield et al. demonstrated that polyclonal antibodies from rabbit sera, able to recognize PS epitopes, conferred protection against GBS infection in animal models[23-25]. During the past two decades, plain GBS polysaccharides have been extensively studied as vaccines in preclinical and clinical studies[26-27]. However, the first human trials conducted in the 1980s showed that the purified native PS from serotype III was not sufficient to induce a robust IgG response in adults[28]. When the full length polysaccharide was conjugated to to TT or CRM_{197}, strong long-term protection has been elicited in mice[29-32]. A pentavalent GBS polysaccharide-protein conjugate vaccine, composed of capsular epitopes from serotypes Ia, Ib, II, III and V, is under development.

In order to study the effect of the saccharide length, a variety of experimental GBS type III PSIII-protein conjugate vaccines have been designed over the years, and their immunogenicity has been tested in animals[33-34]. Generating GBS oligosaccharides is challenging because of the acid-labile, antigenically critical sialic acid residues present at the termini of the side chains of all GBS PS serotypes. Enzymatic digestion of the type III PS with endo-β-galactosidase allowed the production of oligosaccharides with an average weight of 14.5 kDa covalently linked to tetanus toxoid (TT) which proved to be immunogenic in animals[33].

In a follow-up study, oligosaccharide with two fold smaller (7 kDa) or larger (27 kDa) size than the previously reported control (14.5 kDa) were examined. The conjugated medium size polymer gave the optimal immunogenic response (19). Large heterogeneous populations of diverse length fragments, varying as average weight from 11 to 100 kDa, produced according to a method developed by Laferriere and coworkers based on sequential N-deacetylation and nitrous acid deamination[35-36], were shown by Michon

and coworkers to induce comparable immune responses in mice in terms of anti-polysaccharide IgG levels and OPA titers[37].

To explain this peculiar immunological behavior of GBS PSIII, a number of structural studies were undertaken. PSIII was demonstrated to occasionally form extended helices with sialylated side chains arrayed on the exterior surface, interspersed within a major random coil structure[38]. According to the proposed model, the NeuNAc residue would not be immunodominant for PSIII antigenicity but rather be capital for the stabilization of the helical conformation by means of its negative charge and interactions with the PS backbone residues[39].

When the effect of different length oligosaccharides was taken in consideration by studying the inhibition of a monoclonal specific binding to PSIII, it was observed antibody recognition slightly increase when 2 and 3 RUs were used as competitors, to be maximized at 4–5 RUs remaining constant up to 7 RUs, and to finally become much higher at 20 RUs. Since K_D measured by SPR for 1:1 binding with the Fab remained virtually constant from 2 to 7 RUs it was concluded that epitope optimization was occurring from 2 to 7 RUs, while beyond 20 RUs this phenomenon would overlap with the multivalent exposition of stabilized epitopes[40].

Despite it was established that 2 RUs (decasaccharide) were required for suboptimal binding to homologous antibodies[41], the antisera induced by its TT conjugate have been reported to fail at providing significant killing of GBSIII. The antisera raised by 3RU-TT were better but only those conjugates from 4RU-TT gave a comparable killing of GBSIII to antisera raised by native GBSIII-TT. The requirement of at least 4RU to effectively raise good protective antibodies is in agreement to the observation that an optimized conformational epitope forms at 4RU as indicated by binding and inhibition experiments[42].

Intrigued by these unique properties and considering the clinical relevance of GBS PSIII we recently used a structural glycobiolgy approach to map the polysaccharide portion binding to a protective monoclonal rabbit IgG. Notably we found that the epitope consists of 5 disjoined sugar residues comprised in one repeating unit and the GlcNAc moiety of a consecutive one. This observation contrasted the idea that the epitope might be exceptionally large, and convinced us to in depth explore which factors influence the immunogenicity of a glycoconjugate vaccine based on the minimal epitope. Here we disclose how the level of sugar incorporation of this defined PSIII portion onto the protein or its exposition along longer fragments can be tuned to achieve optimization of an anti GBSIII vaccine.

6.2. Results

6.2.1. Influence of the size of the oligosaccharide chains on the immunogenicity of glycoconjugates

In order to determine whether the DP2 was not only the epitope recognized by PSIII specific antibodies (see Chapter 5) but also the minimal structure required to induce an immune response, oligosaccharides of different lengths were evaluated for their immunogenicity. For this purpose, GBSIII fragments have been conjugated to CRM_{197} (see Chapter 3 and 4 and Table 6.1).

Table 6.1. Biochemical characteristics of GBS type III conjugate vaccines.

	Name	Protein concentration (µg/mL)	Sacch. Concentration (µg/mL)	Average n° of saccharide chains per protein
1	**CRM-DP1 linear**	1428	75	3.1
2	**CRM-DP1 Y-shape**	1518	700	26.9
3	**CRM-DP1 branched**	1268	64	3.0
4	**CRM-DP1 branched**	1035	409	23.0
5	**CRM-DP2**	1122	140	3.5
6	**CRM-DP2**	535	160	9.0
7	**CRM-DP3**	383	44	2.0
8	**CRM-DP3**	484	130	4.5
9	**CRM-DP5**	639	159	3.0
10	**CRM-DP5**	349	161	5.5
11	**CRM-DP6,5**	456	79	1.5
12	**CRM-DP6,5**	289	110	3.5
13	**CRM-DP11**	531	235	2.3

In a first set of experiments, oligosaccharide conjugates presenting comparable saccharide (mol) : protein (mol) ratio of 3-4 (n°1, 3, 5, 8, 9, 12, 13 in Table 6.1) were used, to rule out the effect of the glycosylation degree in the immunogenicity comparison. The glycoconjugates were tested in mice for their capability of eliciting specific anti-PSIII antibodies mediating opsonophagocytic killing (OPKA) of strains expressing type III PS.

A total of 16 BALB/c female mice splitted in two identical immunization experiments received three intraperitoneal injections of the prepared conjugates at a saccharide dose of 0.5µg.

The animals received booster doses of the same vaccines 3 and 5 weeks after the first immunization. All the glycoconjugates were formulated with Alum hydroxide and adjuvant alone was used as negative control. A group of mice received PS-III conjugated to CRM for comparison.

Figure 6.1 reports the ELISA Geometric Mean Titer of IgGs raised in each group of mice after I, II, or III vaccine doses.

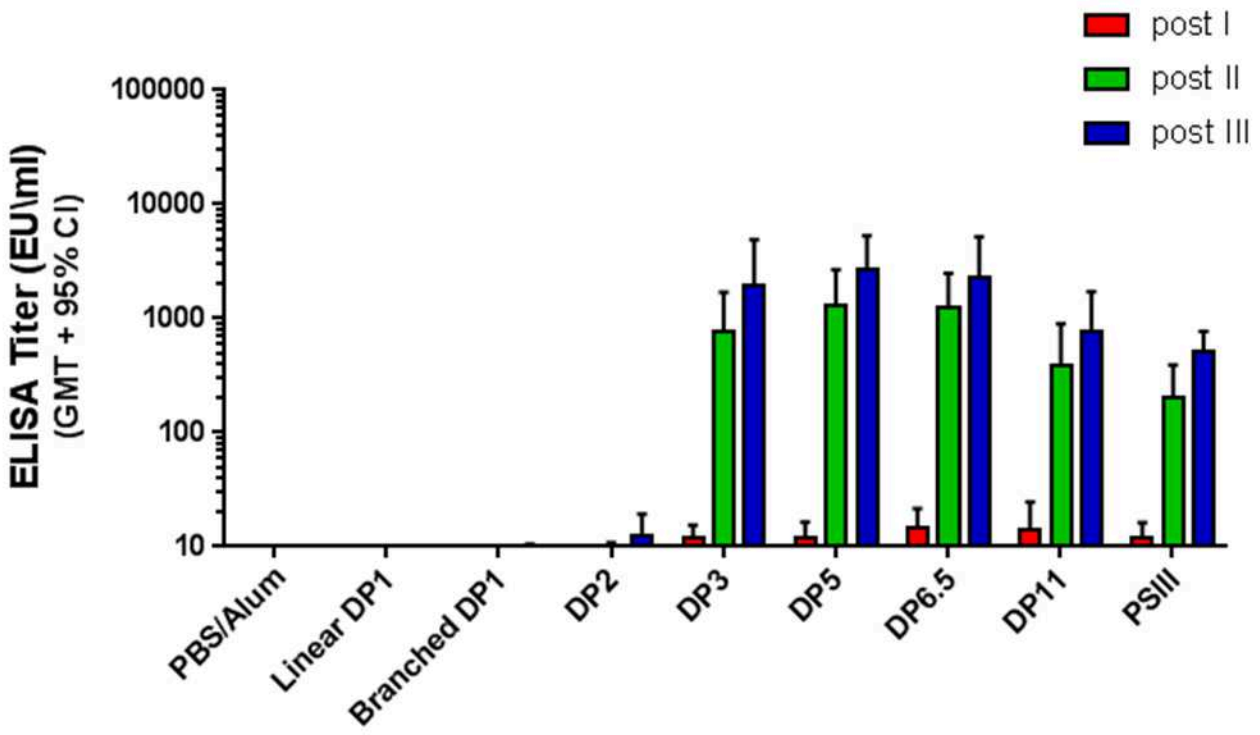

Figure 6.1. Effect of oligosaccharide size on immunogenicity of GBS type III CRM conjugates in mice. IgG titers were obtained from ELISA analysis of sera from mice immunized with 1, 2 and 3 vaccine doses of GBSIII conjugates.

No antibody response was detected after the first immunization, whereas all the CRM-conjugates of the oligomers with DP3 or higher were immunogenic after 1 and 2 booster doses. At this stage, no anti-PSIII antibodies were elicited by synthetic DP1s and DP2. Interestingly, DP3, DP5 and DP6.5 induced significantly higher level of antibodies with respect to the CRM-PSIII vaccine (p value from Mann-Whytney test lower than 0.001).

Antibody functional activity was tested by an *in vitro* OPK assay using pooled sera from animals receiving 3 vaccine doses. OPKA is a well-established assay that mimics the in *vivo* process of GBS killing subsequent to bacterial opsonization by effector cells in the presence of complement and specific antibodies[43]. In this assay, sera are tested at different serial dilutions and the reported OPKA titers are expressed as the reciprocal of the serum dilution leading to 50% bacterial killing. OPKA titers have been shown to correlate with mouse protection levels in a passive immunization/GBS challenge models[44].

As shown in Figure 6.2, all conjugates with saccharide moiety of DP3 or longer elicited functional anti type III antibodies, and the functional activity achieved with DP3, DP5 and DP6.5 was higher than the PSIII conjugate. Differently from previous studies reported in literature[45], this study clearly shows that fragments shorter than avDP4-5, which do not contain a length dependent helical structure, can be effective in eliciting a robust immune response in terms of antibody concentration and functional activity.

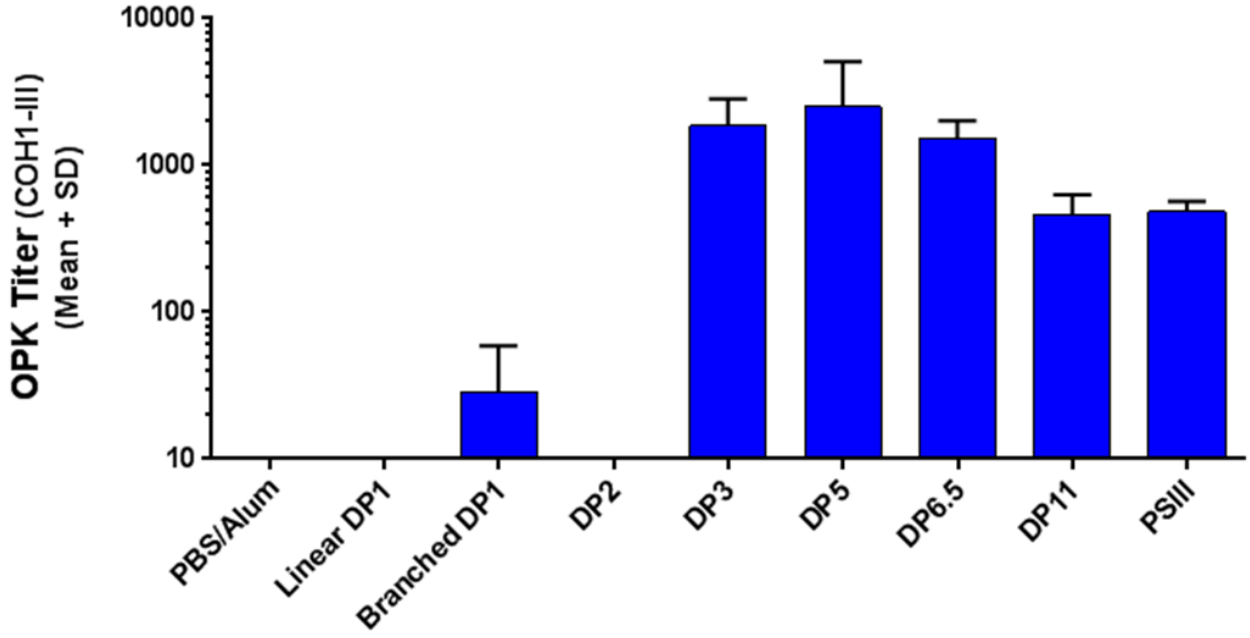

Figure 6.2. Effect of oligosaccharide size on functional activity of antibodies elicited by GBS type III CRM conjugates in mice. OPK titers were obtained from analysis of pool of sera from mice immunized with 3 injections of GBSIII conjugates.

6.2.2. Influence of the saccharide:protein ratio on the immunogenicity of glycoconjugates

Since the conjugate with DP2 did not elicit an anti PSIII response, it has been evaluated whether other parameters would affect the immunogenicity of short oligosaccharides. Hence, an *ad hoc* immunization protocol to investigate the effects of the saccharide:protein ratio on the PS immunogenicity was designed. 8 BALB/c mice /group were immunized with different conjugates of PS fragments showing same length but different glycosylation degree. Branched DP1, DP2, DP3, DP5 and DP6.5 CRM-conjugates were tested. Two glycosylation degrees were compared for each fragment, and conjugated native PSIII was used as control.

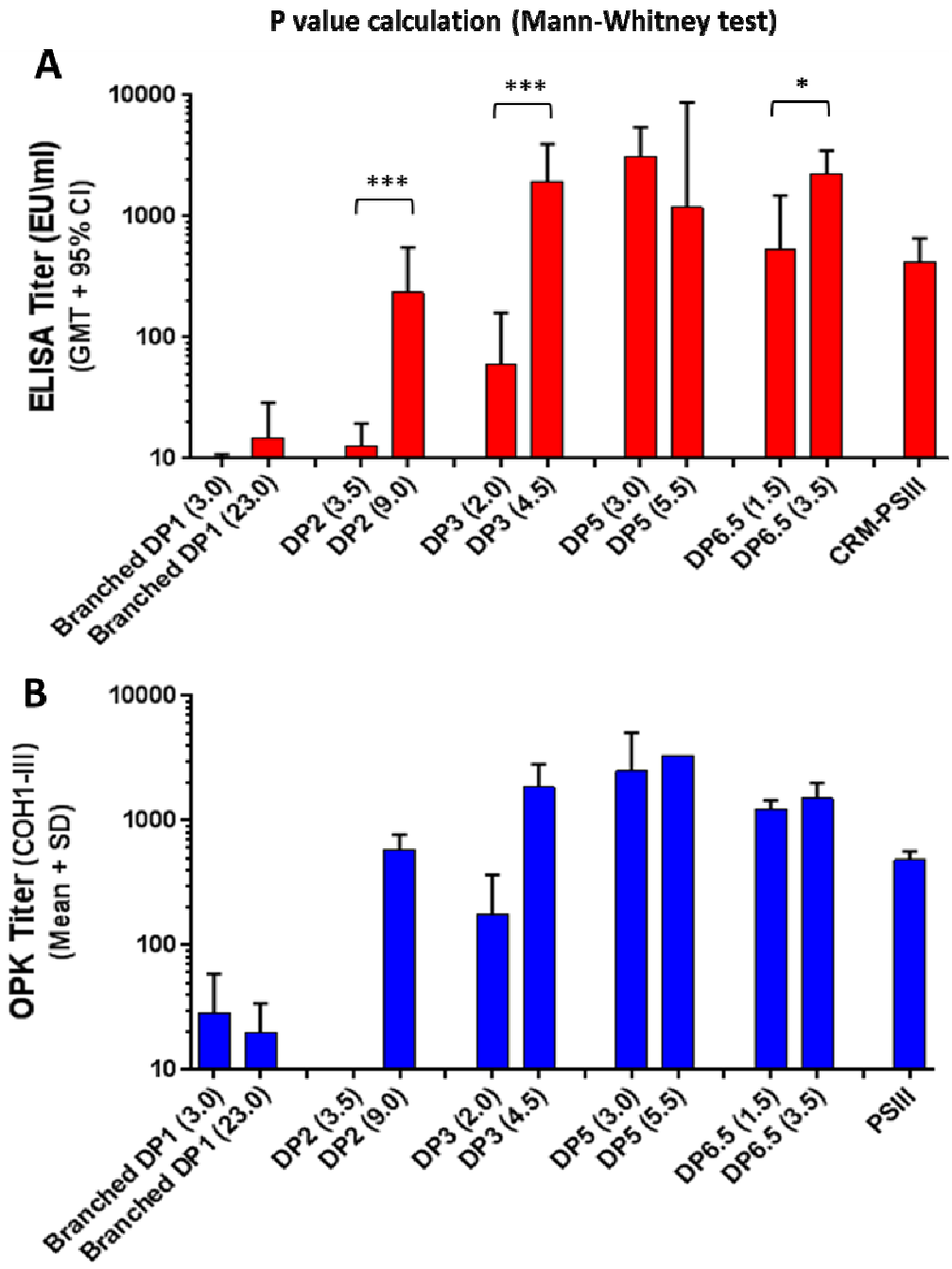

Figure 6.3. Effect of saccharide:protein ratio size on (A) immunogenicity and (B) functional activity of antibodies elicited by GBS type III CRM conjugates in mice. ELISA and OPK titers were obtained from analysis of sera from mice immunized 3 doses of GBSIII conjugates.

ELISA and OPK titers for each immunization group are reported in Figure 6.3 and, also in this case, a similar correlation between ELISA and functional data was observed.

As shown, CRM conjugates elicited higher antibody titers at increasing saccharide/protein ratio. In particular the influence of glycosylation degree was crucial for the shortest oligosaccharides. With the exception of the branched DP1, where the IgG titer remained very low also for the more glycosylated

conjugate, DP2 and DP3 were remarkably influenced by this factor. In particular, CRM-DP2 oligomer conjugate was not immunogenic at glycosylation degree of 3.5 while it became highly immunogenic with a glycosylation degree of 9.0, eliciting functional antibodies comparable to the conjugated PSIII. The CRM-DP3 oligomer conjugate with higher glycosylation degree elicited statistically higher functional IgGs compared to its low glycosylated counterpart and the native PS. The difference in immunogenicity between lower and higher saccharide/protein ratio became less evident for longer fragments, such as DP5 and DP6.5. This finding highlights the potential of multivalent presentation of oligosaccharides on the carrier protein to achieve immunogenicity levels similar or higher than larger glycans. In particular, the minimal epitope appears comprised in the DP2 fragment, in line with our structural studies, and optimization of saccharide/protein ratio in CRM-DP2 results in a conjugate vaccine as effective as CRM-PSIII (Figure 6.3). Moreover an optimal immunogenicity can also occur by presentation of the short defined epitope in longer structures.

6.2.3. Influence of the saccharide dose on the immunogenicity of glycoconjugates

Since the novel constructs with short oligosaccharides presented higher immunogenicity levels compared to CRM-PSIII, it has been evaluated if this result was dose dependent. To this end, two different glycoconjugates were compared to CRM-PSIII at different dosages: CRM-branched DP1 (glycosylation degree 23.0) and CRM-DP3. Eight mice per group were immunized with 3 injections at 0.17 (except branched DP1), 0.5 and 1.5μg dose, respectively. Sera were analyzed by ELISA for IgG titers after 2^{nd} and 3^{rd} injection (Figure 6.4).

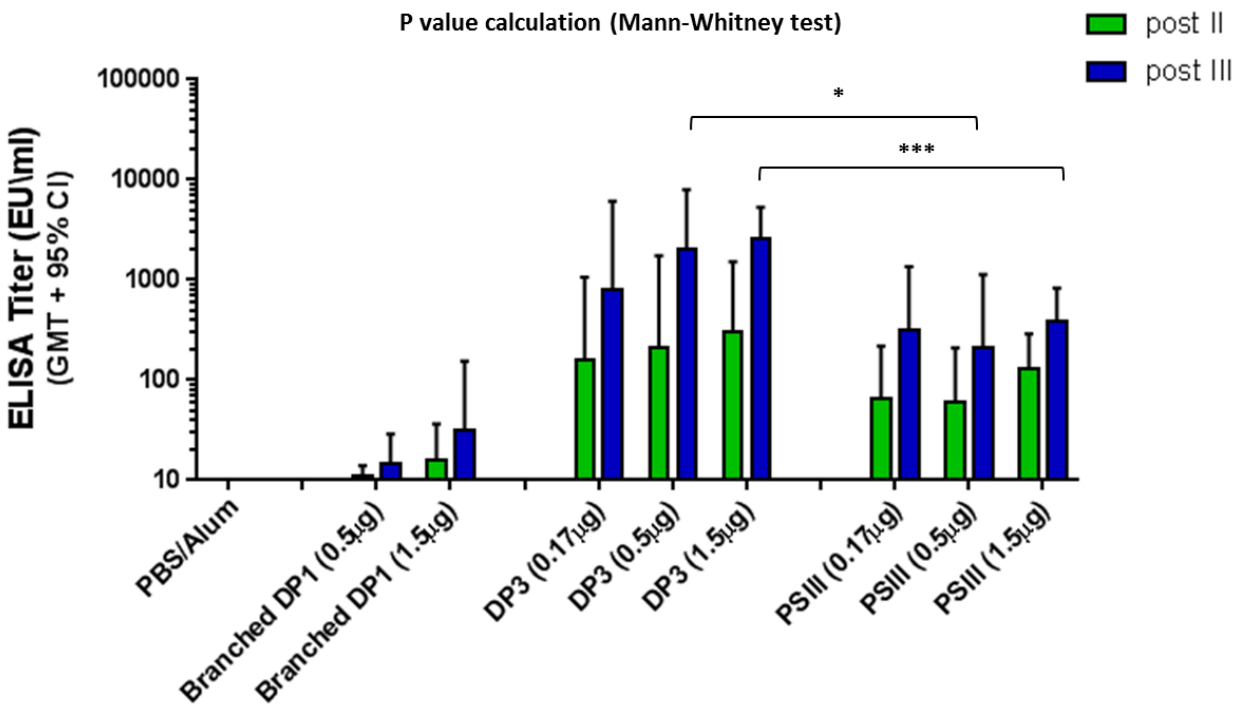

Figure 6.4. Effect of saccharide dose on immunogenicity of GBS type III CRM conjugates in mice. IgG titers were obtained from ELISA analysis of sera from mice immunized 2 and 3 injections of different vaccine doses of GBSIII conjugates.

For the conjugates of the fragments DP1 and DP3, IgG titers slightly increased by injecting a higher quantity of the antigen; the increment was not statistically significant. For CRM-PSIII, the antibody response did not change, varying the dosage from 0.17 to 1.5μg. Importantly, the difference in immunogenicity between DP3 and PSIII becomes significant only at higher dosages (0.5 and 1.5μg).

It is worth of note that the OPK titer measured for the branched DP1 was higher at the highest dose (OPK titer of 136 for 1.5μg *vs* 20 for 0.5μg). This information could be explained considering that the antigenic determinant recognized by functional mAbs is almost totally contained inside the branched DP1. This portion would lack of the glucosamine of the second repeating unit in respect to the epitope identified by X-ray analysis, however it would be sufficient to elicit moderate levels of functional antibodies and this feature would appear only at higher doses.

6.3. Discussion

Specific features of the conjugate design that may influence immunogenicity include choice of carrier protein, degree of carbohydrate loading, coupling method (random site or multisite versus single-site coupling), and chemical treatments that may alter the native epitope. In addition, the molecular size of the saccharide used in such a conjugate may be an important factor in the degree to which coupling to protein enhances immunogenicity.

In this study it has been attempted to define the effect of saccharide size on immunogenicity, using model conjugates in which other design parameters have been carefully controlled.

The deaminative cleavage of the native GBS type III polysaccharide followed by an improved method of purification of the obtained fragments allowed for the simple and well-characterized preparation of single-ended glycoconjugates, which gave sufficient uniformity to their structures to enable a legitimate comparison to be made. All of the GBS PS fragments were terminally linked exclusively at the reducing end. In fact, the methodology offers the added advantage of arming the PS fragments with a reactive aldehyde group readily available for subsequent coupling to proteins by reductive amination.

To rule out the effect of other conjugation variables, conjugates were obtained with a comparable saccharide:protein ratio. The results clearly show that fragments with a DP>2 are immunogenic and antibodies elicited are functional. In particular DP3, DP5 and DP6.5 elicit a response significantly higher than the native polysaccharide.

Additional investigation is required to better understand the impact of interdependent parameters on immunogenicity and protective efficacy. There is no established correlation between hapten loading and protective efficacy[8.12.46]. Here, it is clearly shown that it is a critical parameter. Infact, for the conjugates from short oligosaccharides, with the exception of DP1, if the saccharide:protein ratio increase, the CRM conjugates become immunogenic (as for DP2) or elicit higher functional antibody titers (as for DP3). The difference in immunogenicity between lower and higher saccharide/protein ratio became less evident for longer fragments, such as DP5 and DP6.5.

Regarding the influence of the dose, an increased response with higher dosages was observed for conjugates of GBSIII fragments, whereas CRM-PSIII elicited the same quantity of specific antibodies independently from the quantity of saccharide injected. CRM-DP3 can be a valid improvement in terms of immunogenicity for an anti GBSIII vaccine but only injecting saccharide dosages over 0.5μg where the difference in IgG titer is significant as compared to the CRM-PSIII conjugate.

As already demonstrated in the previous chapter, the glycan epitope defined for GBS type III is composed of five disjointed residues, all comprised in the DP2 fragment. Modulating the numbers of saccharide chains per protein in the CRM-conjugates used as a vaccine, it has been highlighted that DP2 is also the minimal immunogenic fragment, eliciting functional antibodies against GBS type III with a response similar to CRM-PSIII. Merging the two different conclusions, it can be summarized that DP2 contains the entire epitope of GBSIII in terms of antibody recognition and immunogenicity.

6.4. References

1. Plotkin SA. Vaccines: correlates of vaccine-induced immunity. *Clin. Infect. Dis.* **47**, 401–409 (2008).
2. Astronomo RD, Burton DS. Carbohydrate vaccines: developing sweet solutions to sticky situations? *Nature Reviews Drug Discovery* **9**, 308-324 (2010).
3. Jones C. Vaccines based on the cell surface carbohydrates of pathogenic bacteria. *An. Acad. Bras.Cienc.***77**, 293–324 (2005).
4. Pace D. Glycoconjugate vaccines. *Expert Opin. Biol. Ther.* **13**, 11-33 (2013).
5. Avci FY, Li X, Tsuji M, Kasper DL. A mechanism for glycoconjugate vaccine activation of the adaptive immune system and its implications for vaccine design. *Nature Medicine* **17**, 1602-1610 (2011).
6. Berti F, Adamo R. Recent mechanistic insights on glycoconjugate vaccines and future perspectives. *ACS Chem. Biol.* **8**, 1653−1663 (2013).
7. Bolgiano B, Mawas F, Yost SE, Crane DT, Lemercinier X, Corbel MJ. Effect of physico-chemical modification on the immunogenicity of *Haemophilus influenzae* type b oligosaccharide–CRM_{197} conjugate vaccines. *Vaccine* **19**, 3189–3200 (2001).
8. Anderson PW, Pichichero ME, Stein EC, Porcelli S, Betts RF, Connuck DM et al. Effect of oligosaccharide chain length, exposed terminal group, and hapten loading on the antibody response of human adults and infants to vaccines consisting of *Haemophilus influenzae* type b capsular antigen unterminally coupled to the diphtheria protein CRM_{197}. *J. Immunol.* **142**, 2464–2468 (1989).
9. Pozsgay V, Chu C, Pannell L, Wolfe J, Robbins JB, Schneerson R. Protein conjugates of synthetic saccharides elicit higher levels of serum IgG lipopolysaccharide antibodies in mice than do those of the O-specific polysaccharide from *Shigella dysenteriae* type 1. *Proc Natl Acad Sci USA* **96**, 5194–5197 (1999).
10. Pillai S, Ciciriello S, Koster M, Eby R. Distinct pattern of antibody reactivity with oligomeric or polymeric forms of the capsular polysaccharide of *Haemophilus influenzae* type b. *Infect. Immun.* **59**, 4371–4376 (1991).
11. Wessels MR, Paoletti LC, Guttormsen HK, Michon F, D'Ambra AJ, Kasper DL. Structural properties of group B streptococcal type III polysaccharide conjugate vaccines that influence immunogenicity and efficacy. *Infect. Immun.* **66**, 2186–2192 (1998).
12. Benaissa-Trouw B, Lefeber DJ, Kamerling JP, Vliegenthart JF, Kraaijeveld K, Snippe H. Synthetic polysaccharide type 3-related di-, tri-, and tetrasaccharide–CRM(197) conjugates induce protection against *Streptococcus pneumoniae* type 3 in mice. *Infect. Immun.* **69**, 4698–4701 (2001).
13. Jansen WT, Hogenboom S, Thijssen MJ, Kamerling JP, Vliegenthart JF, Verhoef J, et al. Synthetic 6B di-, tri-, and tetrasaccharide–protein conjugates contain pneumococcal type 6A and 6B common

and 6B-specific epitopes that elicit protective antibodies in mice. *Infect. Immun*. **69**, 787–793 (2001).

14. Wang Y, Hollingsworth RI, Kasper DL. Ozonolysis for selectively depolymerizing polysaccharides containing β-d-aldosidic linkages. *Proc Natl Acad Sci USA* **95**, 6584–6589 (1998).
15. Wang Y, Hollingsworth RI, Kasper DL. Ozonolytic depolymerization of polysaccharides in aqueous solution. *Carbohydr. Res*. **319**, 141–147 (1999).
16. Johnson MA, Bundle DR. Designing a new antifungal glycoconjugate vaccine. *Chem. Soc. Rev.* **42(10)**, 4327-4344 (2013).
17. Safari D, et al. Identification of the smallest structure capable of evoking opsonophagocytic antibodies against *Streptococcus pneumoniae* type 14. *Vaccine* **76**, 4615-4623 (2008).
18. Vulliez-Le Normand B, et al. Structures of synthetic O-antigen fragments from serotype 2a *Shigella flexneri* in complex with a protective monoclonal antibody. *Proc Natl Acad Sci U S A.* **105**, 9976-9981 (2008).
19. Baker CJ, Rench MA, Edwards MS, Carpenter RJ, Hays BM, Kasper DL. Immunization of pregnant women with a polysaccharide vaccine of *Group B Streptococcus*. *N. Engl. J. Med.* **319**, 1180–1185 (1988).
20. Harrison LH, Elliot JA, Dwyer DM, Libonati JP, Ferrieri P, Billmann L, Schuchat A. Serotype distribution of invasive Group B streptococcal isolates in Maryland: implications for vaccine formulation. *J. Infect. Dis.* **177**, 998–1002 (1998).
21. Chen VL, Fikri YA, Kasper DL. A maternal vaccine against *Group B Streptococcus*: past, present, and future. *Vaccine* **31**, 13–19 (2013).
22. Munoz FM, Ferrieri P. *Group B Streptococcus* vaccination in pregnancy: moving toward a global maternal immunization program. *Vaccine* **31**, 46–52 (2013).
23. Lancefield RC. A serological differentiation of specific types of bovine hemolytic streptococci (Group B). *J. Exp. Med.* **59**, 441–458 (1934).
24. Lancefield RC. Two serological types of Group B hemolytic streptococci with related, but not identical, type-specific substances. *J. Exp. Med.* **67**, 25–40 (1938).
25. Lancefield RC, McCarty M, Everly WN. Multiple mouse-protective antibodies directed against Group B streptococci. Special reference to antibodies effective against protein antigens. *J. Exp. Med.* **142**, 165–179 (1975).
26. Zalenik DF, Rench MA, Hillier S, Krohn MA, Platt R, Lee MT, Flores AE, Ferrieri P, Baker CJ. Invasive disease due to *Group B Streptococcus* in pregnant women and neonates from diverse population groups. *Clin. Infect. Dis.* **30**, 276–282 (2000).
27. Lancaster L, Saydam M, Markey K, Ho MM, Mawas F. Immunogenicity and physico-chemical characterisation of a candidate conjugate vaccine against *Group B Streptococcus* serotypes Ia, Ib and III. *Vaccine* **29**, 3213–3242 (2011).

28. Baker CJ, Edwards MS, Kasper DL. Role of antibody to native type-III polysaccharide of *Group B Streptococcus* in infant infection. *Pediatrics* **68**, 544–549 (1981).
29. Paoletti LC, Wessels MR, Michon F, DiFabio J, Jennings HJ, Kasper DL. *Group B Streptococcus* type-II polysaccharide-tetanus toxoid conjugate vaccine. *Infect. Immun.* **60**, 4009–4014 (1992).
30. Wessels MR, Paoletti LC, Rodewald AK, Michon F, DiFabio J, Jennings HJ, Kasper DL. Stimulation of protective antibodies against type Ia and Ib group B streptococci by a type Ia polysaccharide-tetanus toxoid conjugate vaccine. *Infect. Immun*. **61**, 4760–4766 (1993).
31. Wessels MR, Paoletti LC, Pinel J, Kasper DL. Immunogenicity and protective activity in animals of a Type-V Group B Streptococcal polysaccharide tetanus toxoid conjugate vaccine. *J. Infect. Dis.* **171**, 879–884 (1995).
32. Paoletti LC, Peterson DL, Legmann R, Collier RJ. Preclinical evaluation of group B streptococcal polysaccharide conjugate vaccines prepared with a modified diphtheria toxin and a recombinant duck hepatitis B core antigen. *Vaccine* **20**, 370–376 (2001).
33. Paoletti LC, Kasper DL, Michon F, DiFabio J, Holme K, Jennings HJ, Wessels MR. An oligosaccharide-tetanus toxoid conjugate vaccine against type III *Group B Streptococcus*. *J. Biol. Chem*. **265**, 18278–18283 (1990).
34. Wessels MR, Paoletti LC, Kasper DL, DiFabio J, Michon F, Holme K, Jennings HJ. Immunogenicity in animals of a polysaccharide- protein conjugate vaccine against type III *Group B Streptococcus*. *J. Clin. Investig.* **86**, 1428–1433 (1990).
35. Laferriere CA, Sood RK, De Muys JM, Michon F, Jennings HJ. *Streptococcus pneumoniae* type 14 polysaccharide-conjugate vaccines: length stabilization of opsonophagocytic conformational polysaccharide epitopes. *Infect. Immun*. **66**, 2441–2446 (1998).
36. Lindberg B, Lonngren J, Svensson S. Specific degradation of polysaccharides. *Adv. Carbohydr. Chem. Biochem*. **31**, 185–240 (1975).
37. Michon F et al. Group B Streptococcal type II and III conjugate vaccines: physicochemical properties that influence immunogenicity. *Clin. Infect. Dis.* **13**, 936–943 (2006).
38. Brisson JR. et al. NMR and Molecular Dynamics studies of the conformational epitope of the type III Group B *Streptococcus* capsular polysaccharide and derivatives. *Biochemistry* **36**, 3278-3292 (1997).
39. Jennings HJ. The role of sialic acid in the formation of protective conformational bacterial polysaccharide epitopes. In Anticarbohydrate Antibodies, P. Kosma and S. Muller-Loennies, eds. (Vienna: Springer), 55-73 (2012).
40. Zou, W. et al. Conformational Epitope of the Type III Group B Streptococcus Capsular Polysaccharide. *J. Immunol.* **163**, 820-825 (1999).
41. Wessels MR, Muñoz A, Kasper DL. A model of high-affinity antibody binding to type III *Group B Streptococcus* capsular polysaccharide. *Proc Natl Acad Sci U S A*. **84**, 9170-9174 (1987).

42. Zou W, Jennings HJ. The molecular immunology of complex carbohydrates - 2 of the series *Advances in Experimental Medicine and Biology* . The conformational epitope of type III *Group B Streptococcus* capsular polysaccharide. **491**, 473-484 (1981).
43. Brigtsen AK, Kasper DL, Baker CJ, Jennings HJ, Guttormsen H. Induction of cross-reactive antibodies by immunization of healthy adults with types Ia and Ib Group B Streptococcal polysaccharide–tetanus toxoid conjugate. *Vaccines* **185**, 1277–1284 (2002).
44. Guttormsen H, Liu Y, Paoletti LC. Functional activity of antisera to group B streptococcal conjugate vaccines measured with an opsonophagocytosis assay and HL-60 effector cells. *Hum. Vacc.* **4**, 370–374 (2008).
45. Zou, W. & Jennings, H.J. The conformational epitope of type III Group B Streptococcus capsular polysaccharide. *The Molecular Immunology of Complex Carbohydrates-2,* Edited by Albert M. Wu, Accademic/plenum Publishers, 473-484 (2001).
46. Laferriere CA, Sood RK, de Muys JM, Michon F, Jennings HJ. The synthesis of *Streptococcus pneumoniae* polysaccharide-tetanus toxoid conjugates and the effect of chain length on immunogenicity. *Vaccine* **15**, 179–186 (1997).

CHAPTER 7: CONCLUSIONS

In this study we aimed to characterize the antigenic determinant of the capsular polysaccharide from the clinically relevant serotype III of GBS, a pathogen for which a vaccine is under evaluation in clinical trials.

The GBS polysaccharide III has been considered as a conformational epitope prototype, based on NMR simulation studies indicating the formation of one of several potential helical structures, where sialylated side chains are arranged on the exterior surface of the helix. However a question was not addressed: Is the helical conformation pivotal for binding of PSIII to antibodies?

We undertook a structural glycobiology approach to deeply investigate the interaction of GBSIII oligosaccharides obtained by synthetic and depolymerization procedures, with a protective monoclonal antibody: a rabbit functional monoclonal IgG belonging to the major PSIII-specific sialic-acid dependent population was selected.

A combination of STD NMR and X-ray crystallography was used and the information obtained by these two techniques was in good agreement. In summary, from the results of these experiments, the glycan epitope for GBS PSIII is composed of five non-consecutive residues highlighted by the trapezoidal area (Figure 5.10a), and it would involve an additional GlcNAc residue of the vicinal repeating unit, as demonstrated by exploring the branched glycan 1 (Figure 5.6) containing the additional a GlcNAc-A" residue. It is worth of note that, the β-Glc-(1→6)-β-GlcNAc linkage creates a ramification in the carbohydrate structure that is discriminant for mAb affinity and recognition. This creates a spatially defined but discontinuous motif which involves sugars from the branch and the backbone of the polysaccharide, and that can be defined as a conformational epitope.

This observation contrasted the idea that the epitope might be exceptionally large, and convinced us to in depth explore which factors influence the immunogenicity of a glycoconjugate vaccine based on the minimal epitope. Here we disclose how the level of sugar incorporation of this defined PSIII portion onto the protein or its exposition along longer fragments can be tuned to achieve optimization of an anti GBSIII vaccine. Infact, modulating the numbers of saccharide chains per protein in the CRM-conjugates used as a vaccine, it has been highlighted that DP2 is also the minimal immunogenic fragment, eliciting functional antibodies against GBS type III with a response similar to CRM-PSIII.

Merging the two different conclusions, it can be summarized that DP2 contains the entire epitope of GBSIII in terms of antibody recognition and immunogenicity.